**NTNU – Trondheim**
Norwegian University of
Science and Technology

# Development of Protocols for the Extraction, Separation and Characterization of Lipids

Determination of photosynthetic Lipid
Composition under different Light
Environments in the Microalga
*Nannochloropsis oceanica*

Ksenia Gulyaeva

Biotechnology (5 year)
Submission date: July 2015
Supervisor: Martin Frank Hohmann-Marriott, IBT
Co-supervisor: Kåre Andre Kristiansen, IBT
Rudolf Schmid, IKJ

Norwegian University of Science and Technology
Department of Biotechnology

# Abstract

The main aim of this research was to develop protocols and techniques for simultaneous extraction, separation and characterization of photosynthetic lipids synthesized in *Nannochloropsis oceanica.* The lipid composition can be changed by changing the environmental conditions of the alga, inducing an alteration of components of the photosynthetic machinery. To understand the mechanisms involved in *Nannochloropsis* in response to changing environmental conditions, the characterization of the photosynthetic lipid composition is a crucial and challenging task. Therefore, the secondary objective of this master project was thus to apply the developed methods for extraction, separation and characterization to investigate the effects of high irradiance on the composition of photosynthetic lipids in *Nannochloropsis oceanica.* Both chromatographic and mass spectrometric techniques were used for this purpose. A particular focus has also been directed toward the investigation of non-photochemical quenching, namely the utilization of the xanthophyll cycle and state transitions during high light. Although state transitions have been widely observed in higher plants, eukaryotic algae and cyanobacteria, the presence of this process have so far not been confirmed for *Nannochloropsis*. The key mechanism of state transitions is based on a flexible binding of antennae complexes to PSII, allowing dissociation of LHCs from PSII in response to over-excitation, in order to prevent photo damage. Spectroscopic techniques have revealed a weak binding between the antennae complexes and PSII, indicating that in addition to having an active xanthophyll cycle, *Nannochloropsis* also may employ state transitions.

# Sammendrag

Hovedmålet med dette prosjektet har vært å utvikle protokoller og teknikker for samtidig ekstraksjon, separasjon og karakterisering av fotosyntetiske lipider fra *Nannochloropsis oceanica*. Lipidsammensetningen i *Nannochloropsis* vil endres når algen utsettes for miljøforandringer, og det samme vil være tilfellet for det fotosyntetiske maskineriet. For å være i stand til å forstå mekanismene som er i virksomhet i *Nannochloropsis* når algens miljø endres, er det viktig å kunne studere hva som skjer med de fotosyntetiske lipidene. Å utvikle protokoller som lar oss analysere disse er dermed en viktig, men også en krevende oppgave.

Det sekundære målet for denne masteroppgaven var å bruke de utviklede metodene for ekstraksjon, separasjon og karakterisering av pigmenter til å undersøke hvilken effekt høy lysintensitet har på det fotosyntetiske maskineriet i *Nannochloropsis*. I denne delen av prosjektet ble både kromatografiske metoder og massespektrometri tatt i bruk. Det har også vært et spesielt fokus å undersøke hvilke prosesser involvert i ikke-fotokjemisk reduksjon av eksitasjonsenergi (forkortet NPQ, fra det engelske uttrykket non-photochemical quenching) som tas i bruk i *Nannochloropsis*-celler som utsettes for høy lysintensitet. De vanligste prosessene som inngår i NPQ er xanthofyllsyklusen og re-distribusjon av pigmenter mellom PSII og PSI. Re-distribusjon av pigmenter mellom fotosystemene har blitt observert i høyere planter, flere eukaryote alger, samt cyanobakterier, men så langt er det ikke blitt påvist at denne prosessen finner sted i *Nannochloropsis*. Når det gjelder hvordan denne prosessen skjer, baserer man seg på en antagelse om at bindingen mellom PSII og de tilknyttede antennekompleksene er fleksibel, slik at lyshøstingskomplekser kan dissosiere fra PSII og i stedet binde seg til PSI ved lysintensiteter som potensielt kan være skadelige for det fotosyntetiske maskineriet. Spektroskopiske målinger gjort i forbindelse med dette prosjektet har indirekte påvist en forflytning av lyshøstingskomplekser fra PSII til PSI under høyt lys. Dette indikerer at *Nannochloropsis* i tillegg til å ha en aktiv xanthofyllsyklus, sannsynligvis også bruker re-distribusjon av pigmenter mellom fotosystemene som en av mekanismene som tas i bruk for å forhindre skade på det fotosyntetiske maskineriet i høyt lys.

# Acknowledgments

Working on this project has probably been my most challenging time of my education here at NTNU. The last year has been filled both with new exiting discoveries and lots of frustration. But now I am finally done! However, the completion of this work would not be possible without the contribution from several people, whom I really would like to thank.

Especially I would like to thank my advisor, Associate Professor Martin Hohmann-Marriott for giving me this research opportunity and being very helpful and patient with me. Our conversations has both helped me interpreting my results and kept me calm upon meeting unexpected challenges. I also would like to thank my dear friend and my mentor, PhD student Gunvor Røkke. Thank you for being there for me, and helping me when I needed it most. Thank you for being patient and not minding explaining me something ten times until I finally get it. Nothing of this would have been possible without you. You are everything I would like to be some time in a not so distant future.

I am also grateful to Kåre Kristiansen for all his help in the MS lab, to Thor Bernt Melø at the department of Physics for helping me around the 77 K lab, and to Rudolf Schmid at the department of Chemistry for helping me with the HPTLC setup, and letting me use the instrumentation by letting me work at the chromatography lab. I also owe a thank-you to Jake and Marianne for letting me work at their offices. In addition, I would like to thank my dear friend and fellow student Axana for cheering me up with mindful conversations in Russian.

I would also like to thank the staff at the department of Biotechnology, and especially Cecilie Skagfjord and Jo Esten Hafsmo for helping me out with administrative issues. I am also grateful to Merethe for providing me with everything I needed in order to perform my work at the lab.

Finally, I would like to thank my family, who has always supported my choices and motivated me every single day of those six years I have studied at NTNU.

# Contents

# Chapter 1: General introduction

## 1.1 Algae and photosynthesis

The sun is the universal source of energy for life on Earth. About 99% of the sun's radiation is in the range between 300-4000 nm, and within this range, the wavelengths of visible light, ranging from approximately 400-700 nm are called photosynthetic active radiation (PAR), and can be utilized by photosynthetic organisms. Photosynthesis is the biological process where water, carbon dioxide and light energy are used for production of oxygen and carbohydrates. In other words, photosynthesis converts solar energy into biologically usable energy. The net process of photosynthesis can be written as:

$$nCO_2 + nH_2O + light \xrightarrow{Chlorophyll\ a,} (CH_2O)_n + nO_2$$

In this equation light is presented as a substrate and chlorophyll *a* is a catalytic agent required for conversion of carbon dioxide from its oxidized state into reduced organic matter (carbohydrates). Energy fixation by photosynthetic organisms is critical for the survival of life on Earth, as the fixed energy is made available for non-photosynthesizing organisms. In this way plants form the base of terrestrial food chain, while marine food chain are primarily based on microscopic algae.

Photosynthetic activity of marine phytoplankton (photosynthetic bacteria and algae) roughly accounts for more than 50 percent of the global photosynthesis (Geider and Osborne 1992, Moroney and Ynalvez 2009). Being a very large and diverse group of predominantly aquatic photosynthetic organisms, phytoplankton range in size from microscopic individuals such as cyanobacteria, to multicellular giants such as giant kelp. The large diversity of algae can also be seen in many aspects of the photosynthetic machinery and its parts, where the most obvious variation between different photosynthetic species is the pigment content and composition found in the light harvesting antennae. The wide ranges of colors that can be observed in algae are related to variations in the composition of photosynthetic lipids, or pigments.

## 1.2 Photosynthetic lipids

Quinones and photosynthetic pigments such as chlorophylls, carotenes and xanthophylls are sometimes collectively termed as photosynthetic lipids due to their non-polar and lipophylic character. There are an impressive number of photosynthetic lipids found in photosynthetic organisms, serving their own particular function. The main function of photosynthetic lipids is to harvest the available light and transfer it to the reaction center in photosystem II (PSII). Chlorophylls and carotenoids are the major classes of pigments involved in light harvesting reactions. In addition, carotenes and xanthophylls have an important role in photoprotection under high light conditions. Another important group of lipids found in biological membranes are quinones, compounds involved in electron transport chain reactions. Major photosynthetic lipids exist as a part of photosynthetic machinery in thylakoids. The thylakoid membrane consists of approximately 50% lipids, where 10% are represented by chlorophylls, phospholipids, sulpholipids, carotenoids, xanthophylls, quinones and sterols (Barsanti and Gualtieri 2014). Differences in photosynthetic lipid content often provide a clue to the taxonomic classification of algae, since composition of photosynthetic lipids can vary between the different species. The composition of lipids within a specific alga can also change as a result of environmental conditions they are subjected to.

### Chlorophylls

Chlorophylls are the major class of photosynthetic pigments found in all eukaryotic photosynthetic organisms. The pigment common to all algae, including cyanobacteria is chlorophyll *a*. Other major chlorophylls are represented by chlorophyll *b*, *c* and *d*. These chlorophylls transfer absorbed energy to chlorophyll *a* situated in the reaction center, and are (together with carotenoids) therefore called accessory pigments.

The structures and properties of the major chlorophylls have been reviewed several times (Scheer 1991, Hynninen 1992, Scheer 2006). The structure of chlorophyll does in some way resemble the hemoglobin structure. Chlorophyll *a* is a planar (almost) square molecule with a polar (hydrophilic) porphyrin head, composed of four pyrrole rings surrounding a magnesium atom, and a non-polar (hydrophobic) phytol tail (H. Scheer 2004, Humphrey 2004).

Chlorophyll *b* and chlorophyll *d* differ from chlorophyll *a* in only one structural regard: a formyl group is coupled to C7-position in chlorophyll *b* instead of methyl group in

chlorophyll *a*, and vinyl group found in chlorophyll *a* at C3-position is replaced by formyl group in chlorophyll *d*. Chlorophyll *c* has a unique structure compared to other chlorophylls, as it only has a hydrophilic porphyrin head, and no isoprenoid hydrophobic tail (Falkowski and Raven 1997, Blankenship 2013). The structures of all major chlorophylls are shown in Figure 1.1.

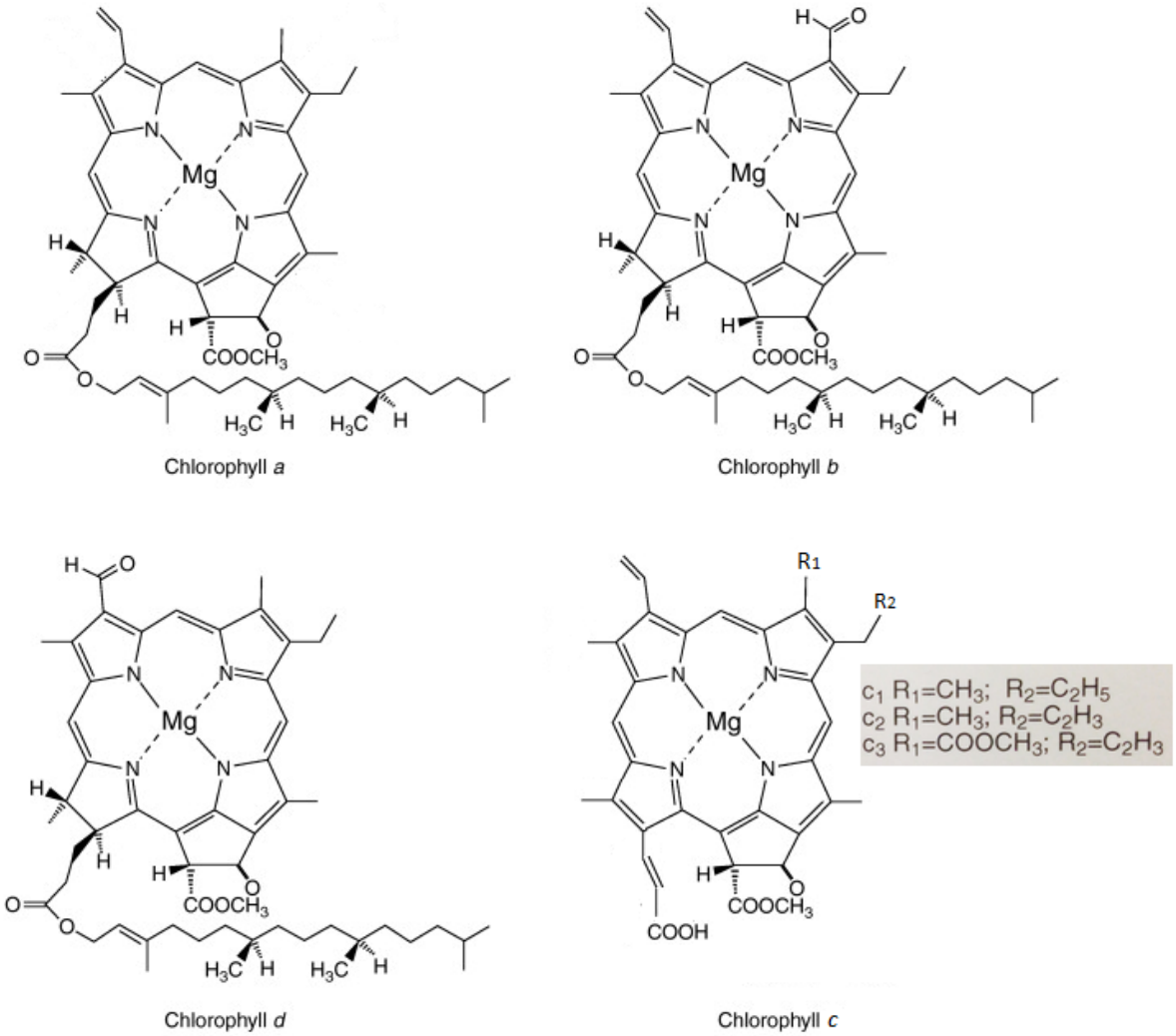


**Figure 1.1 - Chemical structures of chlorophylls *a*, *b* and *c*:** $R_1$ and $R_2$ are side groups referring to structural variants of chlorophyll c. Figure composed from: Chen and Blankenship (2011) and Blankenship (2013).

Structural differences between different chlorophylls result in a maximum absorbance from 660 to 665 nm for chlorophyll a, and maximum absorbance at slightly shorter wavelengths for chlorophylls *b* and *c* (Figure 1.2) (Falkowski and Raven 1997, Hosikian, Lim et al. 2010). In addition each chlorophyll molecule has its distinct absorption property depending on the binding site within the antenna complex and surrounding electrochemical environment.

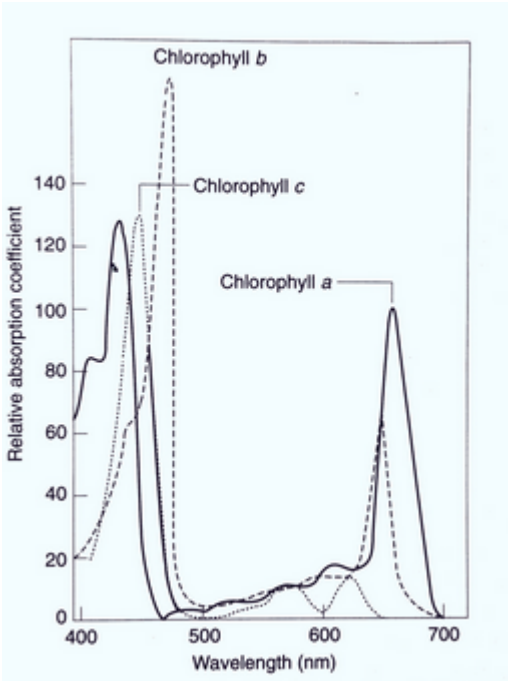


**Figure 1.2:** The normalized absorption spectra for chlorophylls a, b and c in acetone. From: Falkowski and Raven (1997).

## Carotenoids

Carotenoids represent a highly diverse group of naturally occurring chromophores belonging to the compound class of terpenoids. More than 700 chemically distinct carotenoids have been described (Britton, Liaaen-Jensen et al. 2004) that, depending on structural differences, demonstrate a large range of spectroscopic properties (Frank 1999).

All carotenoids can roughly be described as a long molecule consisting of eight isoprene units where 18-carbon conjugated double-bond backbone connects two six-carbon unsaturated rings. Carotenoids differ from each other mainly by the position of different side-groups and the positions of double bonds in the molecule.

Structurally carotenoids can be divided into two groups: carotenes and xanthophylls. Xanthophylls are derived from carotenes by introduction of oxygen and, as a result, formation

of epoxide or hydroxyl groups (Falkowski and Raven 1997, Roy, Llewellyn et al. 2011). Structures of some major carotenoids are shown in Figure 1.3.

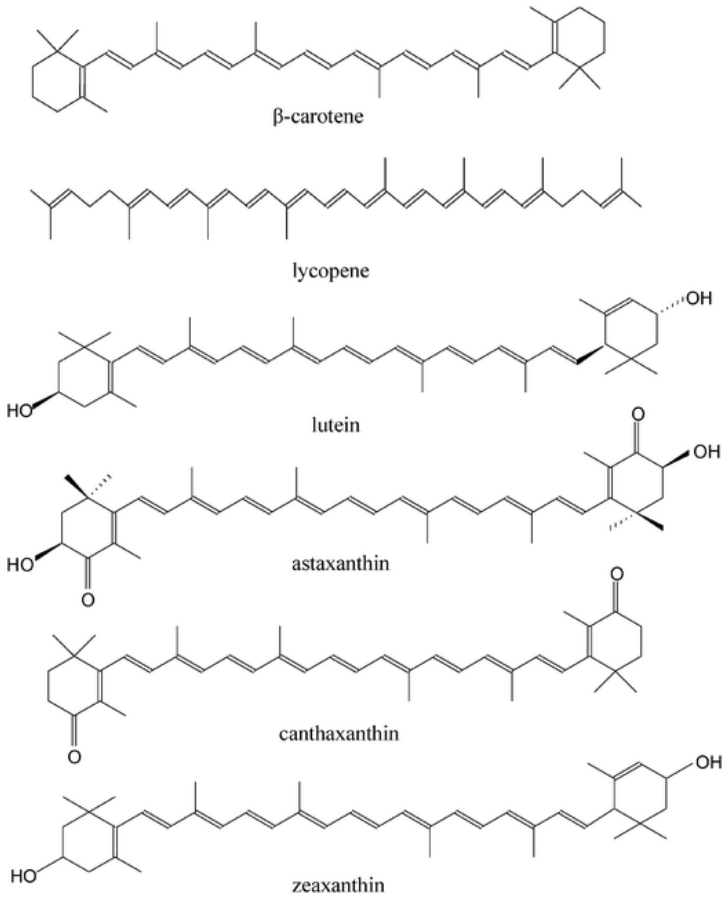


**Figure 1.3 - Chemical structures of some major carotenoids found in algae:** The basic structure is a conjugated isoprene backbone connecting two saturated 6-carnon rings. Carotenes, such as β-carotene and lycopene are pure non-oxygenated hydrocarbons, while xanthophylls contain oxygen. From: Falkowski and Raven (1997).

As mentioned earlier in this chapter, carotenoids can promote energy transfer both to and from chlorophylls working as accessory pigments in addition to their photoprotective role. Since molecular structure and absorption properties are related, different carotenoids have different absorption spectra. Carotenoids having a maximum absorption at a shorter wavelength than chlorophyll *a* can function as energy donors, while an absorption maximum at a longer wavelength than the one of chlorophyll *a*, will yield a carotenoid functioning as an energy acceptor (Falkowski and Raven 1997, Frank 1999).

## Quinones

Quinones are widely distributed in nature and have an important role in electron transport chains. Well known examples are ubiquinone, which acts as an electron carrier in the mitochondrial electron transport chain, and plastoquinone, transferring electrons in the electron transport chain of chloroplasts, being a part of the light-dependent reactions in photosynthetic organisms. A hydrophobic tail with the possibility of being anchored to the lipid bilayer of membranes, alongside with their reverse reduction ability make quinones ideally suited for electron transport-mediated proton transfer across biological membranes.

Naturally occurring quinones can be divided into benzoquinones and naphtoquinones depending on the chemical structure of their hydrophilic head. The aromatic ring of the hydrophilic head can consist of either benzene or naphthalene (Nowicka and Kruk 2010). Both ubiquinone and plastoquinone belong to the benzoquinone group.

Photosynthetic lipids represent high value biochemical compounds used both in production of nutraceutical and pharmaceutical products, in analytical chemistry, as high quality pigment standards, and as additives in food and cosmetics. There is an ongoing search for inexpensive and efficient ways to produce high quality pigments. Photosynthetic organisms, especially algae represent a unique and rich source for the production of aforementioned photosynthetic lipids. The potential of one particular alga to produce the high value chemical compounds will be described further in this chapter.

## 1.3 The potential of *Nannochloropsis*

*Nannochloropsis* is a genus of eukaryotic marine microalgae, first described in 1981 by Hibbered (Hibberd 1981), belonging to the Estigmatopphyceae class within the Heterokontophyta division (Basso, Simionato et al. 2014). The genus includes six species (*N.gaditana, N.oceanica, N.oculata, N.granulata, N.limnetica,* and *N.salina*). As heterokonts, *Nannochloropsis* have unique ultrastructure features, as the result of the secondary endosymbiotic event between a eukaryotic cell and a red algae (Figure 1.4) (Archibald and Keeling 2002, Basso, Simionato et al. 2014). This can be seen by the presence of four membranes enveloping the plastids with interconnections of these membranes to the endoplasmatic reticulum (ER) and the nuclear envelope (Reyes-Prieto, Weber et al. 2007).

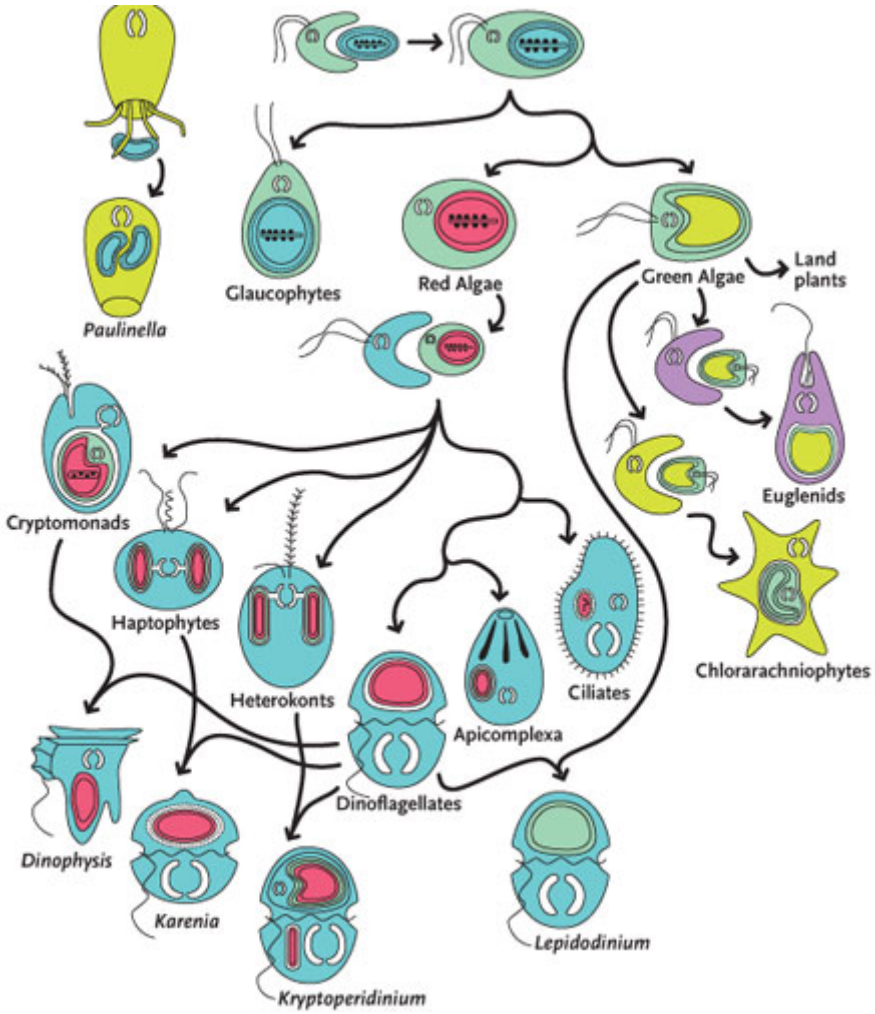


**Figure 1.4 - Evolution of plastids:** Primary (top), secondary (middle) and tertiary (bottom) endosymbiotic events. Three algal lineages with primary plastids are identified by color-coded plastids. Blue: Cyanobacteria and Glauciphyta, Red: red algae (Rhodophyta), Green: green algae (Chlorophyta). From: Keeling (2004).

All members of Estigmatopphyceae are cocoid unicells that can exist as single cells, in pairs or in colonies (Barsanti and Gualtieri 2014). *Nannochloropsis* are small non-motile unicells ranging in size from 2-5 μm. Eustigmatophytes are generally found in freshwater and soil, although *Nannochloropsis* represents species living in marine environment. Because of their relatively small cell size, *Nannochloropsis* species are indistinguishable from each other when using regular light microscopy (Cohen 1999, Fawley and Fawley 2007).

## *Nannochloropsis* as a lipid producer

Lately, microalgae have received much attention, as they represent a unique and inexpensive source for production of high-value biochemical compounds. Due to their capacity to accumulate high amounts of lipids, marine microalgae are seen as a promising source of biofuels (Li, Horsman et al. 2008, Borowitzka and Moheimani 2013). Terrestrial oleaginous crops such as soybean, canola and palm remain the main commercial source for biodiesel production and involve many drawbacks. The use of marine microalgae for bioenergy has several unique advantages over terrestrial crops:

- No pesticides involved
- No need for large quantities of fresh water
- Lower nutritional needs
- Rapid growth and high biomass production
- No food supply conflict
- Higher $CO_2$ uptake and storage
- Production on non-arable land with non-potable water by using portable or large scale outdoor ponds (Wang, Ning et al. 2014).
- Daily harvesting and season-independent growth while growing in photobioreactors (Chisti 2007, Chisti 2008).

Microalgae are also efficient producers of polyunsaturated fatty acids (PUFAs) such as arachidonic acid (AA), eicosapentaenoic acid (EPA), docosahexaenoic acid (DHA) and triacylglycerol (TAG) (Cohen 1999, Borowitzka and Moheimani 2013).

Only a few microalgae are suitable for commercial production of oils (Anandarajah, Mahendraperumal et al. 2012). Among them *Nannochloropsis* species are capable to

accumulate lipids up to 70% of total dry weight. They grow relatively fast, doubling in cell number every 24 hours and accumulating high levels of lipids desired for production of biofuels and PUFAs (Chisti 2007). Several studies indicate that *Nannochloropsis* species also represent a valuable source for production of high-value pigments such as chlorophyll *a*, β-carotene, zeaxanthin, violaxanthin, astaxanthin and canthaxanthin (Lubián, Montero et al. 2000, Nobre, Villalobos et al. 2013). Table 1.1 presents some commercially available phytoplankton pigments, their suppliers and prices. Furthermore, in addition to its use in aquaculture, carotenoids also have important pharmaceutical properties directly related to their antioxidant action, free-radical scavenging and anti-inflammatory effect (Hughes 1999, Paiva and Russell 1999, Miyashita 2009, Anunciato and da Rocha Filho 2012)

**Table 1.1 – Commercial suppliers of pigments:** Prices are given for 1 mg crystals.

| Pigment | Supplier | Isolated from | Price |
|---|---|---|---|
| Antheraxanthin | *CaroteneNature* | Not given | € 370 |
| Astaxanthin | CaroteneNature | Synthesis | € 245 |
| Chlorophyll *a* | Sigma | Spinach | € 97.10 |
| Violaxanthin | CaroteneNature | Not given | € 370 |
| Zeaxanthin | Fluka | Not given | € 362 |

*From:* Commercial suppliers of phytoplankton pigments by Einar Skarstad Egeland and Louise Schluter (Roy, Llewellyn et al. 2011)

As already mentioned, microalgae are considered a valuable source for the production of high-value biochemical compounds and a promising feedstock for biofuels production. However, utilization of microalgae for the aforementioned purposes has several limitations related to formation of biomass and its productivity in terms of production of desirable compounds. Closer understanding of the photosynthetic machinery and its components, and how these can be affected, provides an opportunity for maximizing the total biomass production. Two most important environmental factors that can potentially affect biomass productivity are light and $CO_2$-supply. Overproduction of biomass and desirable products such as various pigments, quinones, lipids and PUFAs, can be achieved either by using a molecular genetics approach, or by modification of cultivation conditions. In addition, optimization of extraction methods and separation techniques, and improvement of

preservation methods are the main criteria for a successful establishment and commercialization of microalgal high-value chemicals.

## 1.4 Photosynthetic machinery of *Nannochloropsis*

*Nannochloropsis* performs oxygenic photosynthesis and is capable of converting light energy into biochemical energy due to the action of particular protein complexes embedded in the thylakoid membrane. These large energy transforming units are termed photosystem I (PSI) and photosystem II (PSII), and are surrounded by light harvesting complexes (LHCs) (Figure 4.1) that, in addition to light capture, also have photoprotective functions (Blankenship 2013).

### Pigment composition

As mentioned above, *Nannochloropsis* belongs to Eustigmatophyceae, a class of eukaryotic microalgae that most probably is derived from a secondary endosymbiotic event between a eukaryotic cell and a red alga (Figure 1.4). The photosynthetic apparatus of *Nannochloropsis* represents distinct features with respect to other members of Heterokontophyta division. The photosynthetic machinery of *Nannochloropsis* is characterized by the absence of accessory chlorophylls and phycobilins, presenting only chlorophyll *a* (Brown 1987). The major carotenoids found in *Nannochloropsis* algae are β-caroten, violaxanthin and vaucheriaxanthin (Lubián, Montero et al. 2000), although zeaxanthin and antheraxanthin are mostly detected after the cells have been exposed to high irradiance (Figueroa, Jiménez et al. 1997). Violaxanthin is the major carotenoid present in the antenna complexes. This is unusual, as violaxanthin in most other photosynthetic species exist as a minor component with respect to other carotenoids (Lubián, Montero et al. 2000, Basso, Simionato et al. 2014). According to the work of S. Basso and colleagues on characterization of photosynthetic apparatus of *Nannochloropsis gaditana* (Basso, Simionato et al. 2014) violaxanthin and vaucheriaxanthin are found to be associated with the antenna complexes. The *Nannochloropsis* PSII core is strongly enriched with β-carotene, while PSI-LHC contains both violaxanthin and β-carotene. Zeaxanthin and antheraxanthin are found to be bound to both photosystem antennas.

## Distribution and dissipation of excess light energy

When the chlorophyll *a* molecules in the light-harvesting antennae absorbs light, it is promoted from its ground state to a single-state excitation form (Blankenship 2013). Most of the excitation energy is used to run photochemical processes. Excitation energy received in quantities larger than the amount of energy that can be utilized in photosynthesis results in an increased yield of single-state excited chlorophyll. The increased fraction of excited chlorophylls leads to the formation of reactive oxygen species that can cause oxidative damage to the thylakoid membrane and its components. This is termed photodamage (Barber and Andersson 1992, Han 2002).

Photodamage caused by excess of light energy can be avoided by either distributing the excess energy differently between the two photosystems, or by disposing of the excess light energy as heat. When the amount of excitation energy absorbed by one of the photosystems exceeds its capacity, the flux of energy is then redirected towards the energy-deficient photosystem in the process known as state transitions (Minagawa 2011). In the green alga model it has been demonstrated that when PSII is over-exposed to light, some of the LHCII complexes are being transferred from the stacked regions of the thylakoids that contain mainly PSII to the unstacked regions and stromal membranes containing an excess of PSI (Falkowski and Raven 1997, Blankenship 2013). This migration allows the received energy to be re-distributed between the two photosystems. However, despite the fact that state transitions have been widely observed in higher plant and many eukaryotic algae and cyanobacteria, the presence of this process in *Nannochloropsis* is still not been confirmed.

If both photosystems are overexposed to light, a re-distribution of received energy by performing a state transition is not enough to prevent photodamage. Under these conditions, excess light energy is dissipated by the actions of the xanthophyll cycle. The xanthophyll cycle is a very important photoprotective processes in many photosynthetic organisms, and together with the process of state transitions, it is one of the two most important light protection mechanisms included in the term non-photochemical (NPQ). The xanthophyll cycle is characterized by formation of zeaxanthin via enzymatic de-epoxidation of violaxanthin at high light, through the antheraxanthin intermediate (Roy, Llewellyn et al. 2011). The reaction is reverted under low light conditions, and violaxanthin is recreated by epoxidation of zeaxanthin. As already mentioned, zeaxanthin and antheraxanthin can be found in significant amounts in *Nannochloropsis* after exposure to high irradiance. This confirms the

existence of a functional xanthophyll cycle in this marine microalga (Gentile and Blanch 2001).

## Aims of Research

The main aim of this research is to develop protocols and techniques for simultaneous extraction, separation and characterization of photosynthetic lipids in *Nannochloropsis oceanica.* The composition of these lipids can be changed by environmental conditions, indicating an alteration of the photosynthetic machinery. Therefore the secondary objective of this master project is to apply the developed protocols mentioned earlier in this paragraph to investigate the effects of high irradiance on the composition of photosynthetic lipids in *Nannochloropsis oceanica.*

# Chapter 2: Optimization of lipid extraction

## Introduction

Development of efficient extraction methods is critical for the establishment and commercialization of algal high-value compounds such as various pigments, quinones, tocopherols and PUFAs. Optimization of extraction techniques including development of rapid, reproducible and economical methods, in addition to efficient separation of extracted components and improved preservation methods, are the main goals for establishment and commercialization of microalgal high-value chemicals. The aim of the experiments presented in this chapter was to develop a functional and effective protocol for the simultaneous extraction of various photosynthetic lipids from *Nannochloropsis oceanica* (*N. oceanica*).

### *In vitro* absorption spectroscopy

An unusual feature that distinguishes *Nannochloropsis* species from other related microalgae is that they only synthesize chlorophyll *a*, completely lacking other accessory chlorophylls. The carotenoid content is also divergent, and characterized by having violaxanthin, vaucheriaxanthin and β-carotene as its major carotenoids, where violaxanthin accounts for up to 60% of the total carotenoid content (Lubián, Montero et al. 2000). Extraction yields for visible photosynthetic lipids can be quickly evaluated by visual inspection. However, isoprenoid quinones absorb in the UV range of the electromagnetic spectrum and can thus not be detected by the bare eye. Therefore, the identification of pigments and determination of the relative pigment content in prepared extracts can be accomplished by using spectroscopic techniques. Spectral analysis is widely employed for the estimation of pigment content *in vitro.*

As already mentioned, chlorophyll *a* is the only chlorophyll synthesized by *Nannochloropsis species,* and in its pure form it creates two major absorption peaks at approx. 435 nm and 665 nm. However, in photosynthetic organisms chlorophyll *a* are not found as free pigments, but are bound to light harvesting complexes and photosystems. Therefore, the absorption properties of a chlorophyll molecule in the cell can vary, depending on its binding site in the LHC and the surrounding electrochemical environment (Basso, Simionato et al. 2014). The total absorbance of chlorophyll *a* extracted from *Nannochloropsis* species can then be

described as the sum of spectral contributions from several chlorophyll *a* molecules (Cinque, Croce et al. 2000), with absorption maxima slightly higher than 667 nm (Figure 2.1) (Basso, Simionato et al. 2014). Organic solvents do not exclusively extract pigments. Other organic molecules such as fatty acids could also be accumulated in the extract. So even though the pigments are now extracted from the cells, they could still interact with other organic molecules, and this would in turn give rise to differences in the absorption properties of chlorophyll *a*. In addition, spectral properties of the organic solvent the pigments were extracted with will also affect the pigment absorbance.

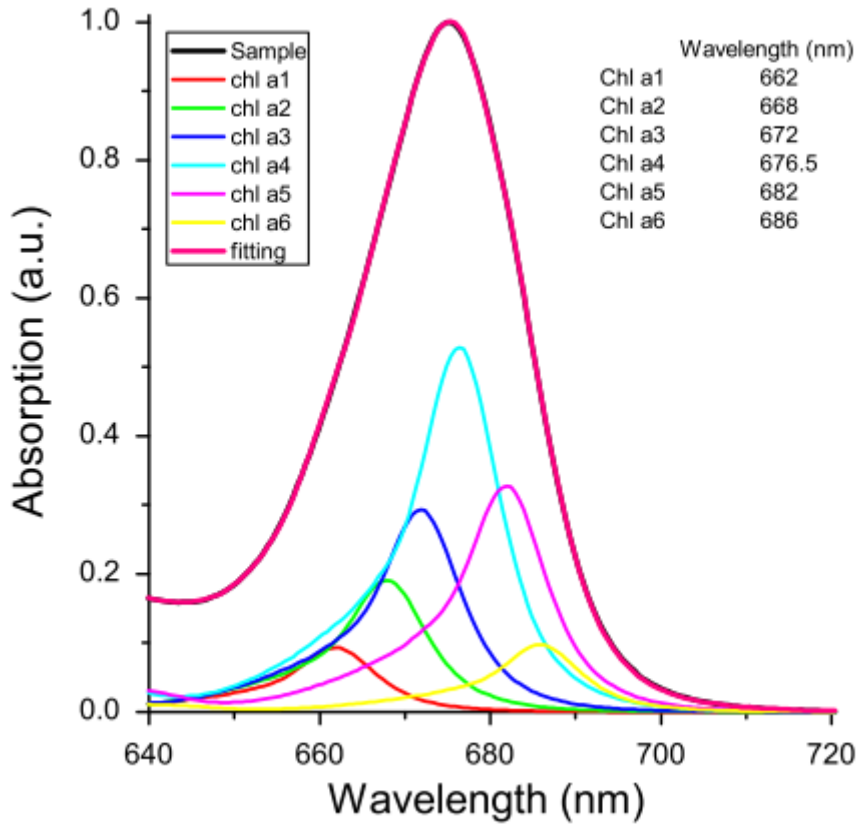


**Figure 2.1 – Distribution of chlorophyll *a* absorbance in *Nannochloropsis gaditana*:** Sample (black) and sample fitting (pink) absorbance as the contribution of several spectral forms of chlorophyll *a* (a1-a6). From: Basso, et al. (2014).

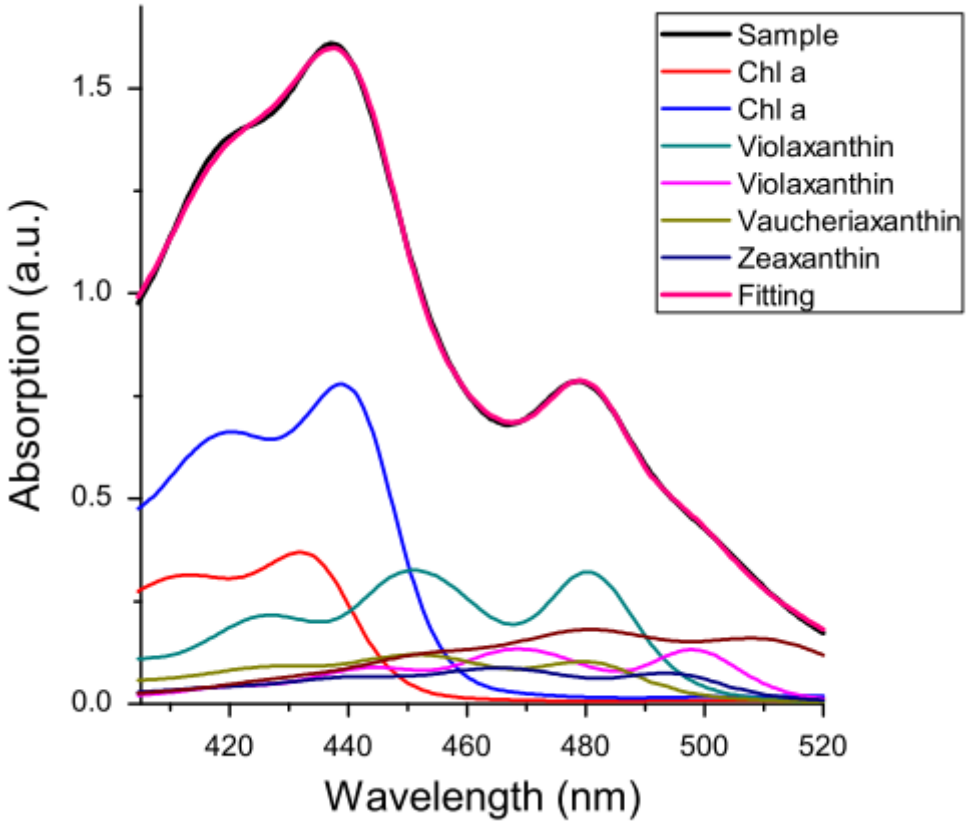


**Figure 2.2 – Distribution of spectral forms of chlorophyll *a* and xanthophylls in *Nannochloropsis gaditana*:** The final appereance of absorbtion spectra as a sum of spectral contributions from chlorophyll *a* and xanthophylls. From: Basso, et al. (2014).

The major carotenoids in *Nannochloropsis* species can be observed in the 430 - 500 nm region, and the largest contribution, as previously stated, comes from violaxanthin. The presence of carotenoids in the analyzed samples affects the overall shape of the obtained absorption spectra, due to a partial overlap between carotenoid / xanthophyll and chlorophyll *a* absorbance (Figure 2.2). Quinones absorb in the UV range of the spectrum, and can be detected in the 230 - 320 nm region. Therefore, quinones do not have overlapping absorption properties with chlorophylls and carotenoids.

To optimize the simultaneous extraction of photosynthetic lipids, experiments were performed to investigate the extraction efficiency of different extraction solvents and effects of different treatments of the sample on the extraction yield. In the following sections (2.1-2.3), the best extraction solvent, the optimal solvent to sample ratio, and the effect of additional treatments will be described.

## 2.1 Choice of organic solvent system

Based on the knowledge from previous studies (Henriques, Silva et al. 2007, Martinis, Kessler et al. 2011) five organic solvents were evaluated for their ability to extract photosynthetic lipids from *N. oceanica*. These five solvents were a mixture of methanol and chloroform (MeOH/CHCl3, 70/30), tetrahydrofuran (THF), acetone, isopropanol (IPA) and methanol (MeOH). Cell pellets were extracted twice and extraction efficiency was evaluated both by empiric examination of the pellets and extracts, and by spectroscopic techniques. Different aspects such as price, toxicity, boiling point and the solvent's compatibility with other analytical techniques have also been considered when assessing the different solvents.

### Materials and methods

#### Growth conditions

*Nannochloropsis oceanica* cells obtained from the National Center for Marine Algae and Microbiota (NCMA, USA) were cultivated in f/2 medium prepared from filtered (0.22 mm disposable filter) and autoclaved seawater. The cells were grown in conical flasks with ribbed sides for increased turbidity. Aeration was achieved by shaking with a Rotamax 120 Orbital Shaker (Heidolph, Germany). Cell cultures were grown at a constant light intensity of 100 μmol photons $m^{-2}s^{-1}$, and the temperature was kept at 23$^{o}$C.

#### Extraction procedure and evaluation

The effect on pigment extraction of five organic solvents was evaluated in a dual extraction procedure. All solvents were prepared by using analytical grade MeOH and $CHCl_3$ (Normapur®, VWR), IPA (GRP®, VWR), THF (Seccosolv®, Merck) and acetone (GRP®, VWR). Cultured cells were harvested by utilizing multiple centrifugations (8000rpm, 15 min) in order to gradually concentrate the cell sample. The concentrated sample was then equally distributed to several Eppendorf tubes (1.5 mL sample in each tube), and cell pellets were prepared by a micro centrifuge using 13000 rpm for 2 min. The masses of the cell pellets were then carefully assessed, and the pellets were extracted twice with five volumes of the selected solvent (e.g. 500 μL solvent for a 100 μg cell pellet). The cells were extracted for 20 min at -20 °C. Extracts were evaluated separately by absorption spectroscopy utilizing a NanoDrop 2000® spectrophotometer (Thermo Scientific, USA) in the range between 220 and 750 nm.

## Results and discussion

The color of extracts and cell pellets can provide valuable information about the extraction efficiency, as it can be quickly evaluated whether or not the pigments of the cell pellet has been extracted to the supernatant. Figure 2.3 shows a cell pellet prior to extraction, while figure 2.4 shows the visual differences between extracts performed with different solvents after the first and second extraction. All samples have been prepared from the same culture, and the extraction conditions for all samples were identical, only differing from each other in use of different organic solvent systems. The visual inspection and measured absorption spectra provide comparable information required for evaluation of extraction ability of the four investigated organic solvents.

**Fig 2.3 – Cell pellet made from harvested cell culture:** The appearance of the cell pellet prior to extraction

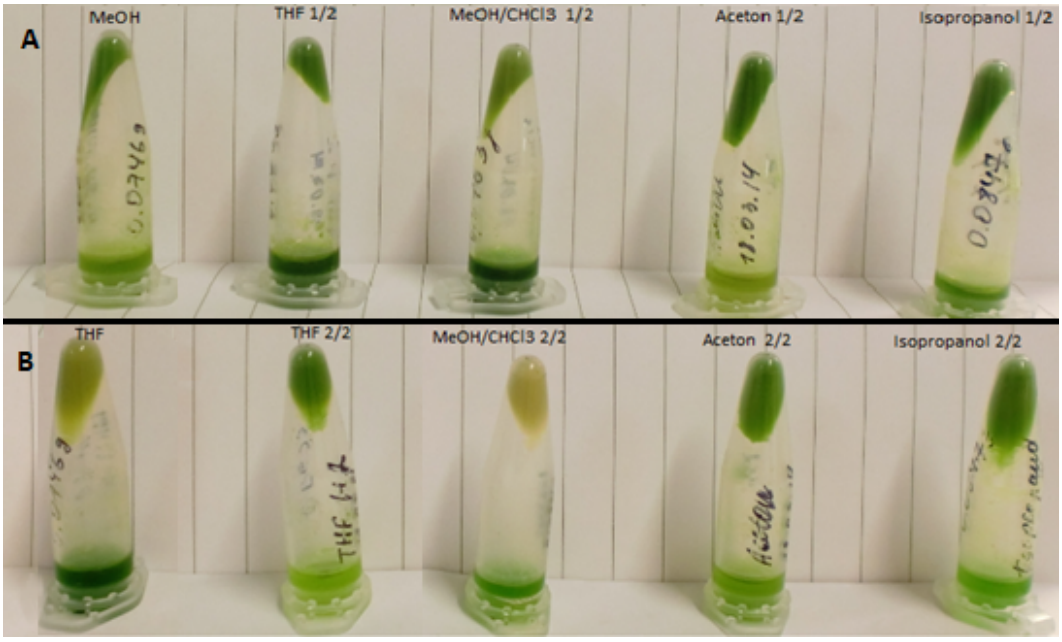


**Figure 2.4 - Prepared extracts and extracted pellets:** Five organic solvents were evaluated for their ability to extracts photosynthetic lipids. Four samples were extracted twice with the same solvent system, while one sample was extracted first with MeOH, and subsequently extracted with THF. 1/2 and 2/2 indicate the first and second extraction of a total of two extractions. **A: first extraction, from left to right:** MeOH, THF, MeOH/CHCl3 (70/30), Aceton, IPA. **B: second extraction, from left to right:** THF, THF, MeOH/CHCl3 (70/30), Aceton, IPA.

The green color of the extracts, predominated by the presence of chlorophyll *a*, was most intense in samples extracted with THF and MeOH/CHCl3. Already after the first extraction, it was noticeable that the green color of the extracts extracted with MeOH/$CHCl_3$ or THF was more intense than in the other samples. Cell pellets treated with MeOH/$CHCl_3$ had the palest color compared to the other samples, especially after the second extraction. Due to predominance of chlorophyll *a* in the extracts it was impossible to evaluate extraction efficiency for carotenoids by visual examination. Furthermore, other photosynthetic lipids such as quinones are not visible by the bare eye. Extraction yields for these photosynthetic lipids can only be assessed by spectroscopic methods.

When investigated by spectroscopy, the presence of carotenoids was observed as a shoulder having a peak in the 450 - 500 nm region (Figure 2.5). Due to overlap between the absorption spectra of carotenoids and chlorophyll in 400 - 500 nm region, the 665 nm peak was identified as chlorophyll. Quinones absorb in the UV-region of the electromagnetic spectrum and were observed as peaks in the 230 - 320 nm region.

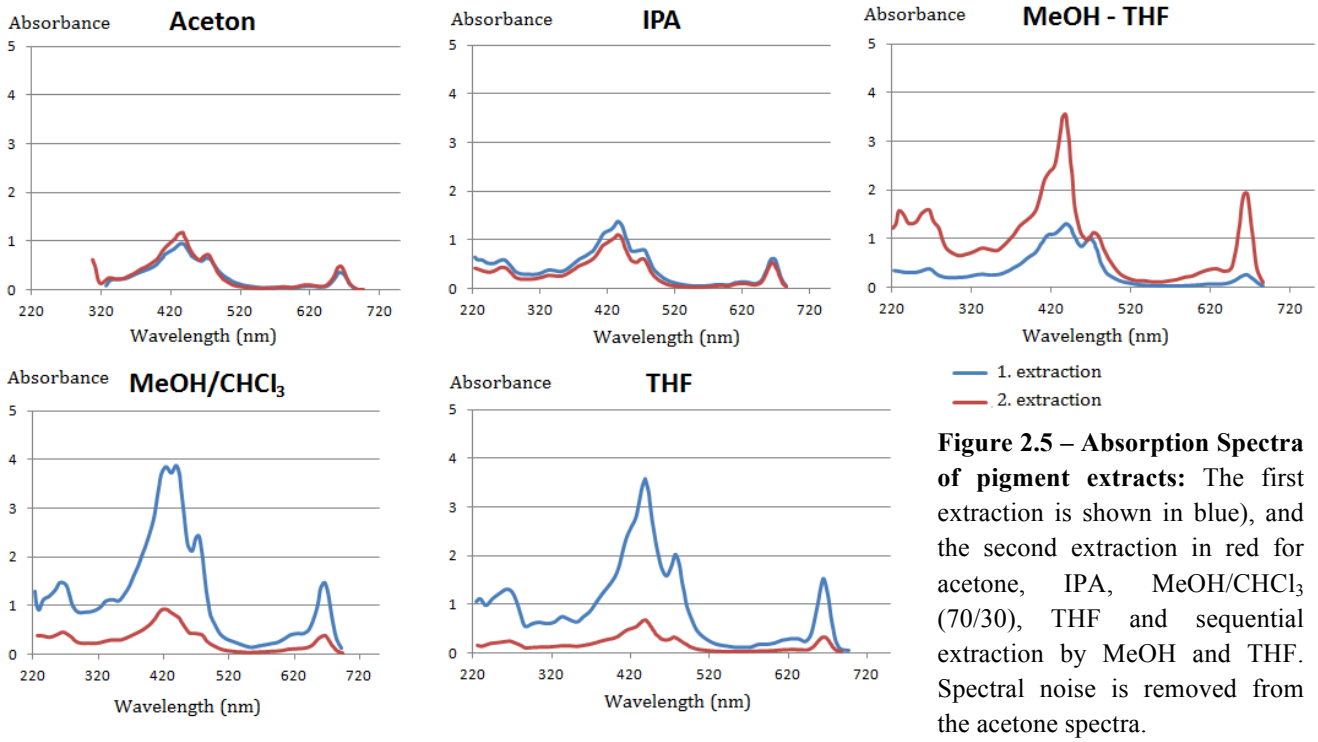


**Figure 2.5 – Absorption Spectra of pigment extracts:** The first extraction is shown in blue), and the second extraction in red for acetone, IPA, MeOH/$CHCl_3$ (70/30), THF and sequential extraction by MeOH and THF. Spectral noise is removed from the acetone spectra.

The highest absorbance after the first extraction was measured for MeOH/$CHCl_3$ and THF. Measurements of absorption properties have shown that the shape of the absorption peaks for the MeOH/$CHCl_3$ extract was smoother than for the THF extract, which appeared more "spike"-like (Figure 2.5). Sequential extraction with MeOH and THF also proved promising.

Despite good extraction yields, the extraction procedure with THF applied in both extractions, proved problematic. Due to differences in polarity between the sample and THF, it was difficult to resuspend the harvested cells in this particular organic solvent. However, the samples extracted with MeOH in the first extraction were easier to resuspend in THF than the samples extracted only with THF. The least efficient extraction was observed for acetone and IPA. This was confirmed by both visual inspection and spectroscopy. Parts of the absorbance spectra recorded for acetone extracts are missing due to high spectral noise between 220 and 300 nm, which have been removed in figure 2.5.

## Conclusion

MeOH/$CHCl_3$ and THF proved to be the most efficient organic solvent systems for extraction of photosynthetic lipids from *N. oceanica*. Sequential extraction with MeOH and THF also showed good results, but the difficulties of upgrading this method to a single extraction procedure excludes it from being a desirable option. Additional treatments need to be applied to improve the extraction with THF. The next step in the optimization of lipid extraction will be the estimation of an appropriate amount of extraction solvent needed for an efficient extraction of photosynthetic lipids from *N. oceanica*.

## 2.2 Solvent to sample ratio

The aim of this experiment was to determine an appropriate amount of organic solvent needed for an efficient extraction of photosynthetic lipids from *N. oceanica*. THF and MeOH/$CHCl_3$ were chosen as the best-suited solvent systems for extraction protocols based on the results from the previous experiment. In this experiment, six different solvent-to-sample ratios (the relationship between the sample mass and solvent volume), were evaluated to see if extraction efficiency could be further improved. The extraction conditions for all samples were identical. The only variation was the amount of applied organic solvents to a sample of fixed weight. The relative ratios of specific pigments were determined by absorbance measurements.

### Materials and methods

#### Growth conditions

All samples were prepared from a single *Nannochloropsis oceanica* culture, grown under the same conditions as described in section 2.1 (Materials and methods – growth conditions).

#### Extraction procedure and evaluation

Cultured cells were harvested by multiple centrifugations (8000 rpm, 15 min) in order to gradually increase cell concentration. Concentrated culture was then equally distributed in Eppendorf tubes (1.5 mL per tube), and cell pellets were prepared by using a microcentrifuge at 13000 rpm for 2 min. Prepared samples were washed with ammonium formate prior the extraction to remove excess salts (Zhu and Lee 1997, Chinnasamy, Bhatnagar et al. 2010) and also to overcome difficulties associated with differences in polarity between the extracted sample and THF. Sample masses were assessed to estimate the required quantities of organic extraction solvents. Six ratios; 1:2, 1:3.5, 1:5, 1:8, 1:12, and 1:15, were used to calculate required volumes of MeOH/$CHCl_3$ and THF. A total of 12 samples were extracted: 6 with MeOH/CHCl3 and 6 with THF in dual-extraction procedure for 20 min at -20 °C. Extracts from the sequential extraction procedure were kept and evaluated separately. The absorption properties of the obtained extracts was measured by a NanoDrop 2000® spectrophotometer (Thermo Scientific, USA) in the range between 220 and 750 nm.

## Results and discussion

Variable solvent-to-sample ratios were investigated, while keeping other extraction conditions identical. This investigation provided comparative results for estimation of the optimal solvent volume required for an efficient extraction of photosynthetic lipids. Extraction efficiency was evaluated by recording absorption spectra of chlorophyll *a*, carotenoids and quinones in prepared extracts. The collected absorbance data were analyzed, and is presented as a function of solvent-to-sample ratio separately for the first and the second extraction in Figure 2.6.

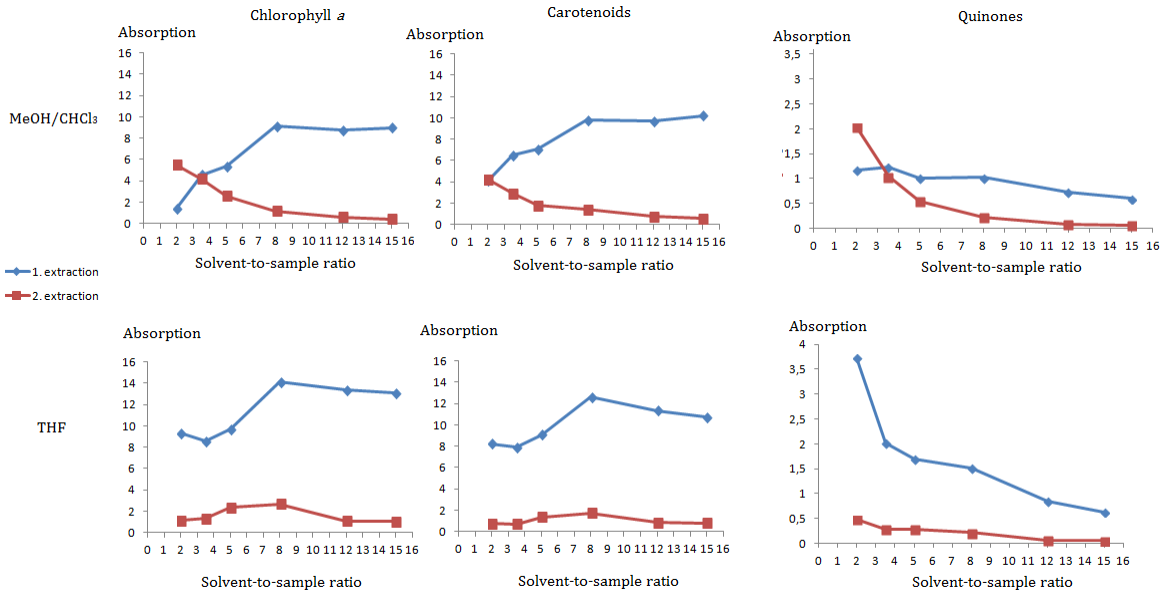


**Figure 2.6 – The effects of solvent to sample ratio on extraction yields:** Absorbance of chlorophyll *a* (664 - 667 nm), carotenoids (472 nm) and quinones (265 nm) in MeOH/$CHCl_3$ and THF as a function of solvent-to-sample ratio. The displayed values indicate the absorption values measured at the indicated wavelength. The first extraction is shown in blue and the second extraction in red. The absorption values have been corrected with the dilution factor.

As mentioned earlier in this chapter, the absorption properties of chlorophyll and other pigments can vary depending on their location in the photosynthetic apparatus and surrounding electrochemical environment, namely solvents pigments were extracted with (Basso, Simionato et al. 2014). Therefore, the observed absorption maxima of chlorophyll *a* vary from 664 to 667 nm.

Observations from preliminary experiments have shown that treatment with a polar solvent, and as a consequence, removal of excess salts facilitates easier resuspension in THF. All cell samples were therefore washed with ammonium formate to remove excess salts and increase solubility in THF. Extraction yields for THF in this experiment were shown to be higher than

extraction yields for MeOH/$CHCl_3$. However, that can also be explained by thin, long and "spike-like" peaks in the absorption spectra of THF-prepared extracts. It was observed that the majority of photosynthetic lipids were extracted using a factor 12 of solvent-to-sample ratio (e.g. 600 μL solvent for a 50 mg cell pellet). Figure 2.4 shows that by using a factor 12 of solvent-to-sample ratio, most of the lipids are isolated already after the first extraction, both for MeOH/$CHCl_3$ and THF. Due to the formation of explosive peroxides in THF, butylated hydroxytoluene (BHT) was added to prevent formation of peroxides and stabilize THF over time. The use of BHT-stabilized THF in the extraction of photosynthetic lipids has a major drawback, as both BHT and isoprenoid quinones absorb in the UV-region of the electromagnetic spectrum, and thus corrupting interpretation of the results. However, chloroform used in the MeOH/$CHCl_3$ mixture is stabilized with ethanol, which does not interrupt the absorption properties of quinones in the prepared extracts. Therefore the organic solvent system consisting of methanol and chloroform (70/30) seems to be more appropriate for the simultaneous extraction of photosynthetic lipids.

## Conclusion

The majority of photosynthetic lipids were isolated already after the first extraction by using a factor 12 of solvent-to-sample ratio, both for MeOH/$CHCl_3$ and THF. However, the presence of BHT in the THF-prepared extracts disrupts the absorption spectra in the absorbance region for isoprenoid quinones. Therefore, it was determined that THF is not the optimal solvent for a simultaneous extraction of all photosynthetic lipids from *N. oceanica*. A single extraction with MeOH/$CHCl_3$ with solvent-to-sample ratio of 12 is therefore considered to be an appropriate option for a simultaneous isolation of all photosynthetic lipids from *N. oceanica*. The additional treatment with ammonium formate prior to the extraction procedure was shown to facilitate extraction of some photosynthetic lipids and needs to be further investigated.

## 2.3 Effects of additional treatments prior to extraction

The extraction efficiency of organic solvents depends on their ability to disrupt cellular membranes, the hydration state and the resistance of the microalga cell wall (Henriques, Silva et al. 2007). The important aspect to be taken into account when working with *Nannochloropsis* is the low permeability and great resistance of the cell wall and plastid membranes of *Nannochloropsis* due to the four membranes acquired by the secondary endosymbiotic event mentioned in chapter 1. Therefore, additional disruption techniques may be helpful in order to increase extraction efficiency. In the experiment presented in this section, the effects of washing with ammonium formate and freeze-drying the sample prior to extraction have been evaluated, both as independent techniques and in combination with each other. Removal of excess salts by washing with ammonium formate prior to freeze-drying also has the advantage of making it easier to gain accurate information about the dry weight of samples. This improved information can in turn be used for quantification of photosynthetic lipid content per microalgae dry weight.

### Materials and methods

#### Growth conditions

All samples were prepared from a single *Nannochloropsis oceanica* culture, grown as described in section 2.1 (Materials and methods – growth conditions).

#### Extraction procedure

Cultured cells were harvested by multiple centrifugations (8000 rpm, 15 min) in order to gradually concentrate the cell culture. The concentrated culture was then equally distributed in Eppendorf tubes (1.5 mL in each tube) and cell pellets were prepared on a micro centrifuge at 13000 rpm for 2 min. The prepared cell pellets were weighed and divided in four groups, with three technical replicates for each group:

1. No wash, No freeze-drying (N.N.)
2. No wash, Freeze-drying (N.F.)
3. Wash, No freeze-drying (W.N.)
4. Wash, Freeze-drying (W.F.)

No additional treatment was applied to samples in group 1. Freeze drying and washing with ammonium formate was used as an independent technique in group 2 and 3 respectively, and in combination with each other in group 4. All samples in group 3 and 4 were washed with ammonium formate prior to proceeding further with freeze drying and extraction. Freeze-drying was performed by a Christ Alpha 1-4 LD freeze-dryer (Martin Christ Gefriertrocknungsanlagen GmbH, Germany) at -55 °C and 0.090 mbar.

After the above-described additional treatment, the prepared samples were extracted once with 12 volumes of MeOH/CHCl3 compared to the weight of the cell pellet (e.g. 600 µL solvent for 50 mg cell pellet) at -20 °C for 20 min. The prepared extracts were evaluated both visually and by spectroscopy using a NanoDrop 2000® spectrophotometer (Thermo Scientific, USA) in the range of 220 - 750nm.

## Results and discussion

In this experiment, additional treatment techniques prior to the extraction procedure were evaluated for their ability to increase extraction efficiency. Relative extraction yields of chlorophyll *a*, carotenoids and quinones were obtained by recording absorption spectra of the prepared extracts (Figure 2.7).

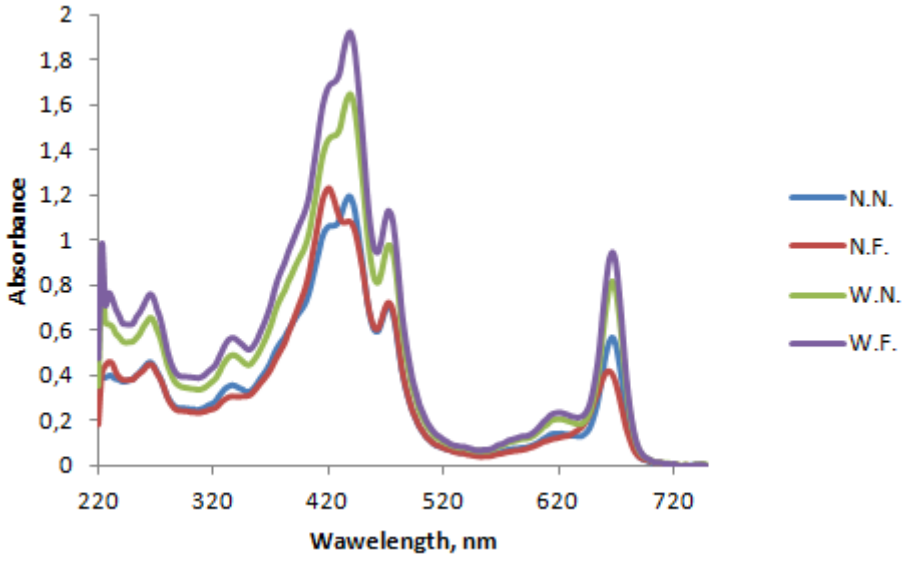


**Figure 2.7 – Comparison between the effects of additional treatments:** Effect of additional treatments prior to the extraction procedure on absorption spectra of photosynthetic lipids extracted from *N.oceanica* with MeOH/$CHCl_3$

Freeze drying alone did not prove to have any significant effect on the extraction quality, although the average absorbance of chlorophyll *a* at 664-667 was slightly lower compared with untreated samples. However, the absorbance of chlorophyll *a* increased with an average of 44% for samples treated with ammonium formate (W.N.) and 67% in combination with freeze drying (W.F.). A significant increase in absorbance was observed for carotenoids (peak at 472 nm) and quinones (peak at 265 nm) both for samples treated only with ammonium formate (W.N.) and in combination with freeze-drying (W.F).

Washing with ammonium formate prior to freeze-drying did, besides increasing the extraction efficiency, also provide the basis of a more accurate estimation of the dry-weight biomass. A correct estimation of dry-weight biomass is important for example for quantification of photosynthetic lipids in extracts and for evaluation of biomass productivity.

## Conclusion

Applications of additional treatments prior to extraction proved to increase extraction yields of photosynthetic lipids extracted from *Nannochloropsis oceanica*. Even though treatment with ammonium formate alone significantly improved the extraction quality, this technique in combination with freeze-drying proved to give the best results.

# Summary

Two solvent systems, THF and MeOH/$CHCl_3$, were shown to be the most efficient organic solvent systems for extraction of photosynthetic lipids from *N. oceanica*. The majority of photosynthetic lipids were successfully isolated by using 12 volumes of organic solvent compared to the weight of the un-dried sample. Even though THF shows a high extractability for photosynthetic lipids and in addition is considered a relative non-toxic solvent compared to the methanol / chloroform mixture, it was still rejected as a candidate for the best extraction solvent. THF is stabilized with BHT, which disrupts absorption spectra in the range where quinones have their main absorption. Because it would be difficult to assess the relative extracted yield of quinones when utilizing THF as a solvent, it was therefore not considered as a desirable solvent for the simultaneous extraction of all photosynthetic lipids from *Nannochloropsis oceanica*. Utilizing MeOH/$CHCl_3$ (70/30) is also much more economical than THF: one liter of MeOH/$CHCl_3$ costs approximately 430 NOK (Sigma Aldrich), while one liter of THF costs 884 NOK (Sigma Aldrich), and when considering extraction of high-value pigments on large scale, the price of the solvent is not without importance. In addition, MeOH/$CHCl_3$ has a lower boiling point compared to THF, which makes it easier to remove it from the extract. After considering extractability, toxicity, chemical properties and price, MeOH/$CHCl_3$ proved to be the candidate best matching the desired criteria for a good solvent, but its toxicity needs to be taken into account, and relevant HSE-procedures need to be followed while working with this solvent system in the lab.

# Chapter 3: Separation and Characterization

## Introduction

The production of photosynthetic lipids in microalgae can be divided into the following steps:

1. Culturing and harvesting
2. Extraction
3. Separation of extracted components
4. Characterization and quantification

The development of separation and characterization methods for photosynthetic lipids can be a quite challenging task. The high diversity of the lipids, their homogenous nature and similar polarity properties creates challenges associated with separation and characterization of the extracted lipids. Another important aspect to be taken into account is the unstable nature of extracted photosynthetic lipids (chlorophylls, carotenoids and quinones). Therefore, the development of efficient and rapid techniques combined with preservation methods is critical for improvement of the quality of separation and characterization.

In this chapter planar chromatography will be evaluated for its ability to separate photosynthetic lipids extracted from *Nannochloropsis oceanica*. Additionally, separation and characterization of pigment standards will be performed by convergence chromatography coupled with mass spectrometry to provide the base for the identification of pigments known to be synthesized in *Nannochloropsis* species.

### Chromatography

Chromatography is the collective term for a number of techniques used for separation of components in a mixture. The Russian botanist Mikhail Semenovich Tswett was one of the pioneers within the field of bio-analytical chemistry. Since his first description of adsorption techniques and chromatography in the early 20$^{th}$ century (Цвет 1903, Tswett 1906), a large number of chromatographic methods and applications have been developed. Separation by chromatographic techniques is now commonly used both for purification and pre-concentration of analytes on the analytical as well as on a preparative scale.

The principle of chromatographic methods is based on the differences between the affinities of components in a mixture to either the mobile or the stationary phase. Components in a mixture interact differently with this two phases depending on their polarity, resulting in different mobility rates allowing separation. There are three main types of chromatography: Liquid Chromatography (LC), Gas Chromatography (GC) and Convergence Chromatography (CC) or Supercritical Fluid Chromatography (SFC) (Braithwaite and Smith 1996).

### Thin Layer Chromatography

Thin layer chromatography (TLC) is a planar adsorption chromatography method used to separate analytes in a mixture. As several other chromatographic techniques, TLC is a separation technique based on the differences in attraction forces between the sample components, and stationary phase and mobile phase. Usually, TLC is performed on a plate made of glass or metal covered with a thin layer of solid adsorbent, usually silica or aluminum oxide (Braithwaite and Smith 1996) .

As is also the case for several other chromatographic techniques, the overall performance of TLC depends on the physical characteristics of the adsorbent, particularly its particle and pore size, and how the particles are distributed in the adsorbent layer. Regular TLC-plates has a 5 - 40 μm particle distribution capable of giving up to 2000 theoretical plates per 5 cm. Theoretical plates is an index used to determine the stationary phase efficiency of separating components in the mixture. High Performance Thin Layer Chromatography (HPTLC) differs from regular TLC in that its stationary phase consists of refined silica with a very tight distribution of particles size with an average size of 5 μm (Zlatkis and Kaiser 2011). HPTLC utilizes a thinner absorbent layer, which gives a smooth and more homogenous surface compared to the plates used in standard TLC. The small particle size and their narrow size distribution reduce the lateral spreading of moving components in a mixture and thus yields higher resolution.

## Convergence chromatography – Mass spectrometry

Mass spectrometry can be considered one of the most powerful tools of bio-analytical chemistry for characterization and quantification of biological molecules. This method can be coupled with other separation techniques such as liquid chromatography (LC), gas chromatography (GC) or convergence chromatography (CC) (Kishikawa and Kuroda 2014).

In combination with mass spectrometry, these techniques give an efficient separation and a high accuracy in the determination process.

### Ultra Performance Convergence Chromatography

As mentioned above there are three main forms of chromatography: GC, LC, and CC. A particular powerful version of CC is Ultra Performance Convergence Chromatography ($UPC^2$). While both GC, LC and $UPC^2$ utilize a stationary phase to interact with compounds of interest, and a mobile phase to move compounds with different polarity through the stationary phase to achieve separation, these techniques differ mainly by the mobile phases used. GC utilizes a gaseous mobile phase, LC uses a liquid phase and CC uses a compressed supercritical fluid (usually $CO_2$) having properties as an intermediate between liquid and gas.

A supercritical fluid is any substance at a temperature and pressure above its critical point, where distinct liquid and gas phases do not exist (Cabovska, Jones et al. 2012). $CO_2$ at its critical point has a polarity similar to n-heptane, but the solvent strength can be increased by increasing density or using a polar co-solvent, for example methanol. Usually, it is a good laboratory practice to dissolve the sample in the mobile phase into which the sample is being injected (Fairchild, Jason F et al. 2013). Therefore, the samples to be analyzed by CC are usually dissolved in heptane prior to application on the column.

### Ionization principle

In a mass spectrometer, the sample molecules are first ionized and then forced into a mass analyzer where they are separated according their mass-to-charge ratio (m/z). Soft ionization techniques such as electrospray ionization (ESI) and atmospheric pressure chemical ionization (APCI) do not cause molecular fragmentation. Instead, these ionization techniques creates molecular ions or quasi-ions such as cations [M+H]+, [M+Na]+, [M+K]+, [M+NH4]+; or anions ([M–H]-, [M–X]-)(Manz, Pamme et al. 2004).

### Time-of-flight and Quadrupole analysis

In time-of-flight (TOF) measurements, ions accelerated in an electric field enter a field free space, where they will move with different velocities according to their m/z ratios. Light ions are accelerated more than heavier ions and will thus reach the detector before the heavier ones. The quadrupole is essentially a mass analyzer which allows ions with only a certain m/z

ratio to pass through and reach the detector (Chernushevich, Loboda et al. 2001, Manz, Pamme et al. 2004)

## 3. 1 Separation of lipids by HPTLC

In order to separate photosynthetic lipids extracted from *Nannochloropsis oceanica* four mobile phase systems of hexane and acetone were tested for their ability to separate chlorophyll *a*, carotenoids and quinones by HPTLC. An overview of the photosynthetic lipids that are expected to be synthesized in *Nannochloropsis oceanica* is provided in Appendix I.

### Materials and methods

Four hexane/acetone ratios were evaluated for their ability to separate chlorophyll *a*, carotenoids and quinones. These were 40% hexane in acetone, 50% hexane in acetone, 40% acetone in hexane and 30% acetone in hexane, adapted from the work of Quach and colleagues (Quach, Steeper et al. 2004) Silica gel HPTLC plates with a concentration zone and a 254 nm fluorescent indicator were utilized for visual inspection of the different acetone/hexane mixture's ability of yielding the desired separation of the extracted pigments. W. F-extracts (50 µL/spot) obtained from the experiment performed to optimize lipid extraction (section 2.3) were applied by using a capillary tube with volume grading. Plates with applied spots were developed horizontally in the HPTLC-specified chamber (Figure 3.1).

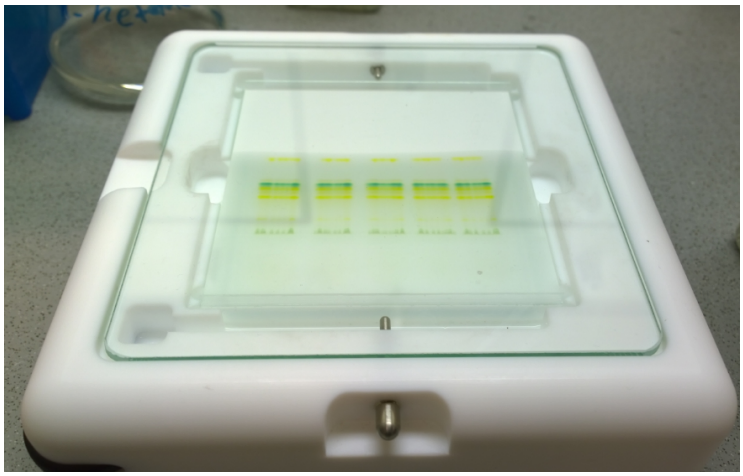

**Figure 3.1 - HPTLC-specified development chamber:** Separation of photosynthetic lipids on HPTLC plates

2 mL of mobile phase were used for each separation procedure. Bands were visualized under UV-light (254 nm). Retention factors ($R_f$ values) were calculated using equation 3.1.

$$R_f = \frac{\text{migration distance by solute}}{\text{migration distance by solvent}} \quad \text{[Equation 3.1]}$$

Separated bands were scraped off the HPTLC plate with the highest obtained resolution and separation. Collected samples were kept separately and dissolved in methanol to isolate the separated molecules from the adsorbent. Silica residues were removed by centrifugation (13000 prm, 1 min) and absorption spectra were recorded for each sample by using a NannoDrop2000 spectrophotometer (ThermoScientific, USA) for identification of separated components.

## Results and discussion

The mobile phase composed of 40% acetone in hexane provided the mobile phase best suited for separation of photosynthetic lipids by HPTLC. In this mobile phase mixture, all separated compounds were clearly visible as strong bands, except from the first yellow band which faded away quickly and lost its color within a few minutes. While the chlorophyll *a* and the carotenoid bands could be detected by the bare eye, the quinone band was visualized by utilizing a UV-visualizer at 254 nm. All bands had a high resolution and were well separated from each other (Figure 3.2). The separated compounds were identified by utilizing spectroscopy. Table 3.1 provides an overview of the photosynthetic lipids extracted from *Nannochloropsis oceanica* separated by HPTLC using hexane/acetone (60/40) as mobile phase. Absorption spectra for the separated components are given in Appendix II.

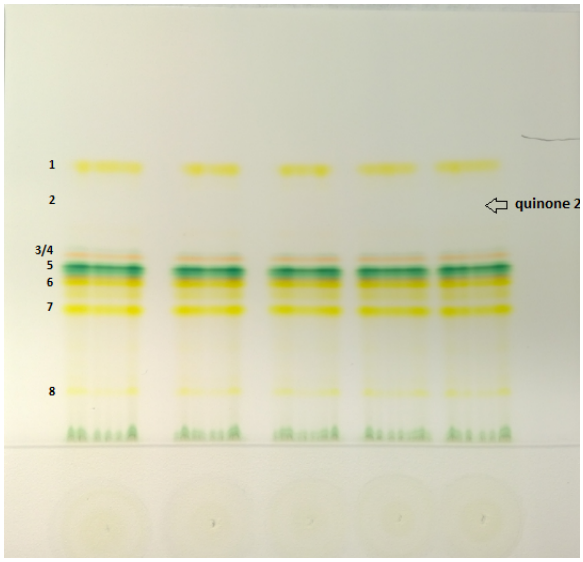


**Figure 3.2 - HPTLC plate with separated pigments:** Photosynthetic lipid extracts from *N. ocenica* separated on HPTLC plates using hexane/acetone (60/40) as mobile phase. The numbers represent separated pigments, and is further described in table 3.1. An arrow shows position of quinone band, which is only visible in UV-light

**Table 3.1 – Pigments separated by HPTLC using hexane/acetone as mobile phase:** Photosynthetic lipids extracts were separated on HPTLC plates using a mixture of hexane and acetone (60/40). Pigment absorption was determined by spectroscopy, and retention factors ($R_f$) were calculated according to equation 3.1. Absorption spectra for the separated photosynthetic lipids are given in Appendix II.

| Band | Color | Absorption peaks (nm) | Identification | $R_f$ |
|---|---|---|---|---|
| **1** | Yellow | 427, 450, 480 | β-carotene | 0.92 |
| **2** | NA | 249, 285 | Quinone2 | 0.87 |
| **3** | Red | — | Canthaxanthin | 0.63 |
| **4** | Grey | 410, 505, 535, 610, 667 | Pheophetyn *a* | 0,62 |
| **5** | Green | 340, 421,616, 667 | Chlorophyll *a* | 0,58 |
| **6** | Yellow | 424, 445, 472 | Antheraxanthin/ Vaucheriaxanthin esters | 0.54 |
| **7** | Yellow | 379, 400, 424, 442, 466 | Auroxanthin/Violaxanthin | 0.44 |
| **8** | Yellow | — | Vaucherixanthin | 0.19 |

In addition to β-carotene, spectroscopic measurements of the first band were absorbing in the 220 - 300 nm region of the spectrum. This indicates the presence of another quinone (quinone-1). Due to similarities in polarity properties between β-carotene and quinone-1, these two components would appear in a single band overlapping each other when using hexane/acetone (60/40) as mobile phase. By decreasing the polarity of the mobile phase, β-carotene and quinone-1 would appear as two separate bands, where the quinone would have the lower $R_f$ value. A second quinone (quinone-2) could also be detected under UV-light (254 nm), but the separation of other more polar components, such as chlorophyll *a* and xanthophylls was insufficient. Absorption spectra of the separated quinones are given in

Appendix II. Based on the absorption spectra and differences in polarity, quinone-1 was identified as phylloquinone while quinone 2 was identified as plastoquinone.

The separated components were identified based on empiric examinations of the band colors, their position on the HPTLC plate and their polarity. The positions of the separated components on the HPTLC plates in this experiment were also compared with earlier studies on separation of photosynthetic lipids utilizing chromatographic techniques such as TLC and HPLC. Based on the results of K. Mikami and M. Hosokawa (Mikami and Hosokawa 2013) and data sheets aiding identification of pigments by E.S. Egeland and colleagues (Roy, Llewellyn et al. 2011) the photosynthetic lipids of interest for this experiment were placed in order of increasing polarity (Table 3.2).

**Table 3.2 - Pigment polarity:** Placed in order of increasing polarity from less polar (1) to most polar (9)

| Non-polar | |
|---|---|
| β-carotene | 1 |
| Canthaxanthin | 2 |
| Pheophetyn *a* | 3 |
| Chlorophyll *a* | 4 |
| Vaucheriaxanthin esters | 5 |
| Zeaxanthin/Antheraxanthin | 6 |
| Astaxanthin | 7 |
| Violaxanthin | 8 |
| Vaucheriaxanthin | 9 |
| **Polar** | |

As already mentioned, the photosynthetic machinery of *Nannochloropsis* displays an unusual composition of carotenoid, with violaxanthin and vaucheriaxanthin as the major xanthophylls. Despite of this knowledge, absorbance spectra typical for violaxanthin were not observed in this experiment. However, the recorded absorbance spectra showed the presence of another xanthophyll structurally related to violaxanthin – namely auroxanthin. Auroxanthin shows absorption peaks at 379, 400, 425 nm when measured in ethanol, and it is an acid-catalyzed alteration product of violaxanthin. Structural rearrangement may occur in slightly acidic

extracts. In this experiment, the band representing auroxanthin had its typical absorption peaks at 379, 400 and 424 nm (measured in methanol) in addition to some minor peaks at 442 and 466 nm that are typical for violaxanthin. HPLC-chromatograms for auroxanthin and violaxanthin (Appendix I) show that these two xanthophylls have an almost identical retention time 13.33 min for auroxanthin and 12.5 min for violaxanthin. Due to their similar structure and polarity, violaxanthin and auroxanthin may overlap each other both in chromatographic methods and spectroscopic measurements. When separated by HPLTC, auroxanthin appears as a strong yellow-orange band, although according to data sheets aiding identification of photosynthetic lipids by E.S. Egeland and colleagues, auroxanthin turns green on silica TLC. The absence of green color in the band-7 may confirm a possible overlap of violaxanthin and auroxanthin, as violaxanthin appears as a yellow-orange band on TLC-plates (Mikami and Hosokawa 2013).

Vaucheriaxanthin is another major pigment found in all *Nannochloropsis* species. Its structure includes three hydroxyl groups, making this xanthophyll the most polar photosynthetic lipid isolated from *Nannochloropsis oceanica*. The polar nature of this xanthophyll results in its high affinity to the stationary phase used in HPTLC. Greatly retarded vaucheriaxanthin appears as the band with the lowest retention ratio (last band from top, Figure 3.2). Despite the fact that vaucheriaxanthin is one of the dominant pigments in eustigmatophytes, it appeared as a weaker band compared to other xanthophylls on the HPTLC-plate. The quantity of vaucheriaxanthin obtained by HPTLC was thus insufficient to obtain its absorption spectrum. Therefore, the identification of this particular photosynthetic lipid was based on its polarity, color and appearance on the HPTLC plate compared to other pigments.

The component of band number 6 was shown to have an absorption spectrum typical for antheraxanthin and vaucheriaxanthin esters. Antheraxanthin is a minor component of the photosynthetic lipid content in *Nannochloropsis* species. As a biosynthetic intermediate between zeaxanthin and violaxanthin in the xanthophyll cycle, this minor xanthophyll is usually detected in cells that have been exposed to a high irradiance level. The cells sampled for this experiment were grown under relatively low light conditions (100 μmol photons $m^{-2}s^{-1}$). Therefore, band number 6 is most likely to be identified as vaucheriaxanthin esters, which are described as one of the dominant pigments in eustigmantophytes (Roy, Llewellyn et al. 2011).

A weak band that is visible between band 6 and 7 (Figure 3.2) is assumed to be a minor xanthophyll isolated from *Nannochloropsis oceanica.* According to its polarity (Table 3.2) and position on the HPTLC-plate, it can be identified as either zeaxanthin, antheraxanthin or astaxanthin. Canthaxanthin is another minor xanthophyll found in *Nannochloropsis.* It is structurally related to β-carotene and echinenone. The introduction of keto groups in the biosynthetic pathway for synthesis of canthaxanthin makes it more polar than β-carotene. The canthaxanthin band will therefore have a lower retention ratio than β-carotene (band number 1 in figure 3.2) and can thus be seen as a thin red band (band number 3).

As expected, HPTLC proved to be the highly efficient and rapid method for separation of photosynthetic lipids. The unstable nature of the separated components, however, calls for modification of the utilized HPTLC-protocol. The application of lipid extracts onto the HPTLC plate needs to be performed in the dark, and ideally while blowing with nitrogen gas to reduce oxidation of the components in the extract as much as possible. Nitrogen gas can also be passed though the development chamber to remove air. The analysis should also, if possible, be carried out at a low temperature.

## Conclusion

HPTLC in combination with spectroscopic techniques has proven to be a suitable method for separation and characterization of photosynthetic lipids extracted from *Nannochloropsis oceanica*. The separation of extracted lipids by HPTLC was optimized, and all separated components were identified. A mobile phase composed of 40% acetone in hexane provided the best-suited mobile phase for separation of photosynthetic lipids by HPTLC. However, a reduction in polarity of the mobile phase may increase the solubility, and thus increase the separation of quinones from β-carotene.

Simplicity, short time required for analysis, reproducible results and small amounts of eluent required for development make HPTLC a desirable analytical method. Being highly efficient and sensitive, this method also provides a basis for the generation of lipid standards. However, further modification of the HPTLC-protocol is necessary in order to improve the yield and reduce the degree of degradation in the separated photosynthetic lipids.

## 3. 2 Characterization of photosynthetic lipids by UPC²- qTOF- MS

The current protocols for separation and identification of photosynthetic lipids by using LC-MS or GC-MS methods are challenging and laborious considering the high diversity of pigment classes present in the cell, their homogenous nature and minimal differences in polarity. Thus to date, no single analytical system exists for simultaneous analysis of all photosynthetic lipids.

The introduction of modern supercritical fluid chromatography methods such as $UPC^2$ offers significant advantages compared to earlier methods, such as fast equilibration, short analysis time, higher efficiency, reduced solvent usage, reduced costs of analysis, and compatibility with MS. In this experiment, $UPC^2$ coupled with qTOF-MS was utilized in order to characterize xanthophyll standards.

### Materials and methods

Standards of canthaxanthin (0.838 mg/L), astaxanthin (0.972 mg/L), violaxanthin (0.911 mg/L), antheraxanthin (0.512 mg/L), zeaxanthin (1.023 mg/L) (all from DHI, Denmark) and β-carotene (Sigma-Aldrich, USA) were used to assess the separation and identification of compounds from the biochemical classes of carotenes and xanthophylls.

A volume of 30 µL of each standard was evaporated at SpeedVac vacuum centrifuge concentrator (Thermo Scientific, USA) and re-dissolved in 30 µL of heptane prior to application on the column. The samples were analyzed separately in a system consisting of a Waters Acquity $UPC^2$ (Milford, USA) coupled to a Waters Synapt G2 qTOF-MS supplied with both an ESI and an APCI ionization source. Separation of the standards was performed by an Acquity $UPC^2$ HSS C18 SB column (1.8 µm, 100 mm) using a gradient of $CO_2$ (A) and methanol (B) (information provided in table 3.3). The temperature of the column was set to 45°C.

**Table 3.3 – Mobile phase gradient** Flow rate and $CO_2$ (A) - methanol (B) gradient in percent.

| **Time** (min) | **Flow rate** | **% A** | **% B** |
|---|---|---|---|
| **Initial** | 2.500 | 98.0 | 2.0 |
| **1** | 2.500 | 98.0 | 2.0 |
| **4** | 2.500 | 70.0 | 30.0 |
| **5** | 2.500 | 70.0 | 30.0 |
| **6** | 2.500 | 98.0 | 2.0 |
| **7** | 2.500 | 98.0 | 2.0 |

The injection volume was 2 μL, and the flow rate was 2.5. Data were collected with a scan time of 0.2 sec over a mass range of 50 - 2000 with a total run time set to 7 min. The source temperature was 120 °C and the probe temperature was 500 °C. The pressure was set to 1600 psi. Ionization of the sample components was performed by APCI in a positive mode. The accuracy of the collected mass data was insured by the LockSpray of leucine enkephalin at a flow rate of 10 μL/min. The corona voltage was set to 3 kV with cone gas flow and desolvation gas flow set to 100 and 1000 L/Hr, respectively. The collected data were analyzed in the MassLynx software (v. 4.1) and the Progenesis QI software (Waters, USA). The detailed description of the instrument parameters applied in this experiment is provided in Appendix III.

## Results and discussion

APCI proved to be the appropriate ionization method for characterization of photosynthetic lipids. Mass spectra recorded by utilizing APCI provided spectra with minimal background noise, and molecular ions of the type $[M+H]^+$ were detected for all of the xanthophyll standards. The response, however, was extremely low, due to the low concentration of standards. But even so, peaks could still be detected by searching for their exact mass. Table 3.4 provides retention times and mass-to-charge ratios in positive APCI mode for all the separated xanthophyll standards. Mass spectra and corresponding chromatograms are given in Appendix IV.

**Table 3.4:** Mass-to-charge ratios detected for standards at positive APCI mode and their corresponding retention times

| Standard | Retention time, min | m/z $[M+H]^+$ |
|---|---|---|
| **Canthaxanthin** | 2,97 | 565,43 |
| **Astaxanthin** | 2,93 | 597,42 |
| **Violaxanthin** | 3,18 | 601,46 |
| **Antheraxanthin** | 3,31 | 585,46 |
| **Zeaxanthin** | 3,43 | 569,46 |
| **β-carotene** | 2,45 | 537,46 |

The mass spectra of astaxanthin and antheraxanthin both had a base peak at 578,29 in addition to the expected molecular ions (597,42 and 585,46, respectively) (See Appendix IV). It is assumed that this signal was produced by the background noise, as it has been detected at several different retention times during the 7-min run time.

## Conclusion

The standards analyzed in this experiment represent a good basis for characterization of carotenoids in *Nannochloropsis oceanica*. However, the extraction protocol implemented in this work does not exclusively extract photosynthetic lipids. Therefore, the extract matrix of *Nannochloropsis* will also contain a large amount of other components, yielding a massive output of information in the recorded mass spectra. Hence, in order to efficiently interpret the collected data, the expected masses need to be calculated beforehand, in order to make searching for specific lipids in the Progenesis QI software and the mass spectrograms easier. This method will, however, only work when characterizing photosynthetic lipids known to be synthesized by *Nannochloropsis*. Further improvement of the protocol is needed to be able to screen also for unknown lipids.

# Chapter 4: Physiological Adaptations to High Irradiance in *Nannochloropsis oceanica.*

## Introduction

Algae are a very large and diverse group of photosynthetic organisms, and can be found almost anywhere; from soil and shallow pounds to hot springs and large oceans. A considerable number of algae are also adapted to life on land. However, most algae species are considered being predominantly aquatic organisms.

Oceans, covering more than 70% of the earth's surface, represent a highly variable aquatic environment where conditions could change both slowly and rapidly. Changes occurring on a longer time scale can result from seasonal changes, changing weather conditions or movement of seawater that gradually transports algae through the water column. The changes that occur on shorter time scales, such as rise and fall of the sea level during the tidal movement, expose algae to drastic changes in light conditions as well as in temperature and oxygen level. To cope with this highly variable environment, photosynthetic organisms have evolved a set of elegant mechanisms in order to optimize photosynthetic performance according to environmental changes. This way, variations in environmental conditions are reflected in the modification of photosynthetic machinery and its components.

### PSII and PSI: structure, function and organization

Oxygenic photosynthesis is a series of redox-coupled reactions where light energy is being converted into biochemical energy through the action of particular protein complexes imbedded into the thylakoid membrane. These large energy-transforming units, termed PSII and PSI, contain light-harvesting chlorophylls and carotenoids embedded into their internal antenna domain. In addition to these internal light-harvesting domains, PSII and PSI are also associated with external antenna complexes termed LHCII and LHCI (Figure 4.1). The main function of LHCs is to harvest light and transfer excitation energy to the reaction center core of PSII and PSI. The reaction center core of both photosystems contain a set of special chlorophyll *a* molecules, P680 in PSII and P700 in PSI. P680 is the primary donor of PSII which, in its excited state, initiates the extraction of electrons from water, thus activating the flow of electrons through the electron transport chain (Blankenship 2013).

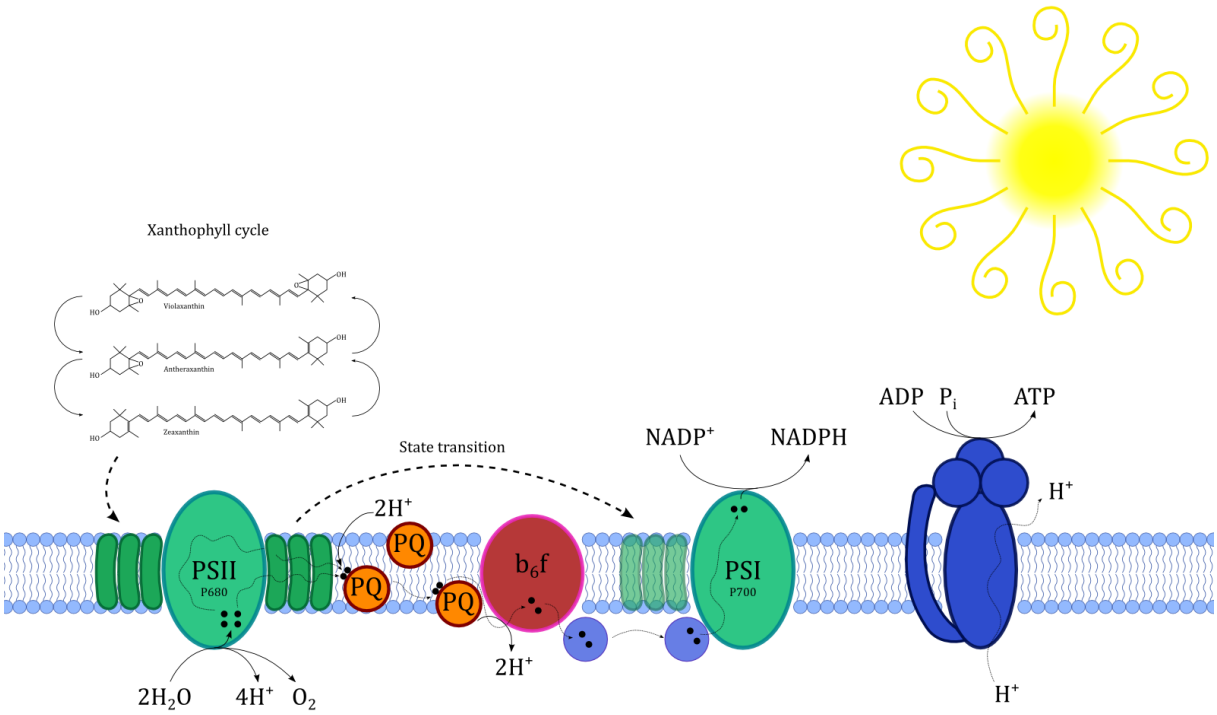


**Figure 4.1 – Overview of oxygenic photosynthesis:** The excitation energy received by the light harvesting complexes of PSII and PSI may be used to either drive photosynthesis, it may be dissipated as fluorescence, or it may be directed to PSI instead of PSII because a state transition has occurred. Dissipation of excess excitation energy through a heat emission, termed the xanthophyll cycle, is another protective mechanism involved in non-photochemical quenching. The figure was provided by Gunvor Røkke (NTNU, 2015).

The core complex of PSII is structurally similar in oxygen-producing photosynthetic organisms both of eukaryotic and prokaryotic origin. Two PSII form homodimer, and each monomer is composed of 17-20 subunits and contains about 36 chlorophyll *a* and 7 β-carotene molecules (Iwata and Barber 2004, Barsanti and Gualtieri 2014). PSI in cyanobacteria is trimeric, and each monomer consists of 12 subunits, whereas PSI in higher plants is a monomer composed of 15 subunits (Vanselow 2008). The core complex of cyanobacterial PSI includes 96 chlorophyll *a* and 22 β-carotene molecules (Fromme, Jordan et al. 2001, Germano, Yakushevska et al. 2002, Amunts, Drory et al. 2007), whereas PSI in higher plant binds approximately 200 cofactors(Ben-Shem, Frolow et al. 2003). Although the overall composition of the photosynthetic machinery is conserved in all photosynthetic organisms, it should be highlighted that heterokont algae, such as Nannochloropsis, appear to have a more cyanobacteria-like PSI.

## NPQ and State transitions

Although being a part of the same process, PSII and PSI are in most algal species spatially separated from each other. This has been especially well established in plants and green lage. PSII is often found in the stacked regions of thylakoids, while PSI mainly is located in stromal membranes (Haldrup, Jensen et al. 2001). Therefore, photosynthetic organisms employ a set of delicate mechanisms to optimize the interplay and photosynthetic performance of both photosystems. To balance the excitation energy between photosystems, many photosynthetic organisms have evolved a mechanism for re-distribution of excess light energy between the two photosystems. This mechanism is termed state transitions, and is useful in high-light conditions, as PSII is easily damaged by excessive photon-fluxes (Murata, Takahashi et al. 2007). A commonly accepted understanding of state transitions in plants and green algae is based on a reversible phosphorylation of LHCII by the action of a kinase imbedded into the thylakoid membrane (Rintamäki, Salonen et al. 1997, Carlberg, Rintamäki et al. 1999). When PSII is overexcited, phosphorylation of LHCII leads to the translocation of LHCII proteins from PSII to PSI (state 2). Under light conditions which preferentially excite PSI, the aforementioned process is reversed, and LHCII is being dephosphorylated. Dephosphorylated LHCII is then transferred back to PSII (state 1) (Minagawa 2011). Schematic presentation of state transition is given in Figure 4.1.

Light absorbed by the pigments associated with PSII, can either be utilized in order to drive photosynthetic reactions including water splitting (photochemical quenching) or may be dissipated in a form of fluorescence or heat (Weis and Berry 1987, Suggett, Prášil et al. 2011). Dissipation of excess excitation energy through a heat emission is another protective mechanism involved in non-photochemical quenching. A well-defined mechanism for energy dissipation is termed the xanthophyll cycle, and is based on thermal dissipation of excess energy and thus the prevention of singlet oxygen formation. Changes in LHCII are then characterized by formation of zeaxanthin via an enzymatic de-epoxidation of violaxanthin occurring in high light, through the antheraxanthin intermediate (Roy, Llewellyn et al. 2011).

## The photosynthetic apparatus of *Nannochloropsis*

*Nannochloropsis* is a genus of eukaryotic marine microalgae belonging to the heterokontophyta phylum. It is assumed to have originated from a secondary endosymbiotic event between a eukaryotic cell and a red alga (Figure 1.4) (Archibald and Keeling 2002, Basso, Simionato et al. 2014). This is indicated by the presence of four membranes enveloping the plastids with interconnections of these membranes to the endoplasmatic reticulum (ER) and the nuclear envelope. *Nannochloropsis* differs from other heterokonts by having the unique property of binding only chlorophyll *a* and lacking other accessory chlorophylls in their light-harvesting complexes. Their carotenoid content is also divergent from other heterokonts, and is dominated mainly by violaxanthin, vaucheriaxanthin and β-carotene (Brown 1987).

According to the findings made by S. Basso and colleagues, the organization of the photosynthetic apparatus in *Nannochloropsis* is similar to that observed in other photosynthetic organisms. PSI in *Nannochloropsis* is found as part of a stable PSI-LHC super complex. The number of antennae subunits associated with *Nannochloropsis* PSI is comparable to that found in *Chlamydomonas*, which is known to be nine (Drop, Webber-Birungi et al. 2011). The size of PSI-LHC in *Nannochloropsis* is therefore significantly larger than the one in plants. Different from PSI, PSII is easily dissociated from its antennae subunits. Such an unstable binding has been widely observed in other photosynthetic organisms, where it plays an important role in the adjustments of photosynthetic machinery through the action of state transitions.

*Nannochloropsis* species can be found in subtropical waters, where they are subjected to varying temperatures and high irradiances during the summer. To cope with this variable aquatic environment, these algae are able to adjust their photosynthetic machinery to optimize photosynthetic performance. In fact, zeaxanthin and antheraxanthin can be found in significant amounts in *Nannochloropsis* after exposure to high irradiance. This supports the existence of a functional xanthophyll cycle in this marine microalga (Gentile and Blanch 2001). Another important physiological adjustment to take into account is state transitions. Although state transitions have been widely observed in higher plants, eukaryotic algae and cyanobacteria, the presence of this process is still not confirmed for *Nannochloropsis*.

## Techniques used to investigate the photosynthetic machinery of *Nannochloropsis*

As already mentioned, *Nannochloropsis* species produce a large range of photosynthetic lipids, or pigments, including chlorophyll *a*, carotenes and xanthophylls. To optimize the photosynthetic performance, the relative content of these pigments can be adjusted in response to changes in external conditions (Falkowski 1980, Falkowski and Owens 1980, Gray, Ivanov et al. 1998, Walters 2005). This way; photosynthetic lipids provide the basis for evaluation of the overall state of the photosynthetic apparatus, which can be easily assessed by various spectroscopic techniques.

### 77 K spectroscopy

Light energy absorbed by the photosynthetic pigments associated with PSII may be either transferred to PSI to drive photochemical reactions by state transitions, or may be dissipated in the form of heat or fluorescence. At room temperature, PSI is a highly efficient light converter (Nelson 2009), and will therefore be able to utilize almost all the photons it receives to run photochemistry. PSII is not as efficient, and hence emits some of the photons it has captured as fluorescence. Almost all the fluorescence seen in room temperature is then emitted predominantly by chlorophyll *a* molecules associated with PSII. The high efficiency of PSI is primarily explained by the rapid energy transfer to its primary electron donor. However, at lower temperatures, the rate of electron transfer is changed, and at 77 K, the fluorescence emission of PSI is higher. Spectroscopy at 77 K is routinely applied for the investigation of the excitation energy transfer to PSI and PSII. Chlorophyll *a* excitation is then performed at 440nm, and the obtained emission spectra are used to analyze the ratios of chlorophyll associated with either PSI or PSII. Changes in the distribution between the photosystems are mainly due to changes of the association of LHCs caused by state transition.

### Pulse Amplitude Modulated Fluorometry

As already mentioned, the excitation energy received by the light harvesting complexes of PSII and PSI may be used to either drive photosynthesis, it may be dissipated as heat or fluorescence, or it may be directed to PSI instead of PSII because a state transition has occurred. The processes of photochemistry, fluorescence and NPQ are in a complementary relationship with each other, meaning that if the yield of one process increases, the yield of one of the other two, or both of them, will decrease, as long as the incident light intensity is unchanged. Changes in environmental conditions have the potential of affecting the balance

between these processes, resulting in altering of excitation energy transport and changes in fluorescence emissions. Changes in fluorescence will therefore provide a useful indicator of the overall photosynthetic state. Fluorometry by pulse amplitude modulation (PAM) allows us to obtain both qualitative and quantitative information about the kinetics of the light protection mechanisms of PSII (Maxwell and Johnson 2000).

PAM fluorometry is routinely applied in photobiology for assessment of photosynthetic energy conversion in plants, eukaryotic algae and cyanobacteria (Consalvey, Perkins et al. 2005). The principle of this spectroscopic method is based on signal modulation where series of light pulses are applied to induce fluorescence emission. Samples are then exposed to a low measuring light and saturated light pulses. Measuring light induces minimal fluorescence ($F_0$) to assess the ratio of PSII reaction centers in oxidized (open) state. $F_0$ can also be interpreted as the ground fluorescence of the PSII antennae, as the measuring light is too weak to induce significant photochemistry. In contrast, a saturated light pulse will reduce all reaction centers resulting in maximum fluorescence ($F_m$) (Schreiber 2004). The primary factor affecting fluorescence yield is the oxidation state of $Q_A$ which is modulated by the redox state of the plastoquinone PQ pool, although the proportion of LHCs associated with PSII in addition to reduction state of PSII reaction center and electrochemical potential across the thylakoid membrane have also been identified as modulatory factors (Butler 1972, Wollman and Delepelaire 1984, Genty, Briantais et al. 1989). Obtained quantum yield ($F_m/F_{0)}$ is therefore considered to be proportional to the oxidation state of the PQ pool. An increase in fluorescence therefore indicates that the PQ pool is highly reduced and thus unable to receive more electrons. The relative electron transport rate (ETR) then drops, and excitation energy, unable to be utilized in photosynthetic reactions, is dissipated as heat or as fluorescence. A reduced PQ pool also induces changes in the composition of carotenoids as part of the xanthophyll cycle.

## 4.1 Effects of high irradiance on the photosynthetic apparatus and pigment composition in *Nannochloropsis oceanica*

To understand the effects of irradiance on the photosynthetic apparatus of *Nannochloropsis oceanica* we conducted an experiment under short-term laboratory conditions. It was investigated how different light intensities affect the content and composition of photosynthetic lipids in *Nannochloropsis* grown under phototrophic conditions. The mechanisms of photoprotection against light stress, namely the xanthophyll cycle and state transitions have also been evaluated in this work. The overall state of the photosynthetic apparatus was assessed by means of PAM fluorometry and 77 K spectroscopy. Characterization of the composition of photosynthetic lipids was performed by utilizing $UPC^2$-qTOF-MS.

### Materials and methods

#### Experimental procedure

1500 mL of *Nannochloropsis oceanica* pre-culture was cultivated in 2 L square bottles containing f/2 medium. The cultures were bubbling with air during growth, and the growth temperature was 20 $^{o}$C. The light intensity used for growing the pre-cultures was 160 μmol photons/$m^2$s of constant light. For the main experiment, 180 mL of the pre-culture, having a cell concentration of $42.1 \cdot 10^6$ cells/mL (determined by BD Accuri C6 (BD Biosciences, USA) flow cytometer), were distributed in six 2 L square bottles. The main cultures were then diluted to 1 L with f/2 medium containing ampicillin (100 μg/mL) to achieve the cell concentration of $3 \cdot 10^6$ cells/mL. Three biological replicates were used for each light condition. The two light conditions used were high light (HL) at 1300 μmol photons/$m^2$s and low light (LL) at 5 μmol photons/$m^2$s. The experiment was continued for 72 hours. The incubation temperature during low light and high light exposure was maintained at approximately 23-24 $^{o}$C for both light conditions. The light intensity of irradiation, provided by halogen lamps, was determined by a QSL-100 photometer (Biospherical Instruments Inc., USA).

### Sampling procedure

Sampling was performed at five different time points; at the zero time point; t=0 and after 4, 24, 48 and 72 hours of incubation under low and high light intensities, respectively. For the pigment analysis, 50 mL of t=0 sample was taken from the start culture. Later, when *N. ocenica* samples were subjected to two different illumination intensities, 100 mL of cultures were taken at all sampling points, except for the HL samples for 48 and 72 hours, where 50 mL of cultures were harvested. The reason for this was increased cell growth in the high light samples compared to the low light samples, and hence less volume was needed to obtain sufficient amount of cells for the pigment analysis. Additionally, 1.5 mL of sample were taken for OD measurements, flow cytometry and PAM fluorometry. For spectroscopy at 77K, 10 mL of each culture were taken at all five time points.

### Extraction of photosynthetic lipids

The extraction procedure was performed according to the optimized extraction method described in section 2.3. Cell cultures collected for photosynthetic lipid analysis were gradually concentrated by multiple centrifugations (8000 rpm, 15 min). Concentrated samples were then transferred to Eppendorf tubes and cell pellets were prepared on a microcentrifuge at 13000 rpm for 2 min. The supernatant was discharged and the cell pellets were washed in ammonium formate prior the last centrifugation (13000 rpm, 2 min). Prepared cell pellets were then freeze-dried at Christ Alpha 1-4 LD freeze-dryer (Martin Christ Gefriertrocknungsanlagen GmbH, Germany) at -55 $^{o}$C and 0.090 mbar. Masses of the cell pellets were carefully assessed prior to the freeze-drying procedure. The volume of organic solvent required for extraction of the largest sample was calculated by using factor 12 of solvent-to-sample ratio. This amount of organic solvent was then applied to all samples to secure sufficient extraction and make the extraction procedure less time consuming. During the extraction procedure, samples were resuspended in 500 µL MeOH/$CHCl_3$ mixture (70/30, Normapur®, VWR). A single extraction was performed where samples were exposed to organic solvent for 20 min at -20 $^{o}$C. Suspensions were then centrifuged at 13000 rpm for 2 min and prepared extracts were stored in the freezer at -80$^{o}$C.

### Separation and characterization by UPC$^2$-qTOF-MS

A volume of 300 µL of each extract was evaporated at SpeedVac (Thermo Scientific, USA) vacuum centrifuge and redissolved in 300 µL of heptane prior to application to the chromatographic column. Samples were analyzed separately in a system consisting of an Acquity UPC$^2$ (Waters, USA) coupled to a Synapt G2 qTOF-MS (Waters, USA) supplied with both ESI and APCI source. Separation of pigments was achieved by Acquity UPC$^2$ HSS C18 SB column (1.8 µm, 100 mm) using a gradient of $CO_2$ (A) and methanol (B) provided in table 3.3. The temperature of the column was set to 45 $^oC$. Other parameters were set as described in section 3.2. In this experiment no other standards other than β-carotene (Sigma-Aldrich, USA), α-tocopherol (provided by Professor Kalbe Razi Naqvi, NTNU) and ubiquinone-10 (provided by Professor Julian Eaton-Rye, University of Otago) were available. However, the results of the separation and characterization of carotenoid standards in chapter 3 were used to assess the characterization of photosynthetic lipids in *Nannochloropsis oceanica*. Collected data were analyzed with the Progenesis QI software (Waters, USA).

### PAM Fluorescence

Chlorophyll fluorescence measurements were recorded with a multicolor PAM fluorometer (Heinz Walz GmbH, Germany). Pulse modulated fluorescence was induced by blue measuring light (440nm) of low intensity (relative intensity 1). Maximum fluorescence values was obtained by applying a light pulse (440 nm) of higher light intensity (relative intensity in settings: 20) every 40 seconds. In addition, light induction curves were recorded by applying light pulses (440nm) with background light gradually increasing every 30 seconds from 0 to 2709 µmol photons/m$^2$s. Light induction curves were recorded for HL and LL samples from one biological replicate for the time points 24, 48 and 72 hours. PAM fluorometry was taken for all replicas at all sampling times.

### 77 K Fluorescence

77 K spectroscopy was performed by a custom made setup and a Jaz-fluorometer (Ocean Optics). For 77 K spectroscopy analysis, thawed cultures were transferred into glass capillaries and frozen again prior the fluorometry. Prepared samples were then transferred into a dewar filled with liquid nitrogen. A custom made 3D printed holder holding the excitation light and a fluorescence sensor in a 90-degree angle were fastened on the dewar, and the

fluorescence sensor was coupled to the fluorometer. The samples were exited by a blue light emitting diode (LED), emitting at 435 nm. Fluorescence emission was recorded in a scan from 600 to 850 nm by the SpectraSuite software (Ocean Optics).

## Results and discussion

### Photosystems and Light-Harvesting Complexes

77 K fluorometry spectra were obtained by exciting at 435 nm for the three biological replicates of both high light-incubated and low light-incubated samples for all time points. The recorded data were normalized to maximum fluorescence emission for each spectrum. Due to little difference observed between the three biological replicates one typical recording is shown for each light condition (Figure 4.2 A and B). Additional recordings are given in Appendix V. Two sets of 77 K spectra were recorded, the latter with improved settings of the measurement software in order to obtain more informative data. In the case of the latter data collection round, the samples had however been thawed twice, because an initial round of data recording had already taken place. All samples were treated equally, and multiple freezing and thawing should therefore have had the same impact on obtained fluorometry results in all samples. A clear trend could be observed when comparing fluorometry data of HL and LL samples (Figure 4.2).

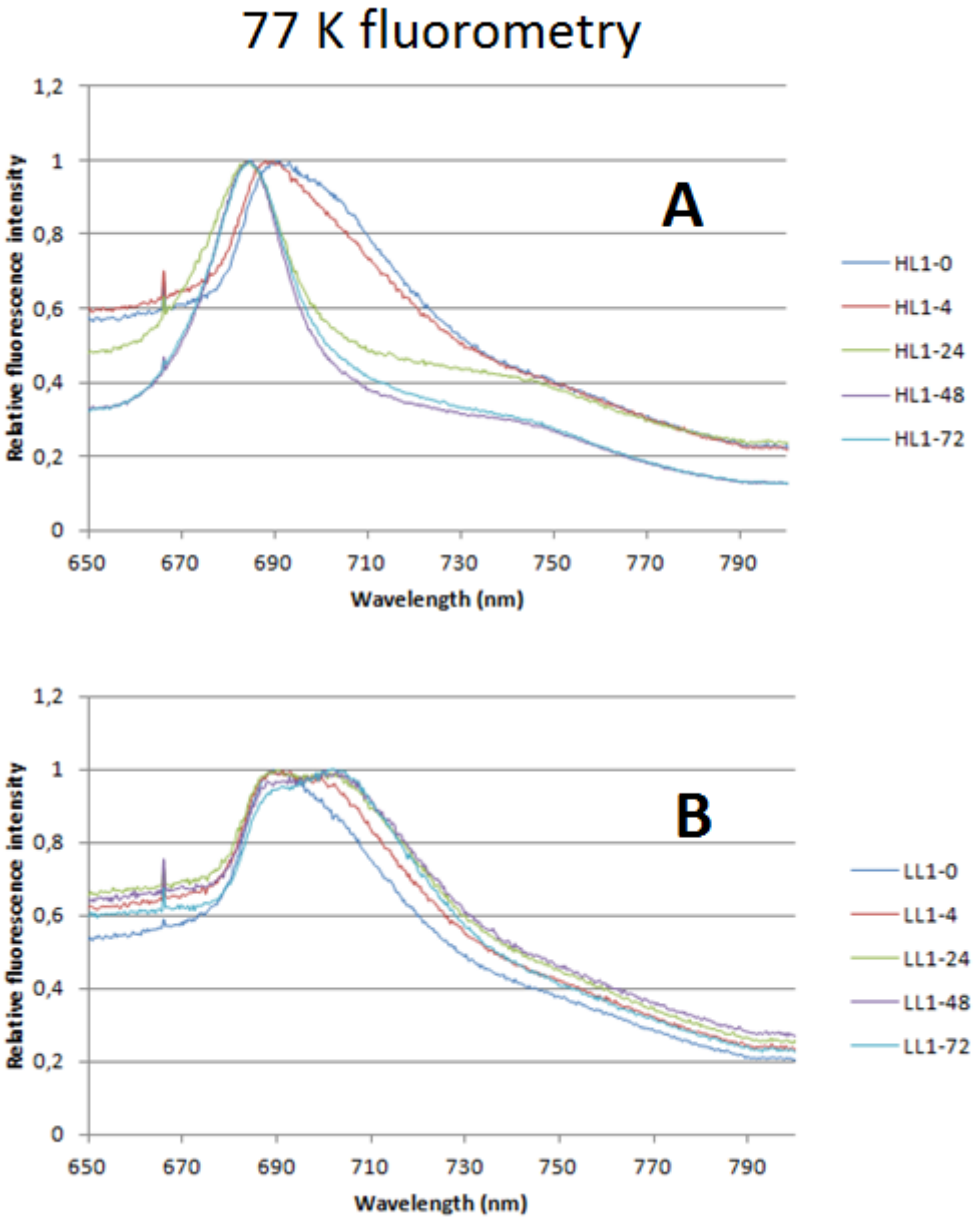


**Figure 4.2 – Normalized 77 K fluorescence emission spectra of *Nannochloropsis oceanica:*** Comparison of fluorescence spectra recorded over time (0-72h). A: under high light (HL) and B: under low light (LL) conditions.

Fluorescence emission spectra obtained from high light samples did not show the typical 685 and 695 nm peaks that can be linked to the core antenna proteins of PSII, CP43 and CP47 (Figure 4.2 A). In this data, the recorded fluorescence emitted by PSII can be seen as a 690 nm peak during the first four hours. This peak then disappears after 24 hours, and the wavelength of its maximum fluorescence shifts to 683 nm. According to the results of S. Basso and colleagues on characterization of the photosynthetic apparatus of *Nannochloropsis gaditana*, the narrow emission peak at 683 nm indicates predominance of LHCII in the

fluorescence emission spectra. The loss of the 690 nm peak and the absorbance shift towards lower wavelengths suggests a dissociation of LHCII from PSII, which would also be the case in a state transition. After 24 hours the fluorescence assumed to be emitted by PSII is mostly lost. These findings suggest that PSII in *Nannochloropsis oceanica* is easily dissociated from its external antenna moiety. This unstable association between antenna complexes and PSII is known to be involved in several adaptation mechanisms in other photosynthetic organisms. In the energy distributing process termed state transitions; the LHCs are easily dissociated from PSII by the action of a protein kinase and transferred to PSI. In this manner, the number of antenna subunits associated with PSII is changed over time as an effect of changing light conditions (Ballottari, Dall'Osto et al. 2007). In addition to state transitions, photosynthetic organisms can also regulate the relative amounts of PSII and PSI situated in the thylakoid membranes in order to optimize photosynthetic performance in response to changing environmental conditions (Escoubas, Lomas et al. 1995, Durnford and Falkowski 1997, Pfannschmidt, Nilsson et al. 1999). The peak shoulder at 700 nm observed at t=0 h and t=4 h is linked to the P700 reaction center chlorophylls of PSI. Fluorescence emitted by P700 becomes drastically reduced after 24 hours of incubation in high light, which could indicate a decrease in LHCs associated with PSI or a decrease in the relative amount of PSI.

77K fluorescence emission recordings of the samples incubated in low light shows the opposite behavior (Figure 4.2 B). The second peak situated at 700 - 703 nm, which is linked to the PSI reaction center chlorophylls (Iwaki, Mimuro et al. 1992) is emerging after four hours in addition to the 690 nm peak for PSII. The narrow 683nm peak linked to LHCII is not visible in this recording. Fluorescence emitted by PSII at 690 nm is slightly decreasing, while fluorescence emitted at 700-703 nm is slightly increasing over time. As mentioned earlier, photosynthetic organisms are able to regulate the relative amount of both photosystems in the thylakoid membranes. Increase in relative fluorescence intensity at 700 nm indicates the increase in LHCs associated with PSI or number of PSI. The maximum fluorescence also shifts toward higher wavelengths in low light conditions, compared with the shift towards lower wavelengths that was observed under high light conditions. The peak linked to PSI (720-730 nm) is not visible in 77 K fluorescence emission recordings for the low light samples, but may be overlapped and predominated by the broad shoulder of 700-703 nm peaks. The width of the 700 nm peak, which slightly shifts to 703 nm after 24 hours, suggests that under low light conditions, several other light-harvesting complexes associate with PSI to optimize photosynthetic performance. According to findings made by S. Basso and

colleagues, the size of the *Nannochloropsis* PSI-LHC supercomplex were shown to be comparable to that in *Chlamydomonas*, where the largest supercomplexes are composed of nine subunits (Drop, Webber-Birungi et al. 2011). As *N.* oceanica possesses several isoforms of LHCs the shift in fluorescence from 700-703 nm could indicate that a new set of LHCs is utilized in low light conditions.

When summing up the observations, it can be assumed that the shift towards a lower wavelength over time in high light is a result of dissociation between the PSII and LHCII, which could be due to a state transition. In the case of a state transition we would expect to see a shift towards higher wavelengths over time, because the pigments leaving PSII would instead be bound to PSI. However, because the samples were thawed two times, it is possible that the light harvesting complexes, which dissociated from PSII by the action of the kinase responsible for initiating state transitions, exist as free LHCIIs instead of being loosely bound to PSI. This possibly indicates that the binding between LHCII and PSI is weaker than the binding between the LHCII and PSII. This explains the absence of 683 nm peak (free LHCIIs) in the fluorescence spectra obtained from low light samples, where most of the LHCIIs are expected to be bound to PSII. As free LHCII has a peak at a lower wavelength than LHCII bound to PSII or PSI (Basso, Simionato et al. 2014), it is still possible that the shift towards a lower wavelength indicate a state transition.

The results obtained by PAM fluorometry also show how *Nannochloropsis* adapts to changes in light conditions. In photosynthetic organisms, absorbed light energy can be utilized either to drive photosynthetic reactions, or it can be dissipated in form of NPQ or fluorescence. The amount of light utilized for one of these three processes is in an inverse relationship with the light utilized for the two other processes, meaning that changes in one process leads to adjustments in the other two. In other words, if the rate of one process decreases, the rates of two other will increase, and vice versa.

In this experiment, the PAM fluorometry data of low light samples subjected to saturating light pulses shows an increase in $F_m/F_0$ over time, while $F_m/F_0$ measured for high light samples decrease over time (Figure 4.3).

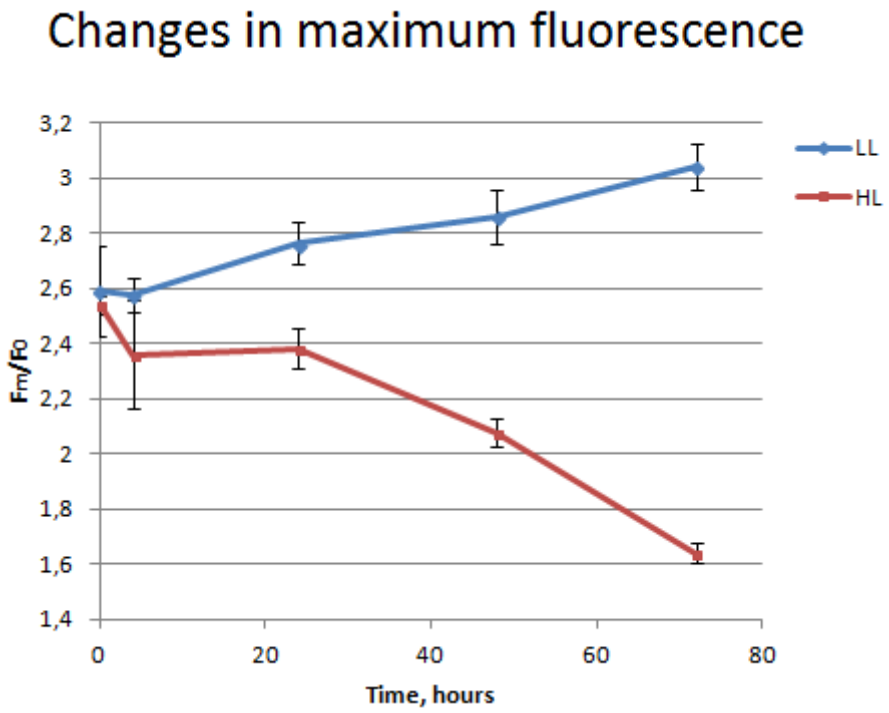


**Figure 4.3 - PAM data recorded for *N. oceanica*:** Relationship between $F_m$ and $F_0$ for high light (HL) and low light (LL) samples over time.

These results indicate that cells treated with high light are more influenced by NPQ than samples treated with low light. This could again indicate that the high light samples are adapted to high irradiances and need to optimize their photosynthetic machinery to a greater extent in response compared with LL-cells. The same observation is made when studying light induction curves. The light induction curves for HL and LL samples harvested at 24 h are shown in Figure 4.4. All other induction curves are shown in Appendix VI.

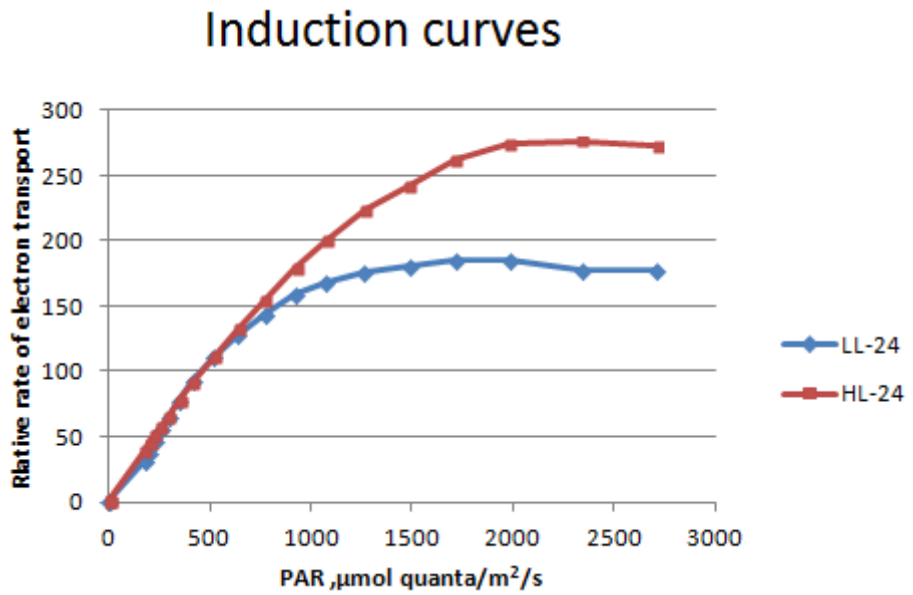


**Figure 4.4** - **The induction curves**: Relative rate of electron transport after 24 hours in low light (LL) and high light (HL) samples as a function of increasing background illumination.

The relative rate of electron transport is dependent on the availability of oxidized PQ pool. Figure 4.4 shows that the relative electron transport rate in HL treated samples is higher at high light intensities compared with LL treated samples. In other words, the PQ pool in cells adapted to high light remains oxidized at high light intensities, were the PQ pool in cells adapted to low irradiation is reduced. It is known that photosynthetic organisms adjust their photosynthetic lipid composition in response to changes in irradiance intensity (Falkowski 1980, Falkowski and Owens 1980, Walters 2005). Results obtained by PAM fluorometry may therefore indicate that the relative amount of PQs is higher in cells grown under high irradiance compared to cells grown in a light depleted environment. This has also been confirmed by results obtained from UPC$^2$-qTOF-MS described later in this chapter. The decrease in maximum fluorescence for HL-samples (Figure 4.3) also indicates that the excess of energy that cells subjected to high light experience is being dissipated through the actions of NPQ. NPQ-linked energy dissipation is reflected in adjustments of the xanthophyll cycle, in addition to the action of state transitions. Adjustments in the xanthophyll cycle is characterized by formation of zeaxanthin via an enzymatic de-epoxidation of violaxanthin occurring in high light, via the antheraxanthin intermediate (Roy, Llewellyn et al. 2011). The effect of high light treatment and low light treatment on carotenoids that are part of the xanthophyll cycle can be assessed by analytical techniques.

### Characterization of Photosynthetic Lipid Composition

Data obtained from UPC$^2$-qTOF-MS were analyzed in Progenesis QI software, and average abundance of photosynthetic lipids was presented as a function of light-exposure time. The detailed overview of plotted data and corresponding standard errors are given in Appendix VII. The retention times and m/z ratios in positive APCI mode for all detected lipids are given in table 4.1.

**Table 4.1 – Photosynthetic lipids detected by UPC$^2$-qTOF-MS:** Compounds identified in extracts from Nannochloropsis oceanica at APCI in positive mode.

| Lipid | Retention time, min | m/z |
|---|---|---|
| **Zeaxanthin** | 3,41 | 569,43 |
| **Antheraxanthin** | 3,36 | 585,43 |
| **Violaxanthin** | 3,14 | 601,42 |
| **Canthaxanthin** | 3,14 | 565,42 |
| **Astaxanthin** | 2,91 | 597,40 |
| **β-carotene** | 3,08 | 537,45 |
| **Plastoquinone (ox.)** | 2,51 | 749,62 |
| **Plastoquinone (red)** | 1,73 | 749,66 |
| **Chlorophyll *a*** | 3,16 | 891,53 |

All photosynthetic lipid data presented in this chapter is an average of lipid abundance observed in the three biological replicates. Interpretation of obtained mass spectrometric data on Progenesis QI has demonstrated variation between the biological replicates. Observed variation in photosynthetic lipid abundance between replicates could result from small

unintentional variation during sample preparation, unequal quantities of light that cultures have been exposed to and degradation of extracted lipids during storage. However, despite high standard error values observed between some samples, the overall evolution of photosynthetic lipid content observed in HL and LL confirms that the photosynthetic apparatus of *N. oceanica* is able to adapt to changes in light conditions.

Characterization of the photosynthetic lipid content in *N. oceanica* has shown the presence of another photoprotective mechanism, namely the xanthophyll cycle. Results obtained by UPC$^2$-qTOF-MS showed that the zeaxanthin and antheraxanthin content increases over time while the violaxanthin content decreases in high light conditions (Figure 4.5). Accordingly, the relative content of zeaxanthin and antheraxanthin decreased while violaxanthin increased in low light conditions.

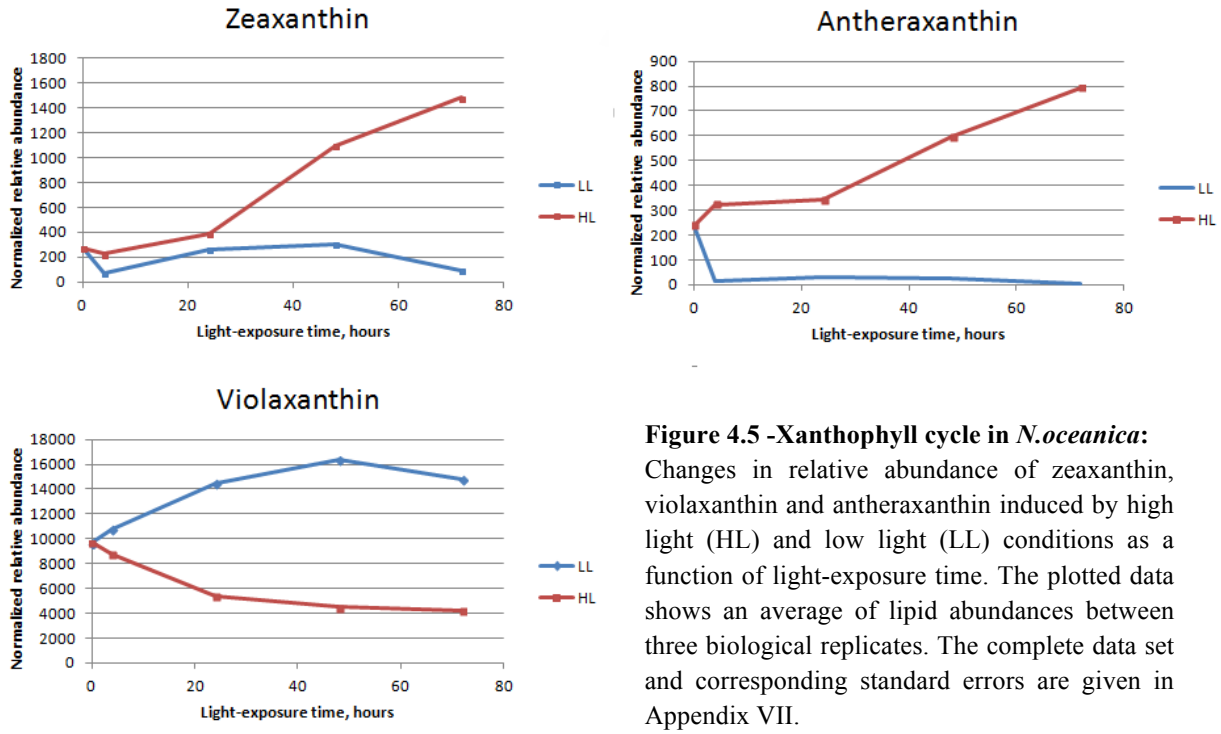


**Figure 4.5 -Xanthophyll cycle in *N.oceanica*:** Changes in relative abundance of zeaxanthin, violaxanthin and antheraxanthin induced by high light (HL) and low light (LL) conditions as a function of light-exposure time. The plotted data shows an average of lipid abundances between three biological replicates. The complete data set and corresponding standard errors are given in Appendix VII.

The carotenoid content of *Nannochloropsis species* is known to be predominated by violaxanthin. Indeed, characterization of xanthophyll cycle-linked pigments in *N. oceanica* has shown that the content of violaxanthin greatly exceeds the quantity of other xanthophylls.

Besides their photoprotective mechanisms, xanthophylls also have a well-established function as light-harvesting pigments. Obtained results in this experiment have shown that the relative abundance of violaxanthin was much higher in cells grown in low light conditions than in cells obtained from cultures exposed to high irradiance. Violaxanthin has more efficient light-

harvesting capabilities than zeaxanthin (Havaux and Niyogi 1999). Therefore, the observed increase in violaxanthin content indicates a modification of the photosynthetic machinery towards more effective utilization of available light and optimization of photosynthetic performance in low light conditions.

Other xanthophylls, than zeaxanthin, are suggested to be involved in photoprotective mechanisms. According to the work of Lubian and Establier on variation in pigment composition in *Nannochloropsis gaditana*, canthaxanthin accumulation increased to 4-fold the initial amount when exposed to high irradiance. In addition, it proved to increase even more in nitrate deficient cultures exposed when exposed to the same irradiance. These observations however have not been confirmed by results obtained in order to characterize the photosynthetic lipid content in *N. oceanica*. Figure 4.6 shows changes in the carotenoid content in cultures during light-exposure time.

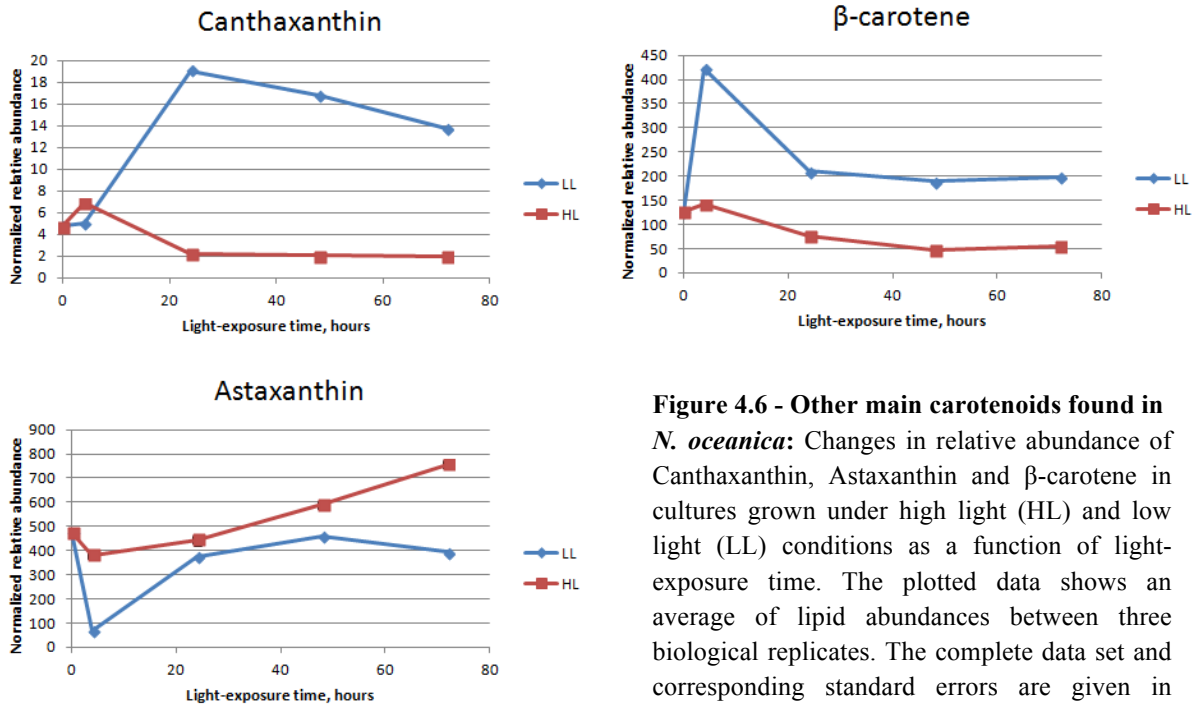


**Figure 4.6 - Other main carotenoids found in *N. oceanica*:** Changes in relative abundance of Canthaxanthin, Astaxanthin and β-carotene in cultures grown under high light (HL) and low light (LL) conditions as a function of light-exposure time. The plotted data shows an average of lipid abundances between three biological replicates. The complete data set and corresponding standard errors are given in Appendix VII.

As shown in Figure 4.6, the canthaxanthin content was much higher in the LL cultures and also greatly increased after 24 hours, before slightly decreasing again during the next 48 hours. The relative abundance of astaxanthin is observed to be increasing in all cultures after 4 hours of light-exposure. However, after 48 hours the relative content of astaxanthin is found to be slightly decreasing in LL-samples, while still increasing in samples obtained from cultures exposed to high irradiance. The relative abundance of β-carotene in LL-cultures drastically increased during the first 4 hours. This increase was then followed by a decrease to

a level that was relatively constant during the next 48 hours. The LL cells contained 4 times as much β-carotene as cells grown in low light conditions. These findings suggest that β-carotene and canthaxanthin participate in adjustments of the photosynthetic apparatus of *N.ocenica* to low light conditions, and thus function as light-harvesting pigments.

Besides carotenoids, quinones are also known to participate in the modification of photosynthetic performance in response to changes in light conditions (Gray, Ivanov et al. 1998). As mentioned above, the results obtained by PAM fluorometry indicate that the relative amount of plastoquinone may be higher in cells grown under high irradiance compared with cells grown in the low light environment. This has been confirmed by results obtained by UPC$^2$-qTOF-MS. Figure 4.7 shows changes in the relative amount of oxidized and reduced plastoquinone in *N. oceanica* cultures incubated at high light and low light.

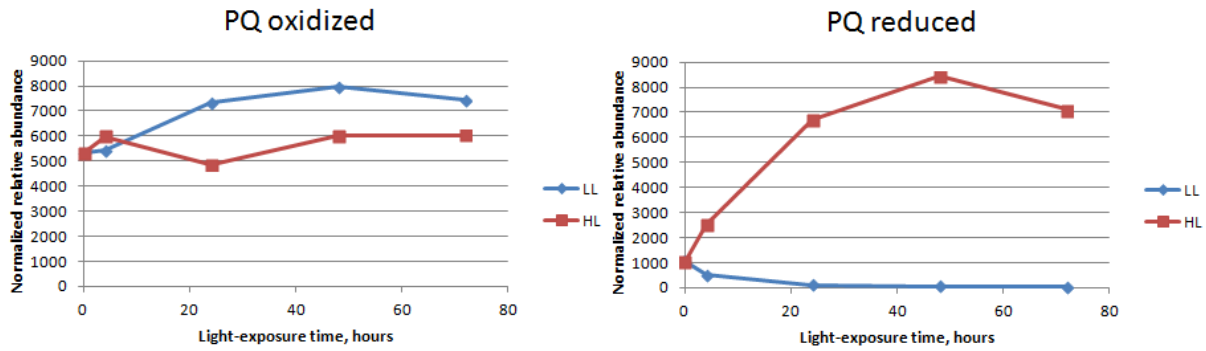


**Figure 4.6 – Relative abundance of plastoquinone in N. oceanica:** Changes in relative content of oxidized and reduced plastoquinone in cultures incubated at high light (HL) and low light (LL) irradiances. The plotted data shows an average of lipid abundances between three biological replicates. The complete data set and corresponding standard errors are given in Appendix VII.

The relative abundance of oxidized PQ was higher in cultures incubated under low light conditions. Accordingly, the relative abundance of reduced PQ was higher in samples obtained from cultures incubated at high irradiance. This is expected because PQs are reduced at higher rate under high light compared with low light conditions. As observed in PAM fluorometry, the high rate of electron transport in cells adapted to high light may indicate that the relative amount of PQs is higher and they are oxidized faster than PQs in cells grown under a low light environment. Indeed, when adding the relative abundance of oxidized PQ and reduced PQ, the total PQ content is found to be higher in cultures exposed to high light (Figure 4.8).

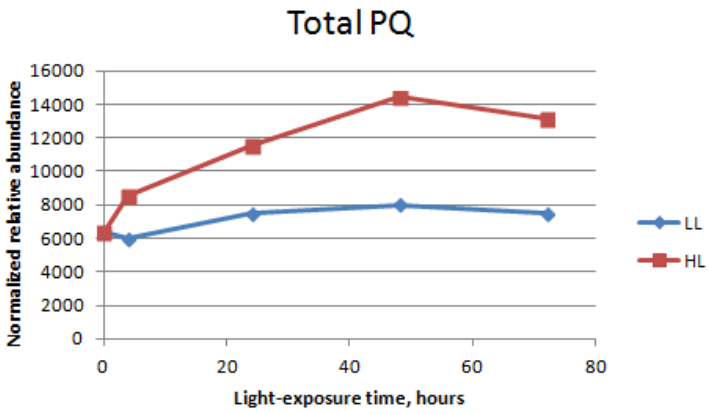


**Figure 4.8 – Total plastoquinone content:** Changes in plastoquinone abundance in cultures over exposure time to high light (HL) and low light (LL).

Analysis of obtained mass spectrometric data on Progenesis QI have shown that ionization of reduced plastoquinone by APCI have produced a molecular ion of lower mass (749,66) than expected. Upon being reduced, plastoquinone accepts two protons, and the expected m/z would then be 450-451 for $[M]^+$ and $[M+H]^+$ adducts. Both molecular ions, identified as oxidized (749,62) and reduced (749,66) PQ, were shown to be structurally related to plastoquinone in Progenesis QI. Having similar masses, they only slightly differed from each other in retention times, indicating differences in polarity. In addition, the relative abundance of the molecular ion with an m/z ratio of 749,66 was higher in the cultures exposed to high light, while the relative abundance of the other ion (749,62) was higher in low light cultures. Knowing that the PQ pool is being continuously reduced under high light conditions, it was assumed that the molecular ion with m/z of 749,66 is the reduced PQ, while the other (749,62) is the oxidized PQ. Due to APCI being a relatively soft ionization technique, the fragmentation of molecular ions most likely occured as a result of oxidation between preparation and storage of samples.

Chlorophyll *a* could also be detected as an adduct of lower mass (891,52) than assumed (m/z 893-894). The relative content of chlorophyll *a* was notable higher in cultures incubated at low light intensity (Figure 4.9). It is known that the relative amount of pigments bound to photosystems is adjusted according to the illumination conditions. Therefore more pigments are expected to be bound to photosystems in cells adapted to low light to effectively harvest available light. Accordingly, under the high irradiance the relative amount of light harvesting pigments and chlorophylls would be decreased to avoid photodamage.

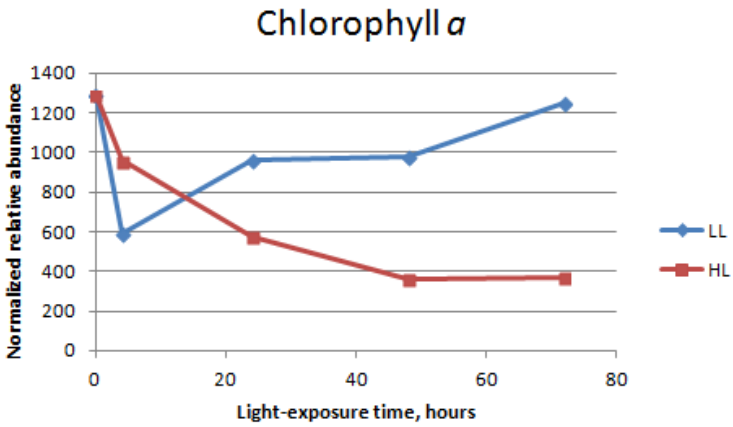


**Figure 4.9 – Changes in chlorophyll *a* content:**
Changes in relative abundance of chlorophyll *a* induced by high light (HL) and low light (LL) conditions as a function of light-exposure time. The plotted data shows an average of lipid abundances between three biological replicates. The complete data set and corresponding standard errors are given in Appendix VII.

## Conclusion

A labile association between antennae complexes and PSII as observed in this experiment indicates that in addition to having an active xanthophyll cycle, *Nannochloropsis* also may employ the another photoprotective mechanism, namely state transitions. The key mechanism of state transitions is based on a flexible binding of antennae complexes to PSII, allowing dissociation of LHCs from PSII in response to over-excitation in order to prevent photo damage. The increase in relative abundance of plastoquinone and the decreased abundance of chlorophyll *a* in cultures exposed to high light conditions indicates that in addition to pigments of the xanthophyll cycle, other photosynthetic lipids are also involved in adaptation to high irradiance. The main mechanism of adaptation to low light conditions is shown to be the possible utilization of a different set of LHCs and the accumulation of light-harvesting carotenoids β-carotene, canthaxanthin and violaxanthin.

# Future research

The main aim of this project was to develop protocols and techniques for simultaneous extraction, separation and characterization of photosynthetic lipids synthesized in *Nannochloropsis oceanica.* However, the method for characterization of lipid composition utilized in this work can only be considered as a semi-quantitative method. This means that the relative abundances, which is the output from the software, can only be used to compare the relative ratios of photosynthetic lipids between different samples. While using this method, large variations were observed between the biological replicas. The variation could be a result of the surrounding environment having a different impact on cultures during incubation, and oxidative processes during sampling and storage. Deviations between the relative abundance of different pigments could also result from small variations during sample preparation for $UPC^2$ and the application of the samples on the $UPC^2$-column. To overcome these problems in the future and improve the sampling procedure, the samples need to be prepared under identical conditions, and preferably analyzed as multiple technical replicates to give an indication of the associated errors. The modification of the $UPC^2$-qTOF-MS protocol should also be made as a development towards a quantitative protocol. To achieve this, standards of various concentrations should ideally be applied while analyzing the samples in order to obtain standard curves, which in turn would make it possible to convert the semi-quantitative data gathered in this project, to fully quantitative data. The following estimation of lipid content can be done per sample dry weight. Therefore, the additional treatment with freeze-drying can be applied not only to improve the extraction yield but also to determine sample dry weight.

Atmospheric pressure chemical ionization (APCI), which is the method utilized in this work to ionize the sample components during mass spectrometry, resulted in molecular ions of chlorophyll *a* and reduced plastoquinone of a lower mass than expected. Due to APCI being a relatively soft ionization technique, the fragmentation of the molecular ions was most likely a result of oxidation during the preparation and storage of the samples. The unstable nature of the separated components, calls for modification of the utilized extraction-protocol. The extraction procedure ideally needs to be performed in the dark, and at low temperature, while blowing with nitrogen gas to reduce oxidation of the components in the extract as much as possible. Assuming that the fragmentation of analytes occurred due to the utilized ionization

technique, an alternative soft ionization method, such as the electrospray ionization, could also be tested and compared to the data gained by utilizing APCI.

# References


Amunts, A., et al. (2007). "The structure of a plant photosystem I supercomplex at 3.4 Å resolution." Nature **447**(7140): 58-63.

Anandarajah, K., et al. (2012). "Characterization of microalga Nannochloropsis sp. mutants for improved production of biofuels." Applied Energy **96**: 371-377.

Anunciato, T. P. and P. A. da Rocha Filho (2012). "Carotenoids and polyphenols in nutricosmetics, nutraceuticals, and cosmeceuticals." Journal of cosmetic dermatology **11**(1): 51-54.

Archibald, J. M. and P. J. Keeling (2002). "Recycled plastids: a 'green movement'in eukaryotic evolution." TRENDS in Genetics **18**(11): 577-584.

Ballottari, M., et al. (2007). "Contrasting behavior of higher plant photosystem I and II antenna systems during acclimation." Journal of Biological Chemistry **282**(12): 8947-8958.

Barber, J. and B. Andersson (1992). "Too much of a good thing: light can be bad for photosynthesis." Trends in biochemical sciences **17**(2): 61-66.

Barsanti, L. and P. Gualtieri (2014). Algae: anatomy, biochemistry, and biotechnology, CRC press.

Basso, S., et al. (2014). "Characterization of the photosynthetic apparatus of the Eustigmatophycean *Nannochloropsis gaditana*: Evidence of convergent evolution in the supramolecular organization of photosystem I." Biochimica et Biophysica Acta (BBA)-Bioenergetics **1837**(2): 306-314.

Ben-Shem, A., et al. (2003). "Crystal structure of plant photosystem I." Nature **426**(6967): 630-635.

Blankenship, R. E. (2013). Molecular mechanisms of photosynthesis, John Wiley & Sons.

Borowitzka, M. A. and N. R. Moheimani (2013). Algae for biofuels and energy, Springer.

Braithwaite, A. and F. J. Smith (1996). Chromatographic methods, Chapman and Hall London,, UK.

Britton, G., et al. (2004). Carotenoids: handbook, Springer Science & Business Media.

Brown, J. S. (1987). "Functional organization of chlorophyll a and carotenoids in the alga, Nannochloropsis salina." Plant physiology **83**(2): 434-437.

Budavari, S., et al. (1989). "The Merck Index, Merck & Co." Inc., Rahway, NJ **1606**.

Butler, W. L. (1972). "On the primary nature of fluorescence yield changes associated with photosynthesis." Proceedings of the National Academy of Sciences **69**(11): 3420-3422.

Cabovska, B., et al. (2012). "Application of UPC2 in extractables analysis." Waters Application Note 720004490en.

Carlberg, I., et al. (1999). "Thylakoid protein phosphorylation and the thiol redox state." Biochemistry **38**(10): 3197-3204.

Chen, M. and R. E. Blankenship (2011). "Expanding the solar spectrum used by photosynthesis." Trends in plant science **16**(8): 427-431.

Chernushevich, I. V., et al. (2001). "An introduction to quadrupole–time-of-flight mass spectrometry." Journal of Mass Spectrometry **36**(8): 849-865.

Chinnasamy, S., et al. (2010). "Microalgae cultivation in a wastewater dominated by carpet mill effluents for biofuel applications." Bioresource Technology **101**(9): 3097-3105.

Chisti, Y. (2007). "Biodiesel from microalgae." Biotechnology advances **25**(3): 294-306.

Chisti, Y. (2008). "Biodiesel from microalgae beats bioethanol." Trends in biotechnology **26**(3): 126-131.

Cinque, G., et al. (2000). "Absorption spectra of chlorophyll a and b in Lhcb protein environment." Photosynthesis Research **64**(2-3): 233-242.

Cohen, Z. (1999). Chemicals from microalgae, CRC Press.

Consalvey, M., et al. (2005). "PAM fluorescence: a beginners guide for benthic diatomists." Diatom Research **20**(1): 1-22.

Crane, F. L. (2010). "Discovery of plastoquinones: a personal perspective." Photosynthesis Research **103**(3): 195-209.

Drop, B., et al. (2011). "Photosystem I of Chlamydomonas reinhardtii contains nine light-harvesting complexes (Lhca) located on one side of the core." Journal of Biological Chemistry **286**(52): 44878-44887.

Durnford, D. G. and P. G. Falkowski (1997). "Chloroplast redox regulation of nuclear gene transcription during photoacclimation." Photosynthesis Research **53**(2-3): 229-241.

Escoubas, J.-M., et al. (1995). "Light intensity regulation of cab gene transcription is signaled by the redox state of the plastoquinone pool." Proceedings of the National Academy of Sciences **92**(22): 10237-10241.

Fairchild, J. N., et al. (2013). "Influence of Sample Solvent Composition for SFC Separations. LC GC." LCGC North America **31**(4): 326-333.

Falkowski, P. G. (1980). Light-shade adaptation in marine phytoplankton. Primary productivity in the sea, Springer**:** 99-119.

Falkowski, P. G. and T. G. Owens (1980). "Light—shade adaptation two strategies in marine phytoplankton." Plant physiology **66**(4): 592-595.

Falkowski, P. G. and J. A. Raven (1997). Aquatic photosynthesis, Capital city press.

Fawley, K. P. and M. W. Fawley (2007). "Observations on the diversity and ecology of freshwater Nannochloropsis (Eustigmatophyceae), with descriptions of new taxa." Protist **158**(3): 325-336.

Figueroa, F. L., et al. (1997). "Effects of high irradiance and temperature on photosynthesis and photoinhibition in< i> Nannochloropsis gaditana</i> Lubián (Eustigmatophyceae)." Journal of plant physiology **151**(1): 6-15.

Frank, H. A. (1999). The photochemistry of carotenoids. Dordrecht, Kluwer.

Fromme, P., et al. (2001). "Structure of photosystem I." Biochimica et Biophysica Acta (BBA)-Bioenergetics **1507**(1): 5-31.

Geider, R. J. and B. A. Osborne (1992). "Algal photosynthesis." Current phycology (USA).

Gentile, M. P. and H. W. Blanch (2001). "Physiology and xanthophyll cycle activity of Nannochloropsis gaditana." Biotechnology and bioengineering **75**(1): 1-12.

Genty, B., et al. (1989). "The relationship between the quantum yield of photosynthetic electron transport and quenching of chlorophyll fluorescence." Biochimica et Biophysica Acta (BBA)-General Subjects **990**(1): 87-92.

Germano, M., et al. (2002). "Supramolecular organization of photosystem I and light-harvesting complex I in Chlamydomonas reinhardtii." FEBS letters **525**(1): 121-125.

Gray, G. R., et al. (1998). "Adjustment of thylakoid plastoquinone content and photosystem I electron donor pool size in response to growth temperature and growth irradiance in winter rye (Secale cereale L.)." Photosynthesis Research **56**(2): 209-221.

H. Scheer, J. L. W., and M. D. Lane (2004). "Chlorophylls and carotenoids". Encyclopedia of Biological Chemistry. New York, NY, USA, Elsevier**:** 430-437.

Haldrup, A., et al. (2001). "Balance of power: a view of the mechanism of photosynthetic state transitions." Trends in plant science **6**(7): 301-305.

Han, B.-p. (2002). "A mechanistic model of algal photoinhibition induced by photodamage to photosystem-II." Journal of theoretical biology **214**(4): 519-527.

Havaux, M. and K. K. Niyogi (1999). "The violaxanthin cycle protects plants from photooxidative damage by more than one mechanism." Proceedings of the National Academy of Sciences **96**(15): 8762-8767.

Henriques, M., et al. (2007). "Extraction and quantification of pigments from a marine microalga: a simple and reproducible method." Communicating Current Research and Educational Topics and Trends in Applied Microbiology Formatex: 586-593.

Hibberd, D. (1981). "Notes on the taxonomy and nomenclature of the algal classes Eustigmatophyceae and Tribophyceae (synonym Xanthophyceae)." Botanical Journal of the linnean Society **82**(2): 93-119.

Hosikian, A., et al. (2010). "Chlorophyll extraction from microalgae: A review on the process engineering aspects." International journal of chemical engineering **2010**.

Hughes, D. A. (1999). "Effects of carotenoids on human immune function." Proceedings of the Nutrition Society **58**(03): 713-718.

Humphrey, A. (2004). "Chlorophyll as a color and functional ingredient." Journal of food science **69**(5): C422-C425.

Hynninen, P. H. (1992). "Chemistry of chlorophylls: modifications." ChemInform **23**(3).

Iwaki, M., et al. (1992). "Fluorescence of P700 and antenna chlorophylls in Photosystem I particles that contain 11 chlorophylls/P700." Biochimica et Biophysica Acta (BBA) - Bioenergetics **1100**(3): 278-284.

Iwata, S. and J. Barber (2004). "Structure of photosystem II and molecular architecture of the oxygen-evolving centre." Current opinion in structural biology **14**(4): 447-453.

Keeling, P. J. (2004). "Diversity and evolutionary history of plastids and their hosts." American Journal of Botany **91**(10): 1481-1493.

Kishikawa, N. and N. Kuroda (2014). "Analytical techniques for the determination of biologically active quinones in biological and environmental samples." Journal of pharmaceutical and biomedical analysis **87**: 261-270.

Li, Y., et al. (2008). "Biofuels from microalgae." Biotechnology progress **24**(4): 815-820.

Lubián, L. M., et al. (2000). "Nannochloropsis (Eustigmatophyceae) as source of commercially valuable pigments." Journal of Applied Phycology **12**(3-5): 249-255.

Manz, A., et al. (2004). Bioanalytical chemistry, World Scientific.

Martinis, J., et al. (2011). "A novel method for prenylquinone profiling in plant tissues by ultra-high pressure liquid chromatography-mass spectrometry." Plant methods **7**(1): 23.

Maxwell, K. and G. N. Johnson (2000). "Chlorophyll fluorescence—a practical guide." Journal of experimental botany **51**(345): 659-668.

Mikami, K. and M. Hosokawa (2013). "Biosynthetic pathway and health benefits of fucoxanthin, an algae-specific xanthophyll in brown seaweeds." International journal of molecular sciences **14**(7): 13763-13781.

Minagawa, J. (2011). "State transitions—the molecular remodeling of photosynthetic supercomplexes that controls energy flow in the chloroplast." Biochimica et Biophysica Acta (BBA)-Bioenergetics **1807**(8): 897-905.

Miyashita, K. (2009). Function of marine carotenoids. Forum Nutr.

Moroney, J. V. and R. A. Ynalvez (2009). "Algal photosynthesis." eLS.

Murata, N., et al. (2007). "Photoinhibition of photosystem II under environmental stress." Biochimica et Biophysica Acta (BBA)-Bioenergetics **1767**(6): 414-421.

Nelson, N. (2009). "Plant photosystem I–the most efficient nano-photochemical machine." Journal of nanoscience and nanotechnology **9**(3): 1709-1713.

Nobre, B. P., et al. (2013). "A biorefinery from Nannochloropsis sp. microalga–extraction of oils and pigments. Production of biohydrogen from the leftover biomass." Bioresource Technology **135**: 128-136.

Nowicka, B. and J. Kruk (2010). "Occurrence, biosynthesis and function of isoprenoid quinones." Biochimica et Biophysica Acta (BBA)-Bioenergetics **1797**(9): 1587-1605.

Paiva, S. A. and R. M. Russell (1999). "β-Carotene and other carotenoids as antioxidants." Journal of the American college of nutrition **18**(5): 426-433.

Pfannschmidt, T., et al. (1999). "Photosynthetic control of chloroplast gene expression." Nature **397**(6720): 625-628.

Quach, H. T., et al. (2004). "An Improved Method for the Extraction and Thin-Layer Chromatography of Chlorophyll a and b from Spinach." Journal of Chemical Education **81**(3): 385.

Reyes-Prieto, A., et al. (2007). "The origin and establishment of the plastid in algae and plants." Annu. Rev. Genet. **41**: 147-168.

Rintamäki, E., et al. (1997). "Phosphorylation of Light-harvesting Complex II and Photosystem II Core Proteins Shows Different Irradiance-dependent Regulation in Vivo APPLICATION OF PHOSPHOTHREONINE ANTIBODIES TO ANALYSIS OF THYLAKOID PHOSPHOPROTEINS." Journal of Biological Chemistry **272**(48): 30476-30482.

Roy, S., et al. (2011). Phytoplankton pigments: characterization, chemotaxonomy and applications in oceanography, Cambridge University Press.

Scheer, H. (1991). "Structure and occurence of chlorophylls."

Scheer, H. (2006). An overview of chlorophylls and bacteriochlorophylls: biochemistry, biophysics, functions and applications. Chlorophylls and bacteriochlorophylls, Springer**:** 1-26.

Schreiber, U. (2004). Pulse-amplitude-modulation (PAM) fluorometry and saturation pulse method: an overview. Chlorophyll a Fluorescence, Springer**:** 279-319.

Sommer, P. and M. Kofler (1966). "Physicochemical properties and methods of analysis of phylloquinones, menaquinones, ubiquinones, plastoquinones, menadione, and related compounds." Vitam Horm **24**: 349-399.

Suggett, D. J., et al. (2011). Chlorophyll a fluorescence in aquatic sciences: methods and applications, Springer.

Tswett, M. (1906). "Physikalisch-chemische Studien über das chlorophyll. Die Adsorptionen." Berichte der Deutschen botanischen Gesellschaft **24**(316-323): 20.

Vanselow, C. (2008). Analysis of the Photosynthetic Components with a Focus on Photosystem I from Galdieria Sulphuraria and Phormidium Laminosum, ProQuest.

Walters, R. G. (2005). "Towards an understanding of photosynthetic acclimation." Journal of experimental botany **56**(411): 435-447.

Wang, D., et al. (2014). "Nannochloropsis genomes reveal evolution of microalgal oleaginous traits." PLoS genetics **10**(1): e1004094.

Weis, E. and J. A. Berry (1987). "Quantum efficiency of photosystem II in relation to 'energy'-dependent quenching of chlorophyll fluorescence." Biochimica et Biophysica Acta (BBA)-Bioenergetics **894**(2): 198-208.

Wollman, F.-A. and P. Delepelaire (1984). "Correlation between changes in light energy distribution and changes in thylakoid membrane polypeptide phosphorylation in Chlamydomonas reinhardtii." The Journal of cell biology **98**(1): 1-7.

Zhu, C. and Y. Lee (1997). "Determination of biomass dry weight of marine microalgae." Journal of Applied Phycology **9**(2): 189-194.

Zlatkis, A. and R. E. Kaiser (2011). HPTLC-high performance thin-layer chromatography, Elsevier.

Цвет, М. (1903). "О новой категории адсорбционных явлений и о применении их к биохимическому анализу." Труды Варшавского общества естествоиспытателей, отд. биологии **14**: 1-20.

# Appendix I

# Photosynthetic lipids in *Nannochloropsis*

There are an impressive number of photosynthetic lipids found in photosynthetic organisms, each having its own particular function. The main function of photosynthetic lipids is to harvest light available for use in photosynthesis, and transfer it to the reaction centers of photosystem II (PSII) and photosystem I (PSI), respectively. Chlorophylls and carotenoids are the major classes of pigments involved in light harvesting. In addition, certain carotenes and xanthophylls play an important role in photoprotection under high-light conditions. Another important group of lipids found in biological membranes is quinones, compounds involved in transporting electrons between PSII and the $b_6f$ complex. *Nannochloropsis* is a eukaryotic marine microalga that synthesizes a wide range of photosynthetic lipids in the aforementioned chemical classes. This appendix gives an overview of the photosynthetic lipids that are known or expected to be synthesized in *Nannochloropsis oceanica*. The data provided for chlorophylls and carotenoids is taken from "Data sheets aiding classification of phytoplankton carotenoids and chlorophylls" by Egeland et al. (2011) in the text book Phytoplankton Pigments (Roy, Llewellyn et al. 2011).

## Chlorophyll *a*

**Recommended abbreviation: Chl *a* (C*a*)**

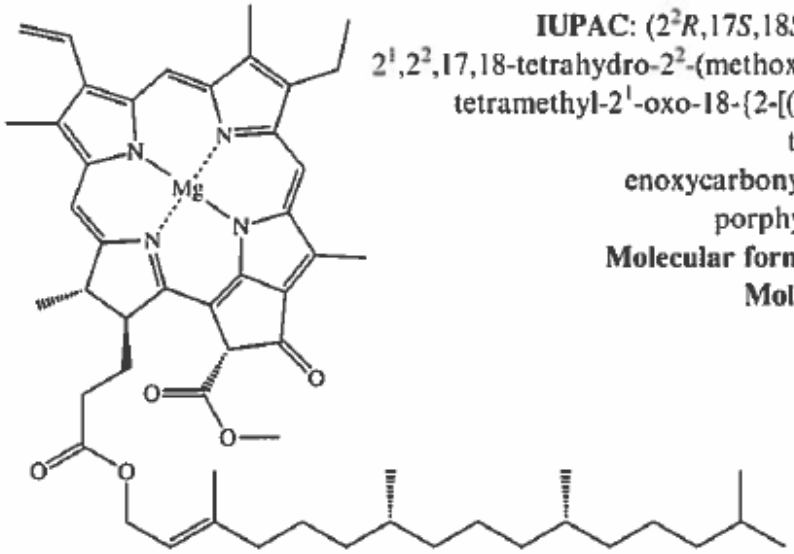

**IUPAC:** ($2^2R$,17*S*,18*S*)-12-Ethenyl-7-ethyl-$2^1$,$2^2$,17,18-tetrahydro-$2^2$-(methoxycarbonyl)-3,8,13,17-tetramethyl-$2^1$-oxo-18-{2-[(2*E*,7*R*,11*R*)-3,7,11,15-tetramethylhexadec-2-enoxycarbonyl]ethyl}cyclopenta[*at*]porphyrinatomagnesium(II)

**Molecular formula:** $C_{55}H_{72}N_4O_5Mg$

**Molecular weight:** 893.49

| | |
|---|---|
| **Biological occurrence** | Characteristic pigment in all photosynthetic algae and plants |
| **Source culture** | *Chroomonas salina* (cryptophyte) |
| **Alteration products** | Chlide *a*, Pheide *a*, Phe *a*, Chl *a*', Chl *a* allo, Pyro derivatives |
| **Biosynthetically related to** | Chl *b*, MgDVP |
| **Occurs together with** | |

**HPLC chromatogram of *Synechococcus* sp. (system 1)**

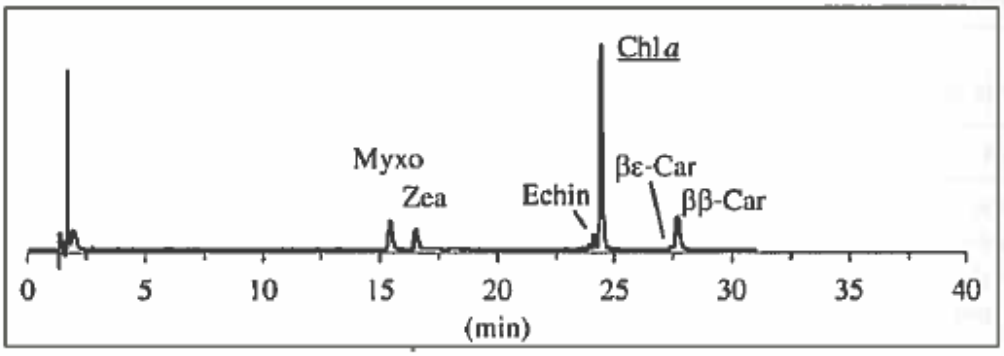


**HPLC chromatogram of *Rhodomonas baltica* (system 2)**

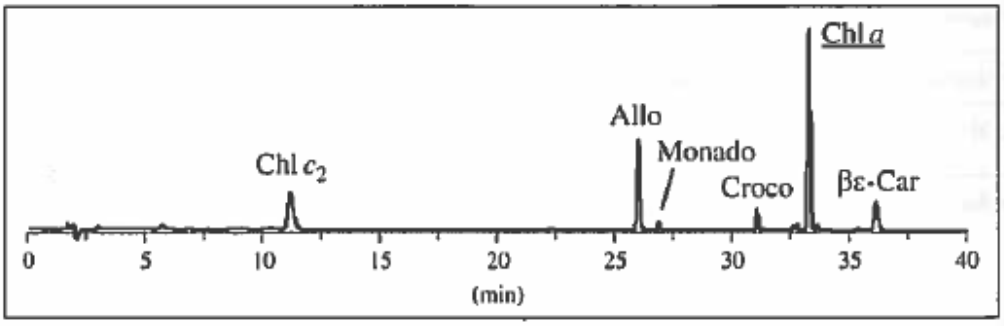

*UV-Vis spectra (see also reference spectra below)*

| Solvent | $\lambda_{max}$ (nm) | Band ratio (blue:red ratio) | Ref. |
|---|---|---|---|
| Acetone | 383, 411, *430*, 534, 580, 617, 662 | 1.2 | [145] |
| Diethyl ether | 409, *428*, 495, 530, 575, 614, 660 | 1.3 | [98] |
| 95% Ethanol | 414, 432, 618, 649, *664* | 0.99 | [121] |
| Methanol | 432, 618, 652, *665* | 0.97 | [121] |
| **Recommended specific absorption coefficient *d*** ($L\ g^{-1}\ cm^{-1}$) | | 129 (at 428 nm, diethyl ether) [98]<br>87.7 (at 664 nm, 90% acetone) [107] | |

**Reference spectra**

**In acetone**

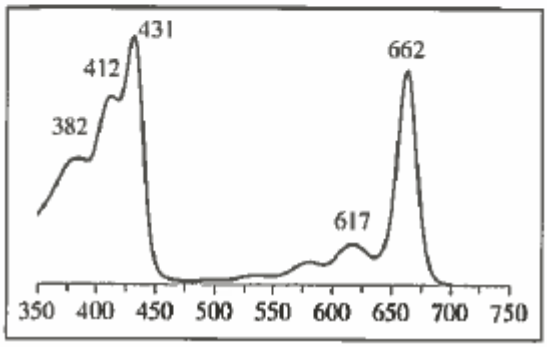


**In HPLC solvent system 1**

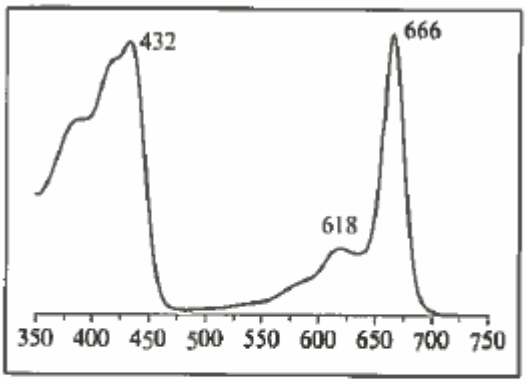


**In HPLC solvent system 2**

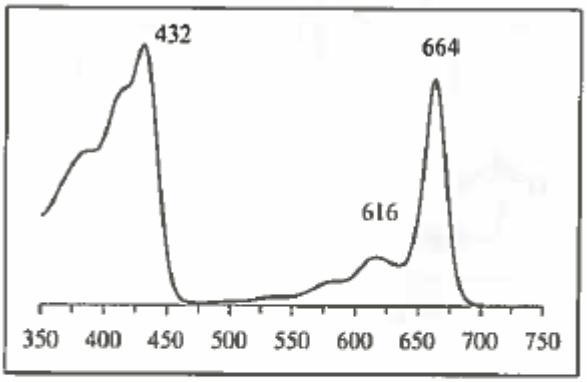


***Mass spectra***

| Ionization technique | Mass analyser type | Diagnostic ions (m/z, rel. intensity) | Ref. |
|---|---|---|---|
| FAB | Magnetic sector | 892 $[M]^+$ (25), 614 $[M\text{-phytyl}]^+$ (100), 555 $[M\text{-}337]^+$ (39), 481 $[M\text{-}60\text{-}351]^+$ (29) | [27] |
| **Remarks** | Fluorescence: excitation 428 nm, emission 666 nm (diethyl ether) [26] | | |

## Pheophytin *a*

**Recommended abbreviation: Phe *a* (Phα)**

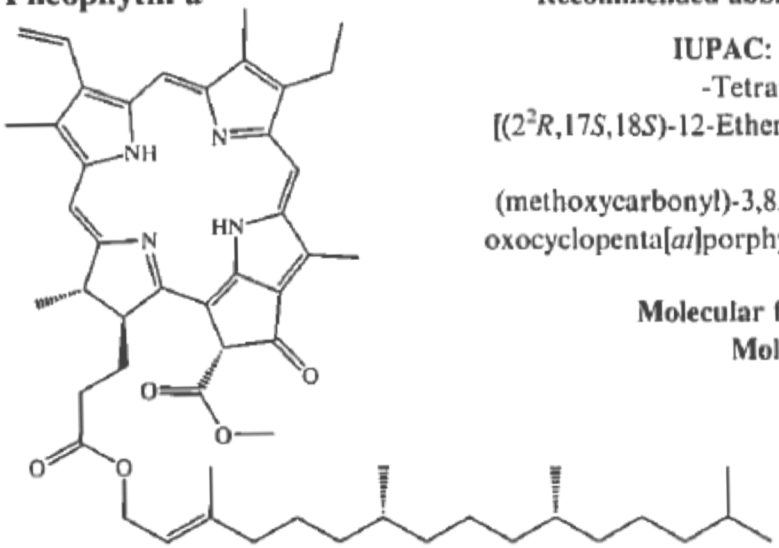

**IUPAC:** (2*E*,7*R*,11*R*)-3,7,11,15-Tetramethylhexadec-2-enyl [(2²*R*,17*S*,18*S*)-12-Ethenyl-7-ethyl-2¹,2²,17,18-tetrahydro-2²-(methoxycarbonyl)-3,8,13,17-tetramethyl-2¹-oxocyclopenta[*at*]porphyrin-18-yl]propanoate

**Molecular formula:** $C_{55}H_{74}N_4O_5$
**Molecular weight:** 871.20

| | |
|---|---|
| **Alteration product of** | Chlorophyll *a*. Found in zooplankton fecal pellets, senescent algae, sediments. The acid-catalysed demetallation also occurs in slightly acidic extracts, especially in prasinophyte extracts |
| **Source culture** | *Chroomonas salina* (cryptophyte) |
| **Alteration products** | Epimer, Allomer, Pheide *a*, Pphe *a* |
| **(Bio)synthetically related to** | Chl *a*, Pheide *a*, Pphe *a* |
| **Occurs together with** | Carotenoid furanoxides |

**HPLC chromatogram of *Amphidinium carterae* (system 1)**

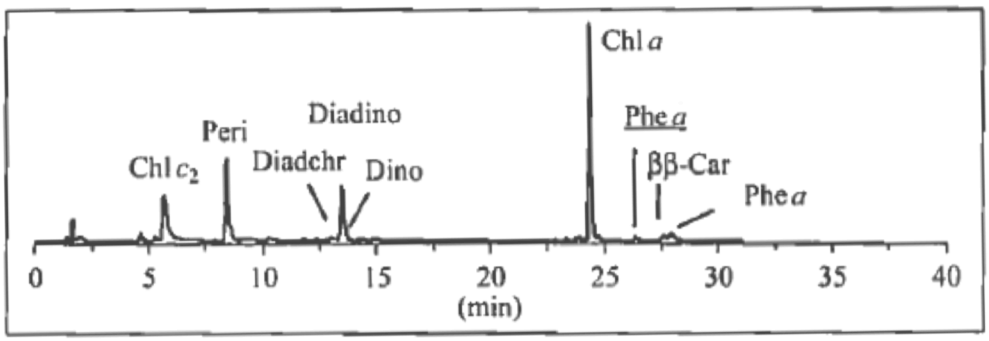


**HPLC chromatogram of a coastal marine sample (system 2)**

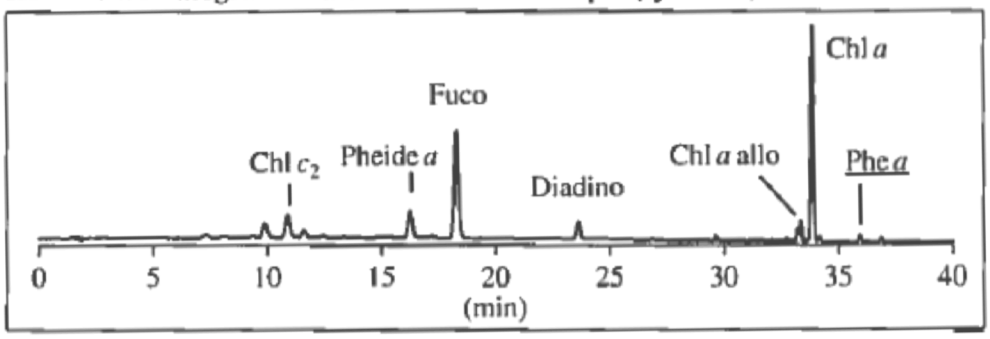

*UV-Vis spectra (see also reference spectra below)*

| Solvent | $\lambda_{max}$ (nm) | Band ratio (blue:red ratio) | Ref. |
|---|---|---|---|
| Acetone | *410*, 505, 535, 560, 610, 666 | 2.3 | [109] |
| Diethyl ether | *408*, 505, 534, 610, 667 | 2.1 | [12] |
| 95% Ethanol | *417*, 507, 536, 564, 662 | 3.3 | [121] |
| Methanol | *417*, 533, 567, 602, 654 | 4.1 | [121] |
| **Recommended specific absorption coefficient *d*** | | 139 (at 411 nm in tetrahydrofuran) [125] | |
| **($L\ g^{-1}\ cm^{-1}$)** | | 51.2 (at 667 nm in 90% acetone) [124, 109] | |

**Reference spectra**

For spectrum in acetone, see [109]

**In HPLC solvent system 1**

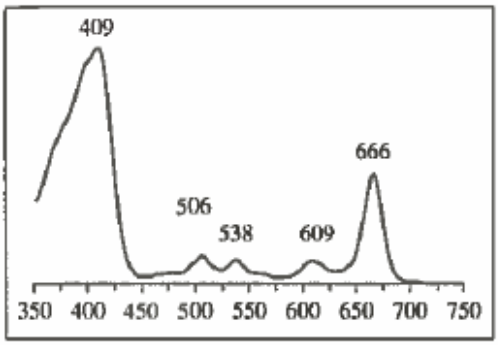


**In HPLC solvent system 2**

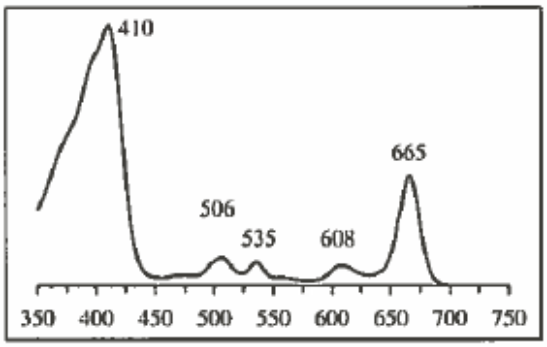


*Mass spectra*

| Ionization technique | Mass analyser type | Diagnostic ions (m/z, rel. intensity) | Ref. |
|---|---|---|---|
| FAB | magnetic sector | 870 $[M]^+$ (100), 592 [M-phytyl]$^+$ (53), 533 (41), 520 (36), 459 (83) | [27] |

| | |
|---|---|
| **Remarks** | Fluorescence: excitation 408 nm, emission 672 nm (diethyl ether) [26]<br>Pheopigments are generally easier to detect using fluorescence |

## β,β-Carotene

**IUPAC:** β,β-Carotene
**Molecular formula:** $C_{40}H_{56}$

**Recommended abbreviation: ββ-Car (ββ)**
(trivial name: β-Carotene)
**Molecular weight:** 536.87

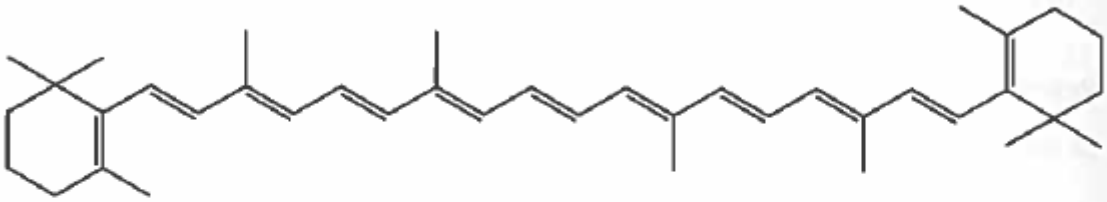

| | |
|---|---|
| **Biological occurrence** | Dominant pigment in chlorophytes, prasinophytes, mesostigmatophytes, rhodophytes and one group of dinoflagellates. Minor in all other algal groups. Also present in plants (notably carrots) [78] |
| **Source culture** | *Pavlova lutheri* (Pavlovophyceae) |
| **Alteration products** | *Cis*-isomers |
| **Biosynthetically related to** | Cantha, Asta, Zea, Viola, Neo, Diato, Diadino, Allo etc. |
| **Occurs together with** | |

**HPLC chromatogram of *Synechococcus* sp. (system 1)**

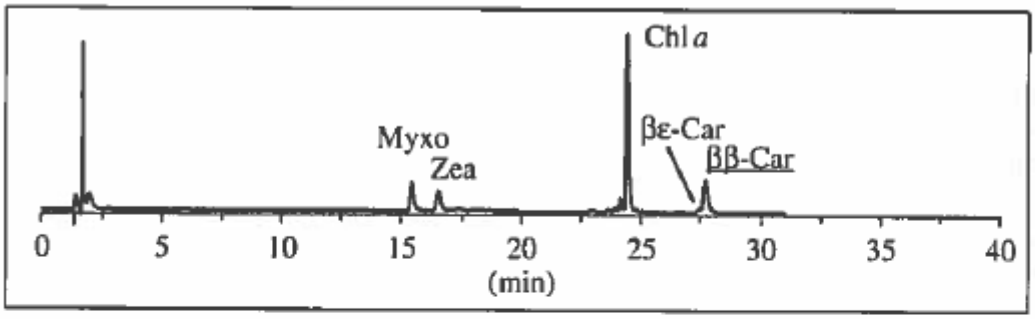


**HPLC chromatogram of *Dunaliella salina* (system 2)**

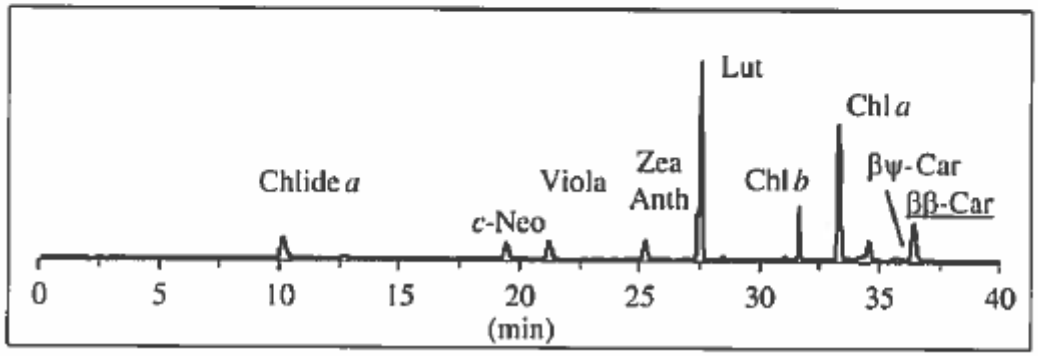

*UV-Vis spectra (see also reference spectra below)*

| Solvent | $\lambda_{max}$ (nm) | Band ratio (% III:II) | Ref. |
|---|---|---|---|
| Acetone | (427), *454*, 480 | 21 | [96] |
| Diethyl ether | (430), *447*, 476 | 5 | [133] |
| Ethanol (see Remarks) | (428), *451*, 480 | 27 | [86] |
| Hexane | (425), *451*, 477 | 29 | [96] |
| Methanol (see Remarks) | (429), *449*, 475 | 25 | [160] |
| **Recommended specific absorption coefficient** $d$ **(L g$^{-1}$ cm$^{-1}$)** | | 259 (at 453 nm, hexane) [103]<br>250 (at 454 nm, acetone) [96] | |

**Reference spectra**

**In acetone**

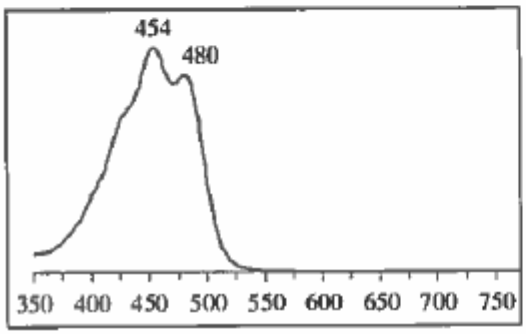


**In hexane**

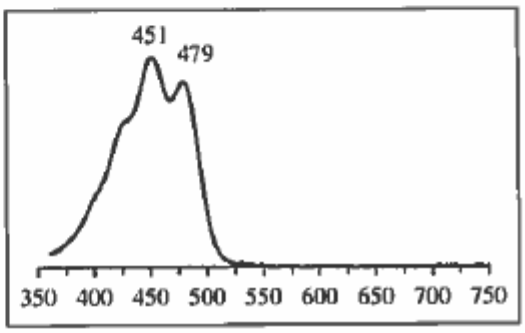


**In HPLC solvent system 1**

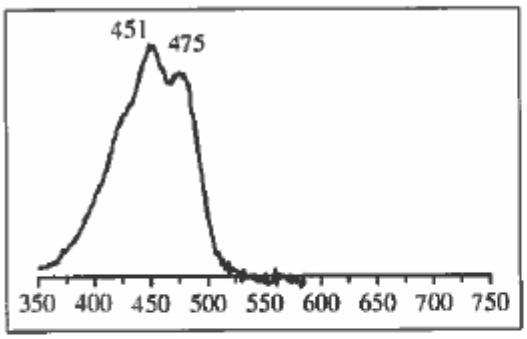


**In HPLC solvent system 2**

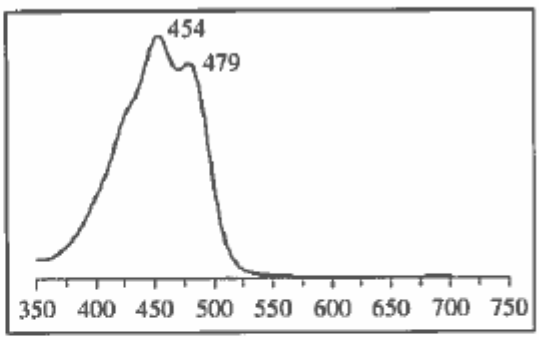


*Mass spectra*

| Ionization technique | Mass analyser type | Diagnostic ions (m/z, rel. intensity) | Ref. |
|---|---|---|---|
| EI | Magnetic sector | 536 $[M]^+$ (44), 444 $[M-92]^+$ (15), 430 $[M-106]^+$ (4), 119 (72), 109 (22), 91 (45), 83 (23), 69 (100) | [144] |

**Remarks** To aid dissolving in alcohol, first dissolve in a drop or two of hexane

## Antheraxanthin

**Recommended abbreviation: Anth (An)**

**IUPAC:** (3*S*,5*R*,6*S*,3′*R*)-5,6-Epoxy-5,6-dihydro-β,β-carotene-3,3′-diol

**Molecular formula:** $C_{40}H_{56}O_3$ **Molecular weight:** 584.87

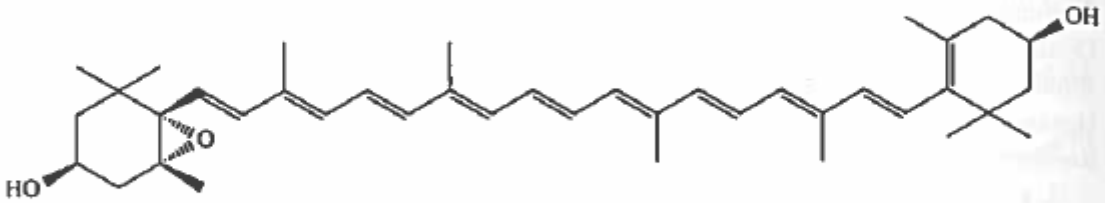


| | |
|---|---|
| **Biological occurrence** | Minor pigment in chlorophytes, prasinophytes, trebouxiophytes, mesostigmatophytes, chlorarachniophytes, and some chrysophytes and eustigmatophytes. Also found in seaweeds and plants. Major in anthers of some flowers [78] |
| **Source culture** | *Dunaliella tertiolecta* (chlorophyte) |
| **Alteration products** | Undergoes rearrangement to Mutato in weakly acidic solutions. *Cis*-isomers |
| **Biosynthetically related to** | Biosynthetic intermediate between Zea and Viola |
| **Occurs together with** | Zea, Viola |

**HPLC chromatogram of *Dunaliella tertiolecta* (system 1)**

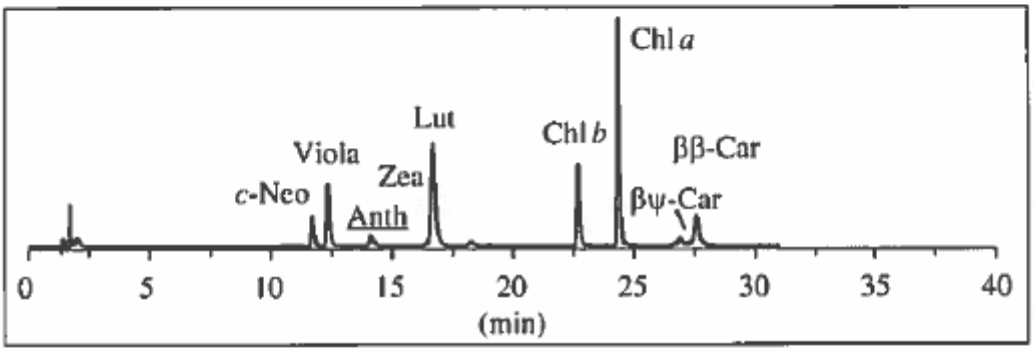


**HPLC chromatogram of *Micromonas pusilla* (system 2)**

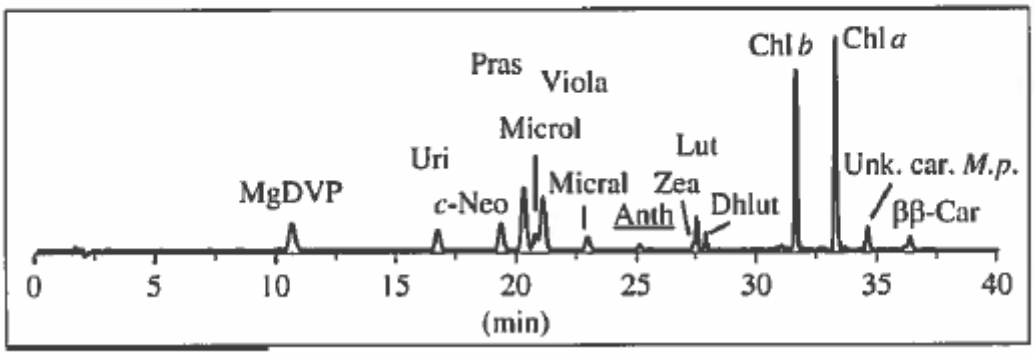

*UV-Vis spectra (see also reference spectra below)*

| Solvent | $\lambda_{max}$ (nm) | Band ratio (% III:II) | Ref. |
|---|---|---|---|
| Acetone | (422), *448*, 475 | 29 | [72] |
| Ethanol | 422, *444*, 472 | 54 | [152] |
| Hexane | 420, *444*, 472 | n.d. | [85] |
| **Recommended specific absorption coefficient *d* (L $g^{-1}$ $cm^{-1}$)** | | 235 (at 446 nm, ethanol) | [84] |

**Reference spectra**

**In acetone**

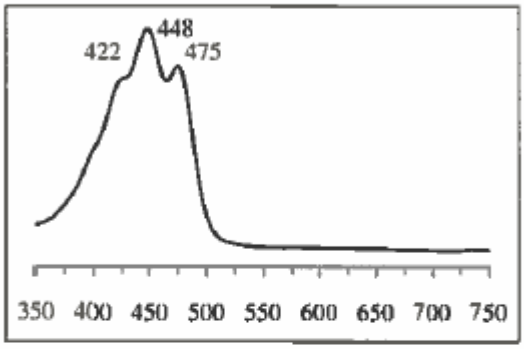


**In ethanol**

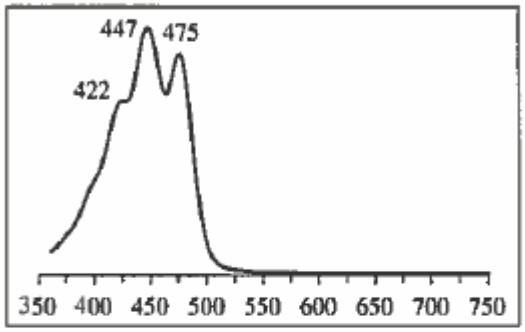


**In HPLC solvent system 1**

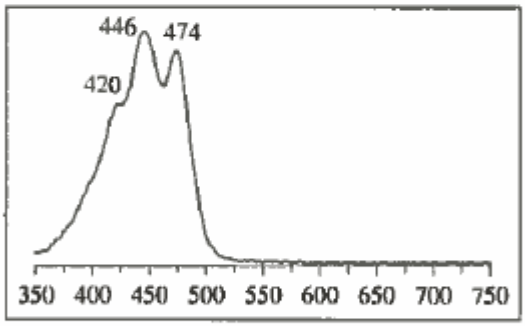


**In HPLC solvent system 2**

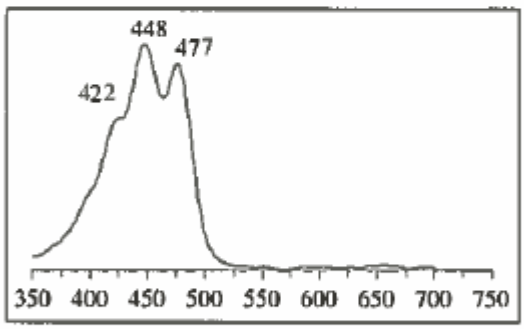


*Mass spectra*

| Ionization technique | Mass analyser type | Diagnostic ions (m/z, rel. intensity) | Ref. |
|---|---|---|---|
| EI | Magnetic sector | 584 $[M]^+$ (60), 504 $[M-80]^+$ (30), 492 $[M-92]^+$ (6), 221 (30), 181 (10), 43 (100) | [127] |
| **Remarks** | Part of a 'xanthophyll cycle' (see Chapter 11, this volume). May be present in diatoms under prolonged high light stress [123] | | |

## Astaxanthin

**Recommended abbreviation: Asta (As)**

**IUPAC:** (3*S*,3′*S*)-3,3′-Dihydroxy-β,β-carotene-4,4′-dione

**Molecular formula:** $C_{40}H_{52}O_4$ **Molecular weight:** 596.84

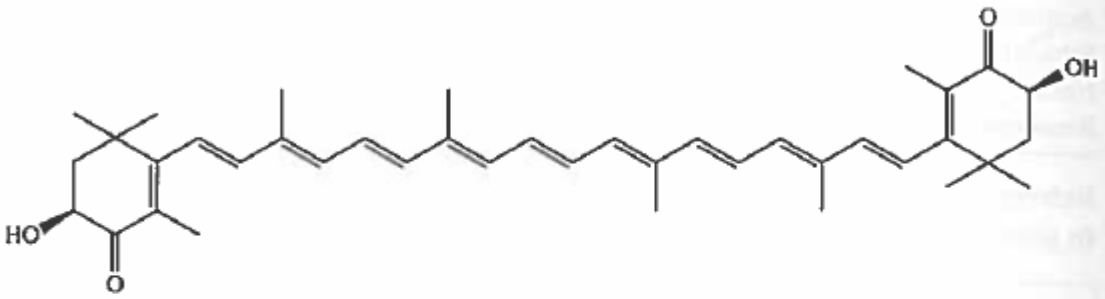


| | |
|---|---|
| **Biological occurrence** | Present in some chlorophytes, but major (mainly as mono- and diesters of fatty acids) in some of these upon nitrogen starvation. Major in salmonids and crustaceans [78, 79] |
| **Source culture** | Synthetic (see Appendix E, this volume) |
| **Alteration products** | *Cis*-isomers; astacene (oxidation product) |
| **Biosynthetically related to** | Zea, Cantha |
| **Occurs together with** | |

**HPLC chromatogram of *Pycnococcus provasolii* (system 1)**

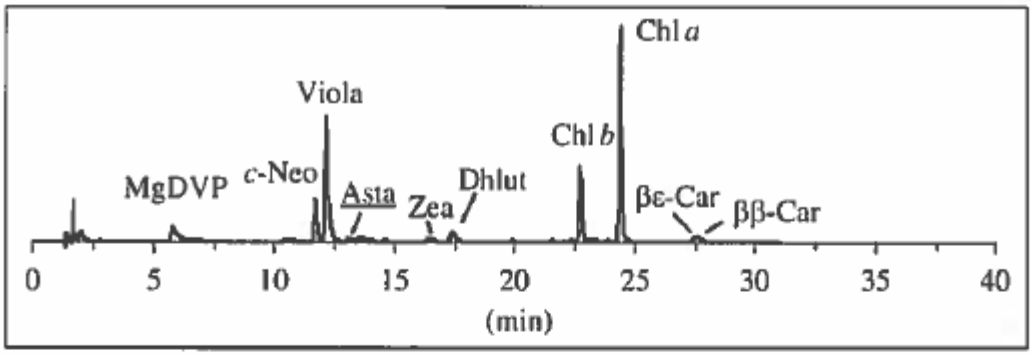


**HPLC chromatogram of synthetic astaxanthin (system 2)**

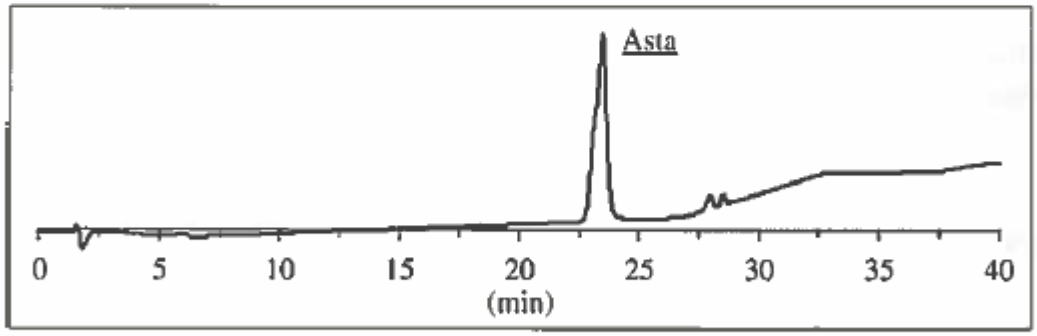

*UV-Vis spectra (see also reference spectra below)*

| Solvent | $\lambda_{max}$ (nm) | Band ratio (% III:II) | Ref. |
|---|---|---|---|
| Acetone | 475 | - | [82] |
| Ethanol | 476 | - | [33] |
| Hexane | 466–467 | - | [41] |
| Methanol | 470–472 | - | [41] |
| Recommended specific absorption coefficient *d* ($L\ g^{-1}\ cm^{-1}$) | | 206 (at 473 nm, methanol) | [79] |

**Reference spectra**

**In acetone**

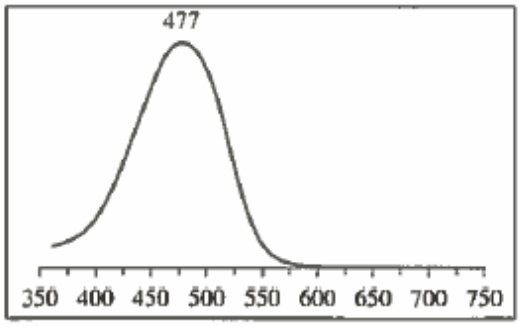


**In methanol**

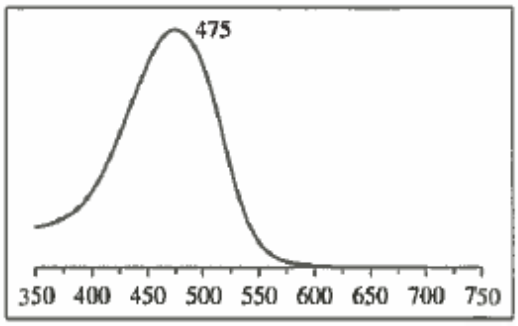


**In HPLC solvent system 1**

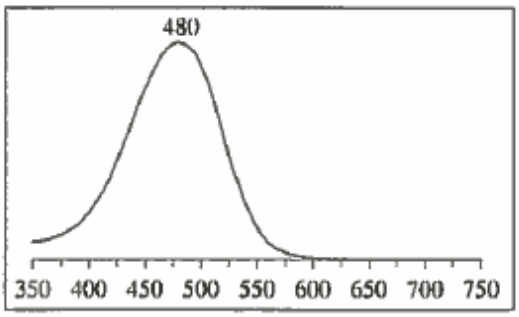


**In HPLC solvent system 2**

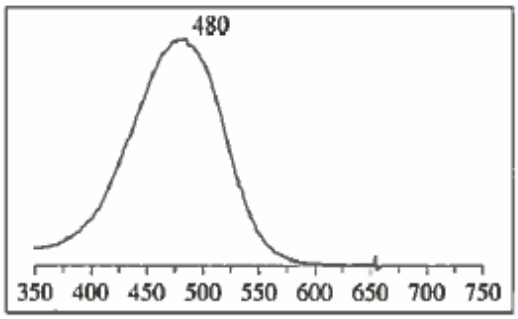


*Mass spectra*

| Ionization technique | Mass analyser type | Diagnostic ions (m/z, rel. intensity) | Ref. |
|---|---|---|---|
| EI | Magnetic sector | 596 $[M]^+$ (7), 580 $[M-16]^+$ (9), 564 $[M-16-16]^+$ (6), 133 (56), 109 (24), 91 (100) | [55] |
| **Remarks** | Mixtures of (3*S*,3′*S*), (3*R*,3′*R*) and (3*R*,3′*S*)-Asta are common in aquatic animals [15]. Esterification will change polarity and hence retention time | | |

## Auroxanthin

**Recommended abbreviation: Auro (Au)**

**IUPAC:** (3*S*,5*R*,8*RS*,3′*S*,5′*R*,8′*RS*)-5,8:5′,8′-Diepoxy-5,8,5′,8′-tetrahydro-β,β-carotene-3,3′-diol

**Molecular formula:** $C_{40}H_{56}O_4$ **Molecular weight:** 600.87

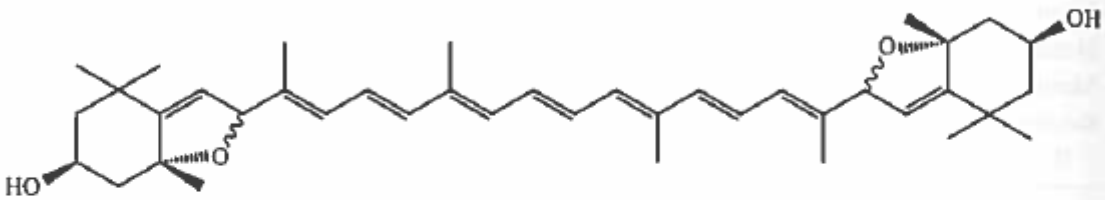


(Always occurs as a mixture of the three (3*S*,5*R*,8*R*,3′*S*,5′*R*,8′*R*), (3*S*,5*R*,8*R*,3′*S*,5′*R*,8′*S*) and (3*S*,5*R*,8*S*,3′*S*,5′*R*,8′*S*) optical isomers)

| | |
|---|---|
| **Alteration product of** | Viola. The acid-catalysed rearrangement occurs in slightly acidic extracts, especially in prasinophyte extracts [91] |
| **Source culture** | *Dunaliella tertiolecta* (chlorophyte) |
| **Alteration products** | *Cis*-isomers |
| **Synthetically related to** | Viola |
| **Occurs together with** | Luteoxanthin, Neochr |

**HPLC chromatogram of acidified *Dunaliella tertiolecta* (system 1)**

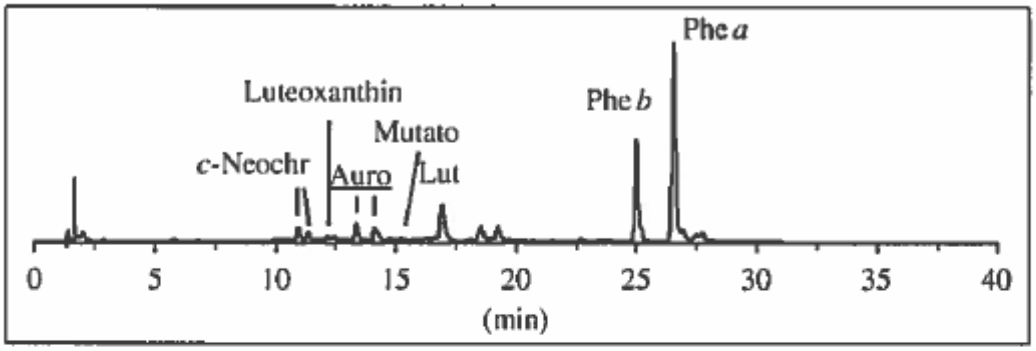


**HPLC chromatogram (system 2)**

NO DATA AVAILABLE

*UV-Vis spectra (see also reference spectra below)*

| Solvent | $\lambda_{max}$ (nm) | Band ratio (% III:II) | Ref. |
|---|---|---|---|
| Acetone | 380, 401, *425* | 125 | [51] |
| Ethanol | 379, *400*, 425 | 92 | [136] |
| Hexane | 380, 400, 425 | n.d. | [167] |
| **Recommended specific absorption coefficient *d* ($L\ g^{-1}\ cm^{-1}$)** | | 181 (at 403 nm, ethanol) [114] | |

## Reference Spectra

**In HPLC solvent system 1**

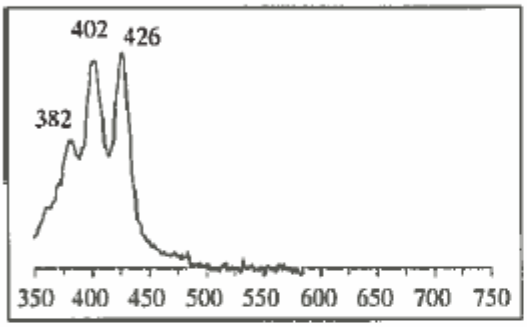


**In HPLC solvent system 2**

NO DATA AVAILABLE

*Mass spectra*

| Ionization technique | Mass analyser type | Diagnostic ions (m/z, rel. intensity) | Ref. |
|---|---|---|---|
| EI | Magnetic sector | 600 $[M]^+$ (44), 584 $[M-16]^+$ (22), 582 $[M-18]^+$ (11), 568 $[M-16-16]^+$ (12), 221 (100), 181 (68) | [51] |
| **Remarks** | Turns green on silica TLC (partly ionised to a blue oxonium ion) | | |

## Canthaxanthin

**Recommended abbreviation: Cantha (Ct)**

**IUPAC:** β,β-Carotene-4,4′-dione

**Molecular formula:** $C_{40}H_{52}O_2$

**Molecular weight:** 564.84

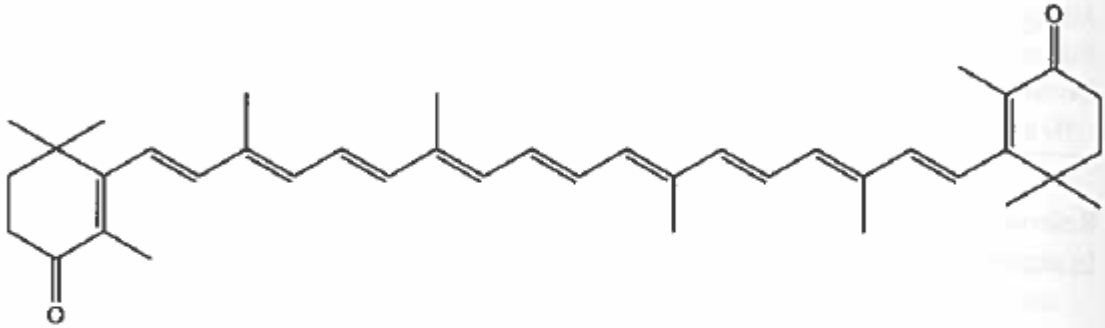

| | |
|---|---|
| **Biological occurrence** | Minor or trace pigment in eustigmatophytes, cyanobacteria (Cyano-1) and some dinoflagellates. Detected in some cultures of chlorophytes, diatoms and prymnesiophytes. Major in some chlorophytes upon nitrogen starvation [78] |
| **Source culture** | Synthetic (see Appendix E, this volume) |
| **Alteration products** | *Cis*-isomers |
| **Biosynthetically related to** | ββ-Car, Echin, Asta |
| **Occurs together with** | |

**HPLC chromatogram of *Guillardia theta* – canthaxanthin: internal standard (system 1)**

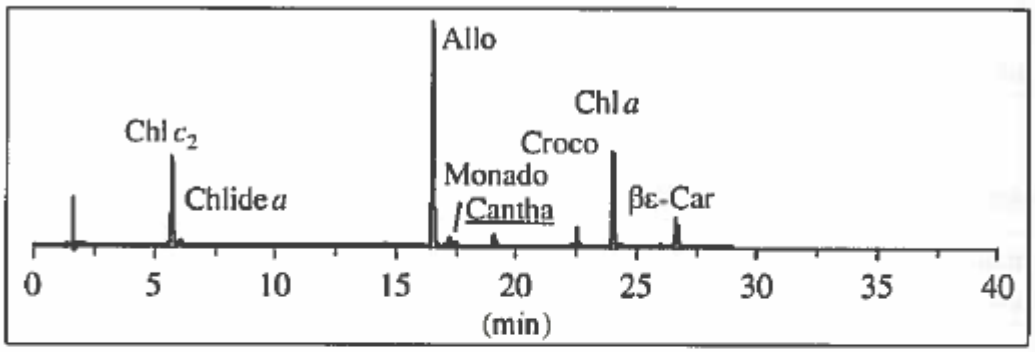


**HPLC chromatogram of synthetic canthaxanthin (system 2)**

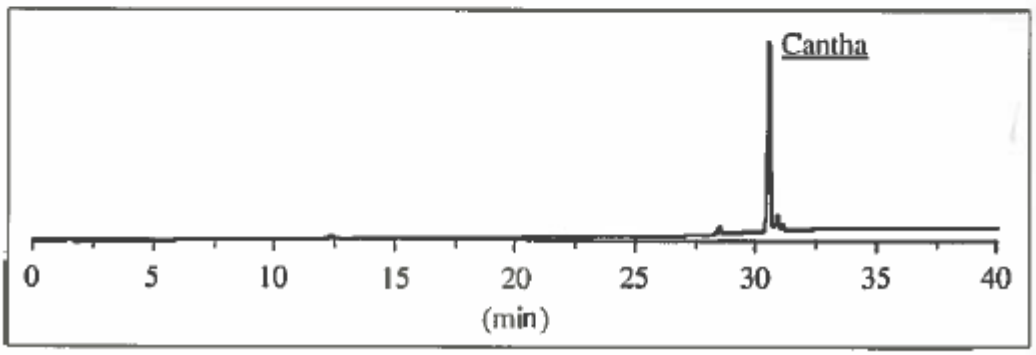

*UV-Vis spectra (see also reference spectra below)*

| Solvent | $\lambda_{max}$ (nm) | Band ratio (% III:II) | Ref. |
|---|---|---|---|
| Acetone | 468 | - | [82] |
| Ethanol | 478 | - | [135] |
| Hexane | 468 | - | [54] |
| **Recommended specific absorption coefficient *d* ($L\ g^{-1}\ cm^{-1}$)** | | 220 (at 469 nm, cyclohexane) | [155] |

**Reference spectra**

**In acetone**

For spectrum in acetone, see [109]

**In methanol**

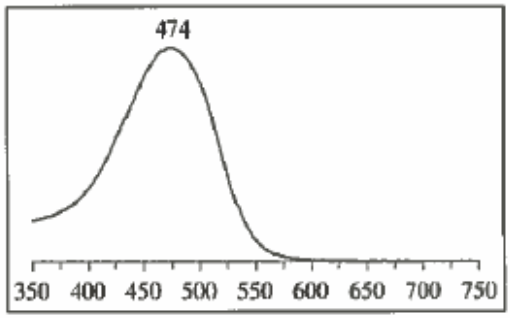


**In HPLC solvent system 1**

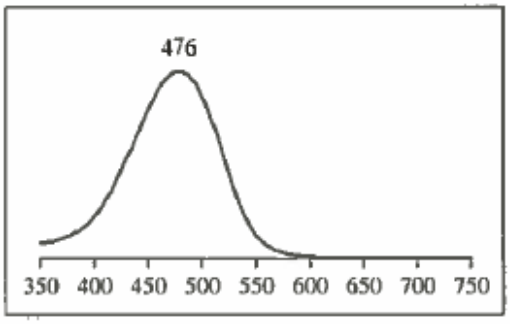


**In HPLC solvent system 2**

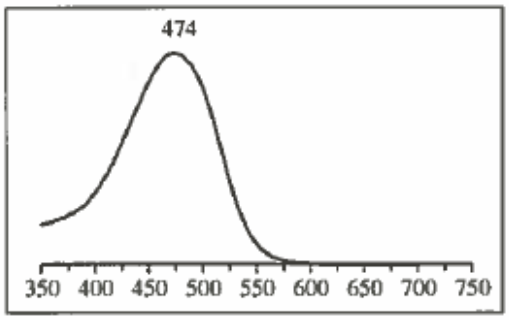


*Mass spectra*

| Ionization technique | Mass analyser type | Diagnostic ions (m/z, rel. intensity) | Ref. |
|---|---|---|---|
| EI | Magnetic sector | 564 $[M]^+$ (41), 562 $[M-2]^+$ (2), 472 $[M-92]^+$ (7), 458 $[M-106]^+$ (2), 91 (19), 83 (100) | [55] |

**Remarks**

## Vaucheriaxanthin

**Recommended abbreviation: Vauch (Va)**

**IUPAC:** (3*S*,5*R*,6*R*,3′*S*,5′*R*,6′*S*)-5′,6′-Epoxy-6,7-didehydro-5,6,5′,6′-tetrahydro-β,β-carotene-3,5,3′,19′-tetrol

**Molecular formula:** $C_{40}H_{56}O_5$ **Molecular weight:** 616.87

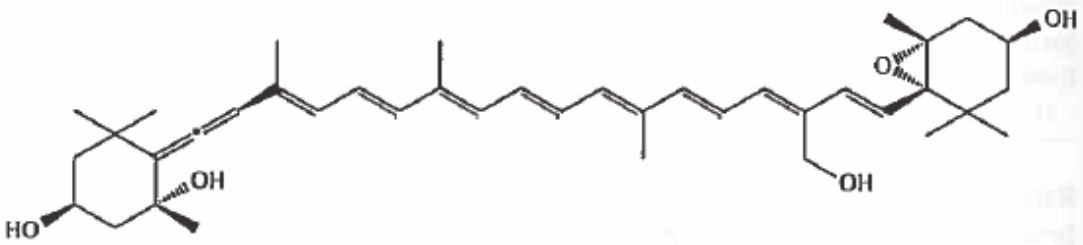


| | |
|---|---|
| **Biological occurrence** | Dominant pigment in eustigmatophytes (see Chapter 1) |
| **Source culture** | *Nannochloropsis oculata* (eustigmatophyte) |
| **Alteration products** | Undergoes rearrangement to Vauchfur in weakly acidic solutions [91]. *Cis*-isomers |
| **Biosynthetically related to** | Zea, Anth, Viola, Neo, Vauch-eo, Vauch esters |
| **Occurs together with** | Vauch esters |

**HPLC chromatogram of *Nannochloropsis oculata* (system 1)**

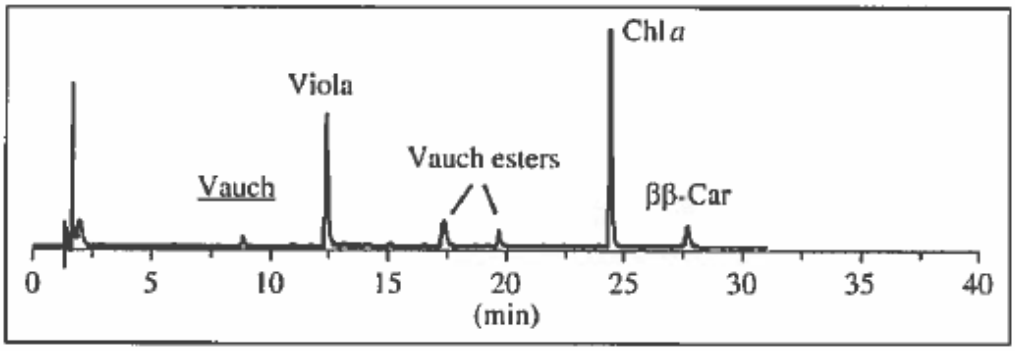


**HPLC chromatogram of *Nannochloropsis gaditana* (system 2)**

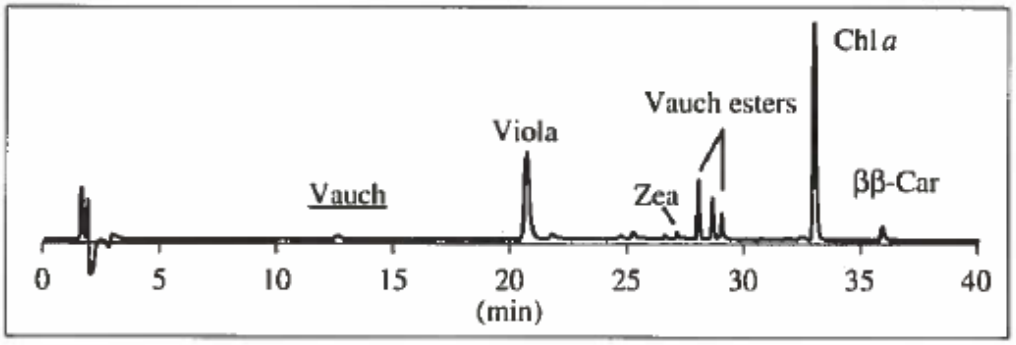

*UV-Vis spectra (see also reference spectra below)*

| Solvent | $\lambda_{max}$ (nm) | Band ratio (% III:II) | Ref. |
|---|---|---|---|
| Acetone | 416, *438*, 466 | 54 | [47] |
| Ethanol | 419, *442*, 471 | 78 | [152] |
| Recommended specific absorption coefficient *d* ($L\ g^{-1}\ cm^{-1}$) | | n.d., see Remarks. | |

**Reference spectra**

For spectrum in acetone, see [109]

For spectrum in hexane, see [109]

**In HPLC solvent system 1**

NO DATA AVAILABLE

**In HPLC solvent system 2**

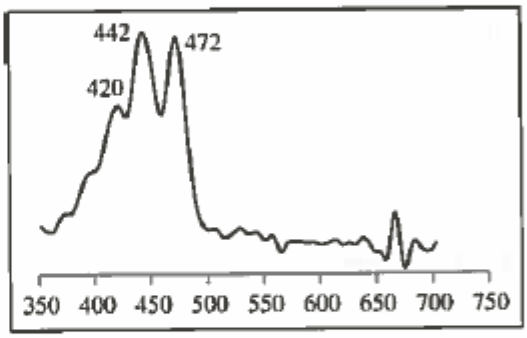


*Mass spectra*

| Ionization technique | Mass analyser type | Diagnostic ions (m/z, rel. intensity) | Ref. |
|---|---|---|---|
| EI | Magnetic sector | 616 $[M]^+$ (11), 598 $[M-18]^+$ (11), 580 $[M-18-18]^+$ (19), 562 $[M-18-18-18]^+$ (30), 544 $[M-18-18-18-18]^+$ (21), 197 (73), 181 (100) | [47] |

**Remarks** $d = 232\ L\ g^{-1}\ cm^{-1}$ (at 442 nm, ethanol) is recommended (calc. from *trans*-Neo), as no value has been determined for Vauch. Vaucheriaxanthin furanoxide is formed in slightly acidic extracts [91]

## Vaucheriaxanthin ethanoate octanoate

**Recom. abbreviation: Vauch-eo**

**IUPAC:** (3*S*,5*R*,6*S*,3′*S*,5′*R*,6′*R*)-5,6-Epoxy-3′-ethanoyloxy-19-octanoyloxy-6′,7′-didehydro-5,6,5′,6′-tetrahydro-β,β-carotene-3,5′-diol

**Molecular formula:** $C_{50}H_{72}O_7$ **Molecular weight:** 785.10

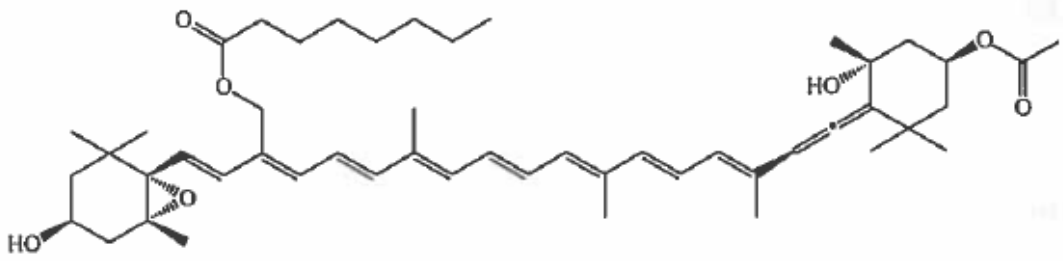

| | |
|---|---|
| **Biological occurrence** | Dominant pigment in eustigmatophytes, minor in xanthophytes (see Chapter 1, this volume) |
| **Source culture** | *Nannochloropsis oculata* (eustigmatophyte) |
| **Alteration products** | Undergoes rearrangement to Vauch-eo-fur in weakly acidic solutions [91]. *Cis*-isomers |
| **Biosynthetically related to** | Zea, Anth, Viola, Neo, Vauch |
| **Occurs together with** | Vauch |

**HPLC chromatogram of *Nannochloropsis oculata* (system 1)**

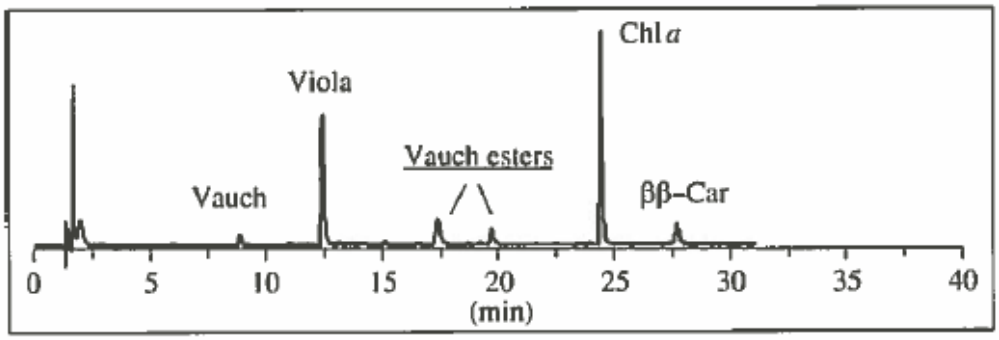


**HPLC chromatogram of *Nannochloropsis oculata* (system 3)**

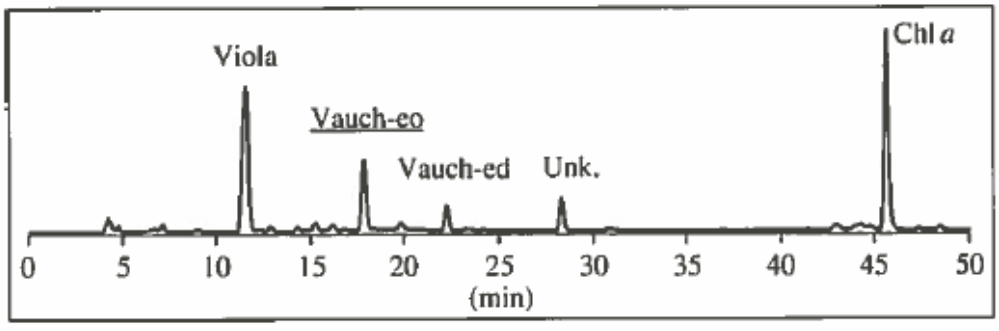

*UV-Vis spectra (see also reference spectra below)*

| Solvent | $\lambda_{max}$ (nm) | Band ratio (% III:II) | Ref. |
|---|---|---|---|
| Acetone | 422, *445*, 471 | 33 | [47] |
| Ethanol | 419, *442*, 471 | 80 | [152] |
| Hexane | 419, *442*, 471 | 64 | [109] |
| **Recommended specific absorption coefficient** $d$ **(L g$^{-1}$ cm$^{-1}$)** | | n.d., see Remarks. | |

**Reference spectra**

For spectrum in acetone, see [109] For spectrum in hexane, see [109]

**In HPLC solvent system 1**

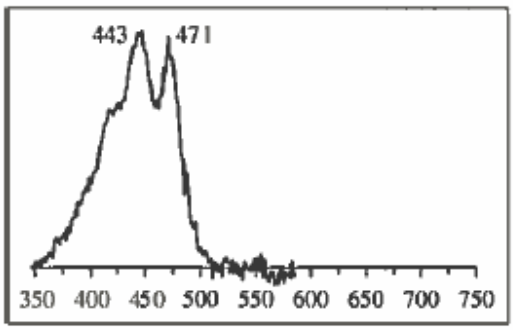


**In HPLC solvent system 3**

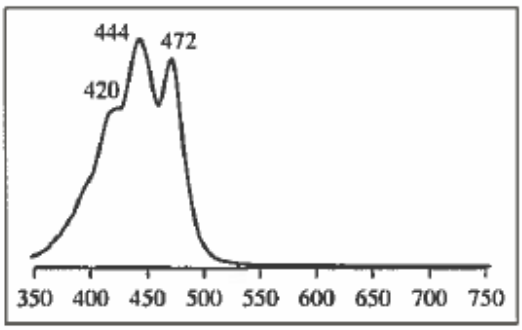


*Mass spectra*

| Ionization technique | Mass analyser type | Diagnostic ions (m/z, rel. intensity) | Ref. |
|---|---|---|---|
| EI | Magnetic sector | 784 $[M]^+$ (6), 766 $[M-18]^+$ (3), 706 $[M-18-60]^+$ (2), 640 $[M-18-126]^+$ (15), 197 (58), 181 (100) | [47] |

**Remarks** Former name: vaucheriaxanthin 3-acetate 19′-octanoate. Found also in mixture with vaucheriaxanthin ethanoate decanoate (Vauch-ed) [47]. Other esters and their acid-catalysed forms exist: [91]. $d$ = 182 L g$^{-1}$cm$^{-1}$ (at 442 nm, ethanol) is recommended (calc. from *trans*-Neo), as no value has been determined for Vauch-eo

## Violaxanthin

**Recommended abbreviation: Viola (V)**

**IUPAC:** (3*S*,5*R*,6*S*,3′*S*,5′*R*,6′*S*)-5,6:5′,6′-Diepoxy-5,6,5′,6′-tetrahydro-β,β-carotene-3,3′-diol

**Molecular formula:** $C_{40}H_{56}O_4$ **Molecular weight:** 600.87

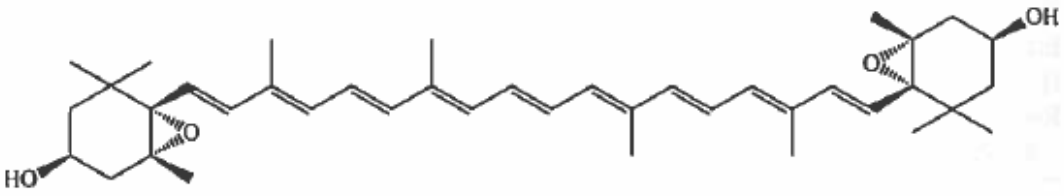


| | |
|---|---|
| **Biological occurrence** | Dominant pigment in chrysophytes, eustigmatophytes, synurophytes, mesostigmatophytes, chlorophytes, prasinophytes, and dinoflagellates Pigment Type 5. Minor in chlorarachniophytes, pinguiophytes and raphidophytes (see Chapter 1, this volume). Also present in higher plants and brown seaweeds |
| **Source culture** | *Dunaliella tertiolecta* (chlorophyte) |
| **Alteration products** | Undergoes rearrangement to Luteoxanthin and Auro in weakly acidic solutions. *Cis*-isomers |
| **Biosynthetically related to** | ββ-Car, Cryp, Zea, Anth, Neo |
| **Occurs together with** | Anth, Neo |

**HPLC chromatogram of *Dunaliella tertiolecta* (system 1)**

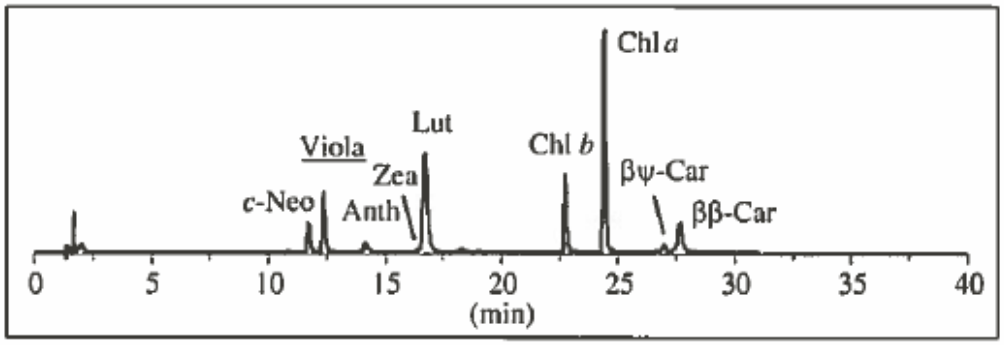


**HPLC chromatogram of *Micromonas pusilla* (system 2)**

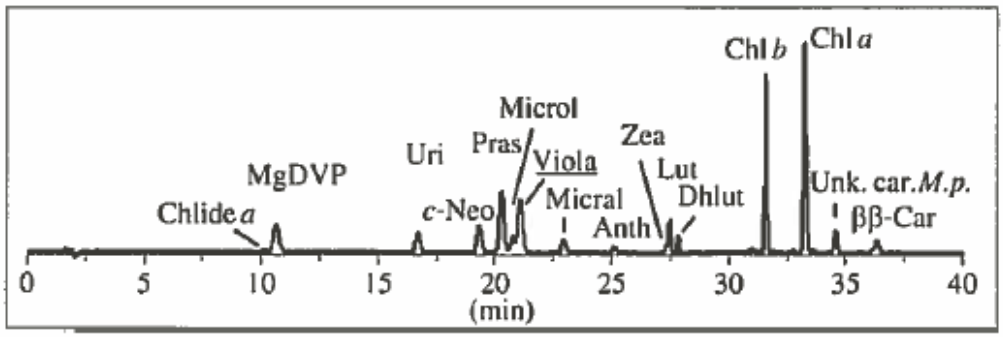

*UV-Vis spectra (see also reference spectra below)*

| Solvent | $\lambda_{max}$ (nm) | Band ratio (% III:II) | Ref. |
|---|---|---|---|
| Acetone | 415, *438*, 467 | 79 | [91] |
| Ethanol | 417, *440*, 469 | 93 | [152] |
| Hexane | 417, *440*, *470* | 100 | [145] |
| Methanol | 415, *436*, 466 | 90 | [160] |
| **Recommended specific absorption coef. *d* (L $g^{-1}cm^{-1}$)** | 254 (at 437 nm in diethyl ether:methylbutane:ethanol 5:5:2) [4] 255 (at 443 nm in ethanol) [44] | | |

**Reference spectra**

**In acetone**

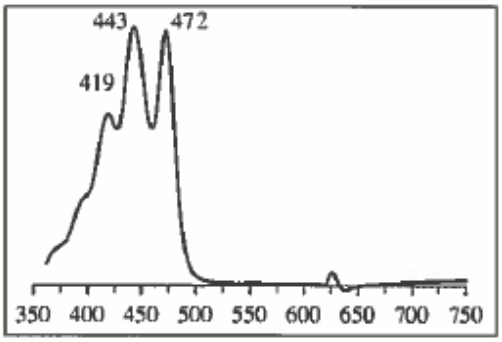


**In ethanol**

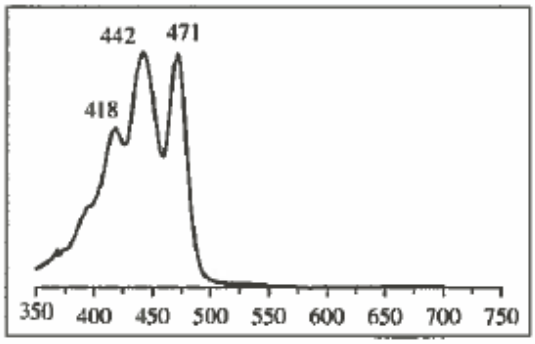


**In HPLC solvent system 1**

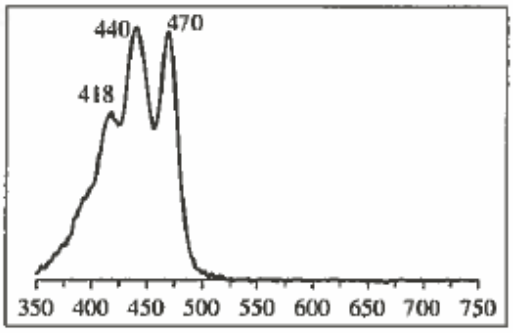


**In HPLC solvent system 2**

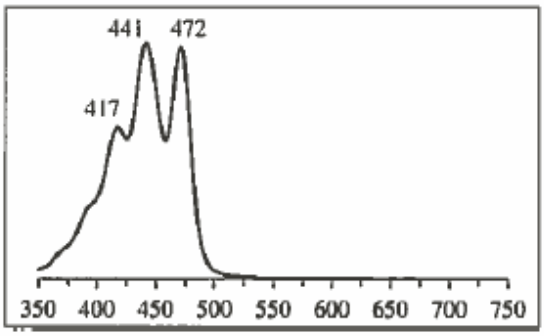


*Mass spectra*

| Ionization technique | Mass analyser type | Diagnostic ions (m/z, rel. intensity) | Ref. |
|---|---|---|---|
| CI | Magnetic sector | 601 $[M+1]^+$ (47), 583 $[M+1-18]^+$ (36), 565 $[M+1-18-18]^+$ (22), 510 (35), 509 $[M+1-92]^+$, 221 (27), 181 (100) | [4] |

**Remarks** Part of a 'xanthophyll cycle': see Chapter 11. May be present in diatoms under prolonged high light stress [123]. Transforms into luteoxanthin and auroxanthin in slightly acidic extracts, particularly in prasinophytes [91]

## Zeaxanthin

**Recommended abbreviation: Zea (Z)**

**IUPAC:** (3*R*,3′*R*)-β,β-Carotene-3,3′-diol

**Molecular formula:** $C_{40}H_{56}O_2$ **Molecular weight:** 568.87

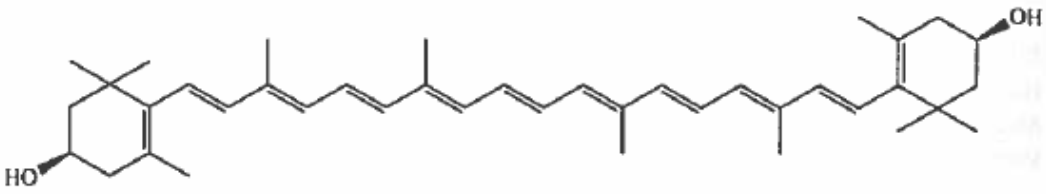


| | |
|---|---|
| **Biological occurrence** | Dominant pigment in cyanobacteria, chrysophytes, eustigmatophytes, pelagophytes, rhodophytes and dinoflagellates Pigment Type 5. Minor in pinguiophytes, raphidophytes, chlorarachniophytes, chlorophytes, prasinophytes and trebouxiophytes. Occasional in dictyochophytes and dinoflagellates Pigment Type 3 (see Chapter 1, this volume) |
| **Source culture** | *Synechococcus* sp. (DC-2) (cyanobacteria) |
| **Alteration products** | *Cis*-isomers |
| **Biosynthetically related to** | ββ-Car, Cryp, Anth, Viola, Neo |
| **Occurs together with** | |

**HPLC chromatogram of *Prochlorococcus* sp. (system 1)**

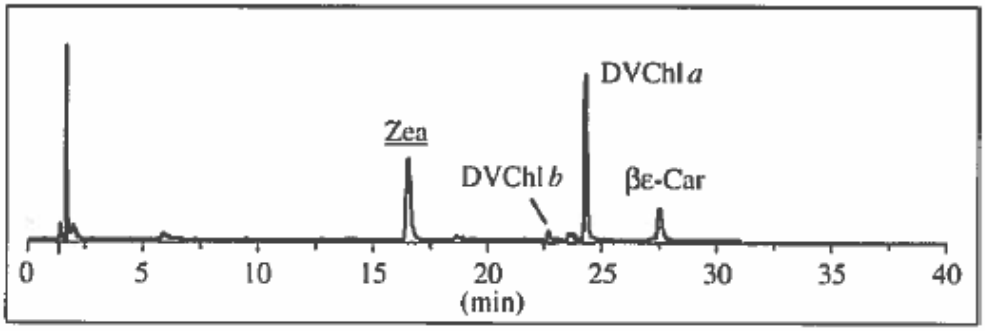


**HPLC chromatogram of *Prochlorococcus* sp. (system 2)**

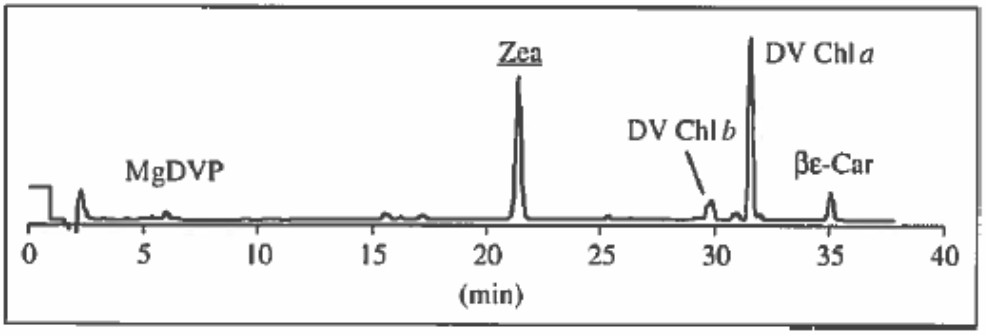

*UV-Vis spectra (see also reference spectra below)*

| Solvent | $\lambda_{max}$ (nm) | Band ratio (% III:II) | Ref. |
|---|---|---|---|
| Acetone | (428), *454*, 481 | 33 | [145] |
| Ethanol | (428), *450*, 478 | 26 | [152] |
| Hexane | (424), *450*, 478 | 46 | [145] |
| Methanol | (429), *449*, 475 | 25 | [160] |
| **Recommended specific absorption coefficient** $d$ **(L g$^{-1}$ cm$^{-1}$)** | | 245 (at 453 nm, ethanol) [148] | |

**Reference spectra**

For spectrum in acetone, see [109]

For spectrum in hexane, see [109]

**In HPLC solvent system 1**

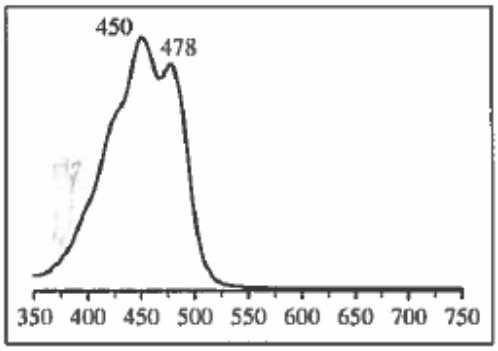


**In HPLC solvent system 2**

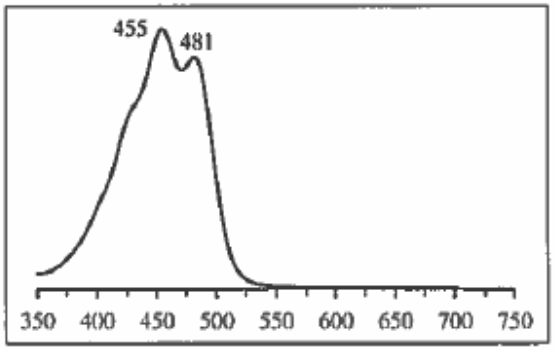


***Mass spectra***

| Ionization technique | Mass analyser type | Diagnostic ions (m/z, rel. intensity) | Ref. |
|---|---|---|---|
| EI | Magnetic sector | 568 $[M]^+$ (100), 550 $[M-18]^+$ (84), 532 $[M-18-18]^+$ (5), 489 $[M-79]^+$ (1), 476 $[M-92]^+$ (13), 462 $[M-106]^+$ (1), 458 $[M-18-92]^+$ (11), 410 $[M-158]^+$ (5) | [19] |

**Remarks** Part of a 'xanthophyll cycle' – see Chapter 11, this volume. May be present in diatoms under prolonged high light stress [123]

## Plastoquinone-9 **Recommended abbreviation: PQ-9**

**IUPAC Name:** 2,3-dimethyl-5-[(2*E*,6*E*,10*E*,14*E*,18*E*,22*E*,26*E*,30*E*)-3,7,11,15,19,23,27,31,35-nonamethylhexatriaconta-2,6,10,14,18,22,26,30,34-nonaen-1-yl]cyclohexa-2,5-diene-1,4-dione

**Molecular formula:** $C_{53}H_{80}O_2$ **Molecular weight:** 749.20

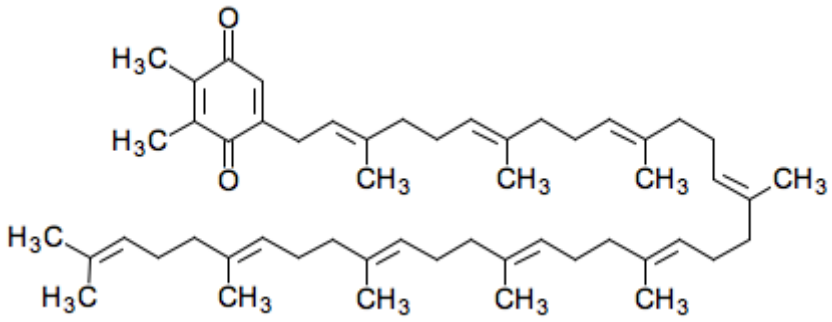


**Absorbance maxima (nm)**: 255 nm (oxidized), 290 nm (reduced) (Crane 2010)

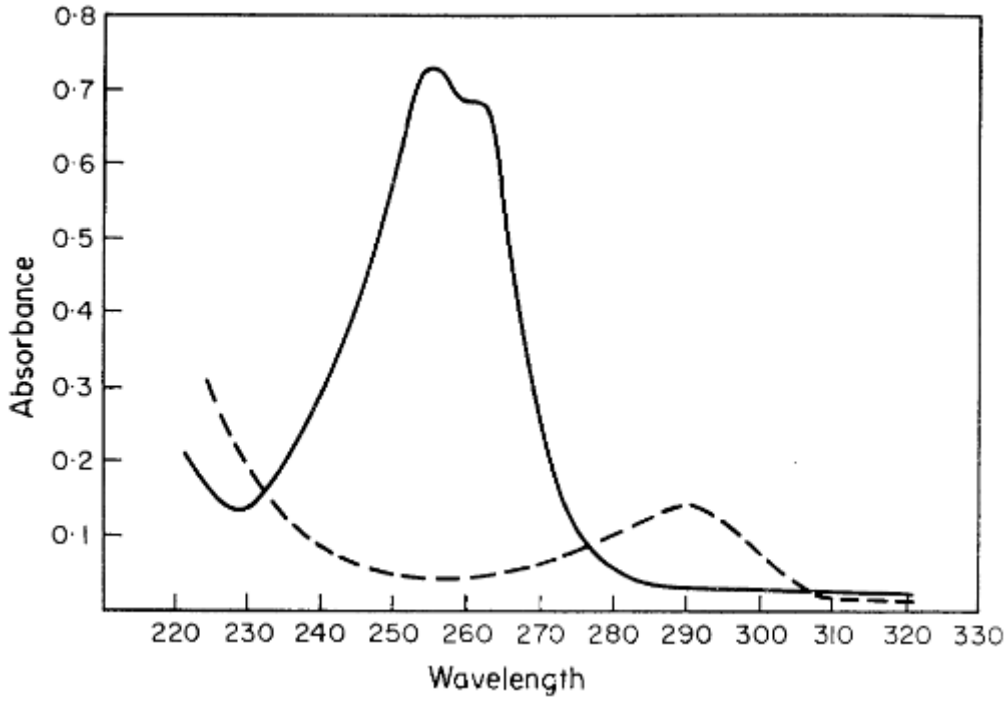


**Figure A1.1 - Absorption spectra of plastoquinone:** Oxidized (solid) and reduced (dashed) (Crane 2010).

## Phylloquinone **Recommended abbreviation: PHQ**

**IUPAC Name:** 2-methyl-3-[(2*E*)-3,7,11,15-tetramethylhexadec-2-en-1-yl]naphthoquinone

**Molecular formula:** $C_{31}H_{46}O_2$ **Molecular weight:** 450.70

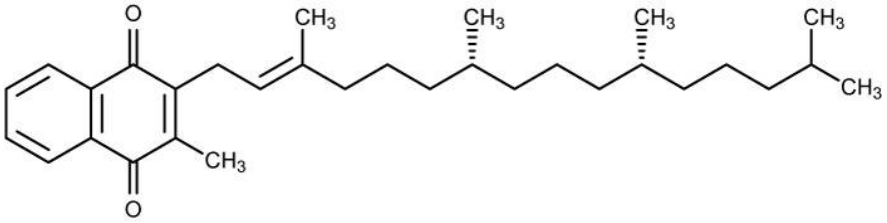


**Absorbance maxima (nm)**: 242, 248, 260, 269, 325 nm (Budavari, O'Neil et al. 1989)

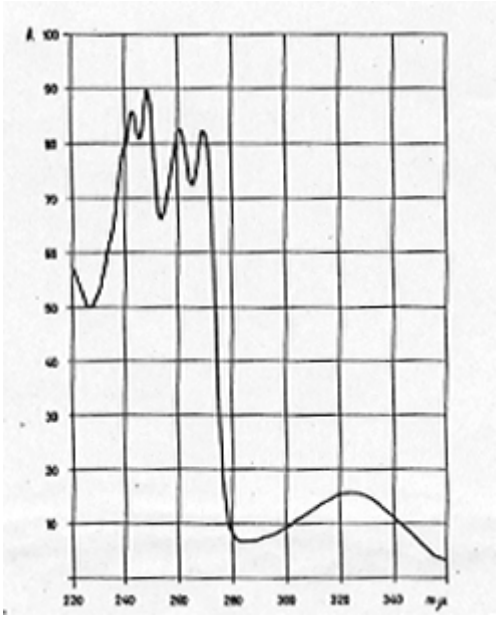

**Figure A2.1 – Absorption spectra of phylloquinone in hexane.** From "Vitamins & Hormones" (Sommer and Kofler 1966) **.**

# References

Budavari, S., et al. (1989). "The Merck Index, Merck & Co." Inc., Rahway, NJ **1606**.

Crane, F. L. (2010). "Discovery of plastoquinones: a personal perspective." Photosynthesis Research **103**(3): 195-209.

Roy, S., et al. (2011). Phytoplankton pigments: characterization, chemotaxonomy and applications in oceanography, Cambridge University Press.

Sommer, P. and M. Kofler (1966). "Physicochemical properties and methods of analysis of phylloquinones, menaquinones, ubiquinones, plastoquinones, menadione, and related compounds." Vitam Horm **24**: 349-399.

# Appendix II

# Separation of photosynthetic lipids by HPTLC

Subsequent to having optimized extraction conditions, the photosynthetic lipids extracted from *Nannochloropsis oceanica* were separated by high performance thin layer chromatography and identified by absorption spectroscopy. The measured spectra are provided in this appendix.

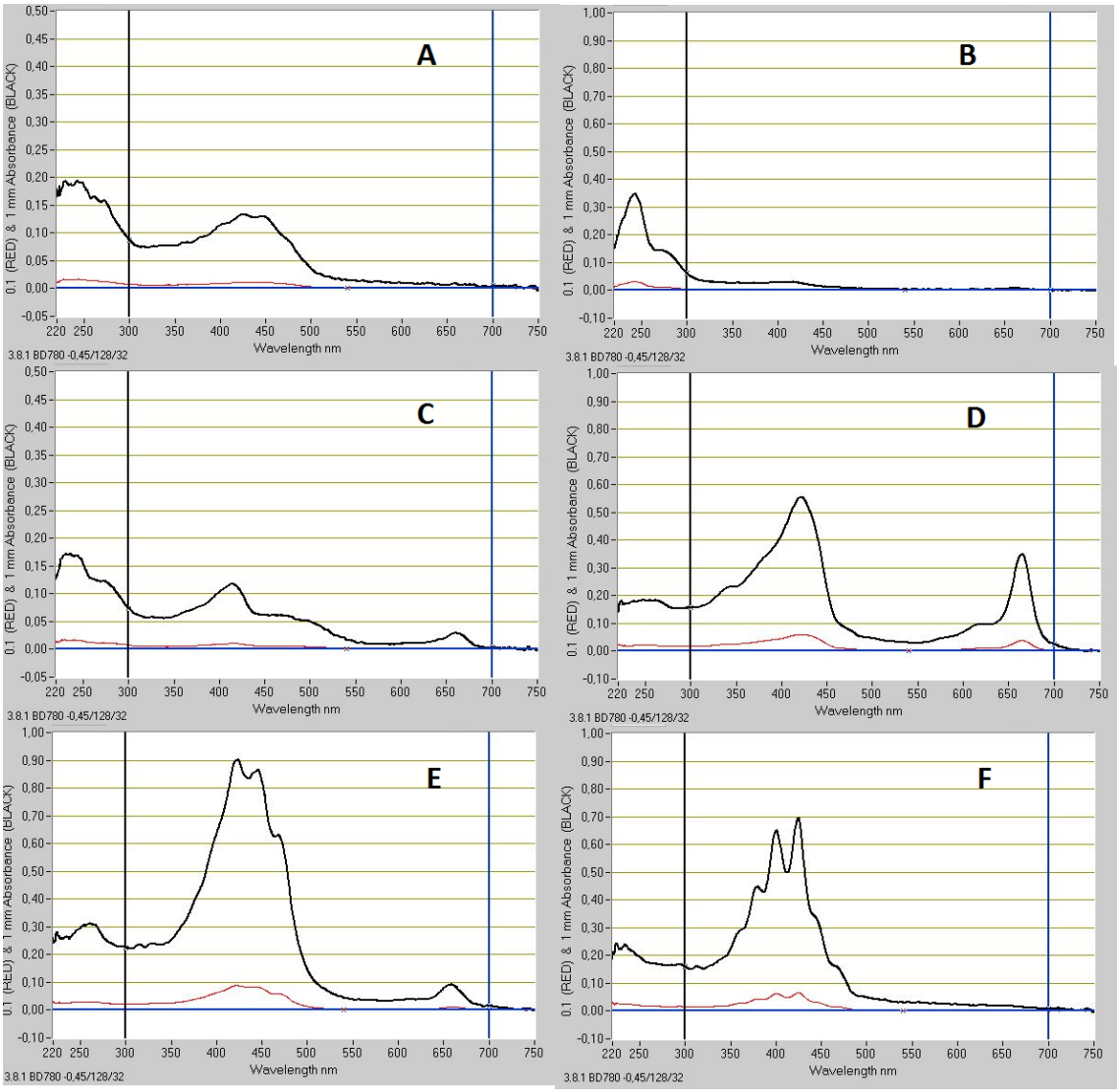


**Figure A2.1 – Absorption spectra of photosynthetic lipids extracted from Nannochloropsis oceanica and separated by HPTLC:** Separated lipids were scrapped off and dissolved in methanol prior to the measurements of their absorption spectra. A-F represent analyzed bands isolated from the HPTLC-plate after development with hexane/acetone (60/40). Bands are represented in order of increasing retention factor. A: β-carotene and phylloquinone (band 1), B: plastoquinone (band 2), C: pheophetyn *a* and canthaxanthin (band 3, 4), D: chlorophyll *a* (band 5), E: antheraxanthin/vaucheriaxanthin esters (band 6), F: violaxanthin (band 7). Band 8 is not shown.

# Appendix III

# UPC$^2$-qTOF-MS instrument parameters

Appendix III gives an overview of the instrument parameters applied for the UPC$^2$-qTOF-MS protocol utilized for characterization of photosynthetic lipid standards.

---

**Acquisition Experiment Report Page 1 of 9**
**File:**
**D:\SYNAPT\2014\KK_20140905_MARTIN_H_M.PRO\DATA\20150119_KK_APCI_B_CAROTENE**
**Printed: Tuesday, May 12, 2015 10:52:03 W. Europe Daylight Time**

---

Note: This file contains a record of the instrument parameters used at the start of the ac
Note: Where parameters are varied through the experimental method refer to that method or
**Header**
Acquired File Name: 20150119_KK_APCi_b_carotene_inj1
Acquired Date: 19-Jan-2015
Acquired Time: 15:48:42
Job Code: 20150119_SFC_Ksenia_samples
Task Code:
User Name:
Laboratory Name:
Instrument: SYNAPT G2-S#NotSet
Conditions:
Submitter:
SampleID:
Bottle Number: 2:A,3
Description:
Instrument Calibration:
Calibration File:
Parameters
MS1 Static: None
MS1 Scanning:
Mass: 50 Da to 1500 Da.
Resolution: 0.0/0.0
Ion Energy: 0.0
Reference File: ESI_NaFormate_Pos
Acquisition File: Commission sodium formate-2015-0O§ú
MS1 Scan Speed Compensation: None
Calibration Time: 18:03
Calibration Date: 01/18/15
Coefficients
MS1 Static: None
Function 1: -0.000000000037*x^5 + 0.000000003617*x^4 + -0.000000123672*x^3 + 0.00000
Function 2: -0.000000000037*x^5 + 0.000000003617*x^4 + -0.000000123672*x^3 + 0.00000
Parameters for
C:\Projects\IBT\KK\2014\KK_20140905_Martin_H_M.PRO\ACQUDB\20140504_KK_APCi_

Created by 4.1 SCN 897
Lock Spray Configuration:
Reference Scan Frequency(sec) 10.000
Reference Cone Voltage(V) 30.000
Reference Trap Collision Energy 4.000
Reference DRE Setting 22.810
Temperature Correction:
Temperature Correction Disabled
Instrument Configuration:
Lteff 1800.0
Veff 7194.50
Resolution 20000
Min Points in Peak 2
Acquisition Device WatersADC
Acquisition Algorithm ADC Mode
ADC Trigger Threshold (V) 1.00
ADC Input Offset (V) -1.68
Average Single Ion Intensity 22
ADC Amplitude Threshold 4
ADC Centroid Threshold -1
ADC Ion Area Threshold 2
ADC Ion Area Offset 10
ADC Pushes Per IMS Increment 1

---



---

EDC Delay Coefficient 1.4100
EDC Delay Offset 0.4000
Experimental Instrument Parameters
Instrument Parameter Filename C:\Projects\IBT\KK\2014\KK_20140905_Martin
Polarity API+
Corona Voltage (kV) 3.0
Corona Current (uA) 2.5
Probe Temp (C) 500.0
Source Temperature (°C) 120
Sampling Cone 50.0000
Source Offset 50.0000
Source Gas Flow (mL/min) 0.00
Cone Gas Flow (L/Hr) 100.0
Desolvation Gas Flow (L/Hr) 1000.0
Nebuliser Gas Flow (Bar) 6.0
LM Resolution 4.7
HM Resolution 15.0
Aperture 1 0.0
Pre-filter 2.0
Ion Energy 1.0
Manual Trap Collision Energy FALSE
Trap Collision Energy 4.0
Manual Transfer Collision Energy FALSE
Transfer Collision Energy 2.0
Manual Gas Control FALSE
Trap Gas Flow (mL/min) 2.00
HeliumCellGasFlow 180.00
IMS Gas Flow (mL/min) 90.00
Detector 3075
DetectorCache 2300

Sample Infusion Flow Rate (µL/min) 20
Sample Flow State LC
Sample Fill Volume (µL) 250
Sample Reservoir C
LockSpray Infusion Flow Rate (µL/min) 10
LockSpray Flow State Infusion
LockSpray Reservoir B
LockSpray Capillary (kV) 3.00
Use Manual LockSpray Collision Energy FALSE
Collision Energy 4.0
Acceleration1 70.0
Acceleration2 200.0
Aperture2 70.0
Transport1 70.0
Transport2 70.0
Steering 0.62
Tube Lens 73
Pusher 1900.0
Pusher Offset -0.71
Puller 1380.0
Pusher Cycle Time (µs) Automatic
Pusher Width (µs) Automatic
Collector 50
Collector Pulse 10.0
Stopper 10
Stopper Pulse 20.0
Entrance 62
Static Offset 180
Puller Offset 0.00
Reflectron Grid (kV) 1.475
Flight Tube (kV) 10.00
Reflectron (kV) 3.780
Use Manual Trap DC FALSE



Trap DC Entrance 0.0
Trap DC Bias 2.0
Trap DC -2.0
Trap DC Exit 1.0
Use Manual IMS DC FALSE
IMS DC Entrance -20.0
Helium Cell DC 1.0
Helium Exit -20.0
IMSBias 2.0
IMS DC Exit 20.0
USe Manual Transfer DC FALSE
Transfer DC Entrance 5.0
Transfer DC Exit 15.0
Trap Manual Control OFF
Trap Wave Velocity (m/s) 300
Trap Wave Height (V) 0.5
IMS Manual Control OFF
IMS Wave Velocity (m/s) 300
IMS Wave Height (V) 0.0
Transfer Manual Control OFF

Transfer Wave Velocity (m/s) 249
Transfer Wave Height (V) 0.2
Step Wave 1 In Manual Control OFF
Enable Reverse Operation OFF
Step Wave 1 In Velocity (m/s) 300.0
Step Wave 1 In Height 15.0
Step Wave 1 Out Manual Control OFF
Step Wave 1 Out Velocity (m/s) 300.0
Step Wave 1 Out Height 15.0
Step Wave 2 Manual Control OFF
Step Wave 2 Velocity (m/s) 300.0
Step Wave 2 Height 1.0
Use Manual Step Wave DC OFF
Step Wave TransferOffset 25.0
Step Wave DiffAperture1 3.0
Step Wave DiffAperture2 0.0
Use Automatic RF Settings TRUE
StepWave1RFOffset 300.0
StepWave2RFOffset 350.0
Target Enhancement Enabled FALSE
Target Enhancement Mode EDC
Target Enhancement Mass 556.0
Target Enhancement Trap Height (V) 4.0
Target Enhancement Extract Height (V) 15.0
Mobility Trapping Manual Release Enabled FALSE
Mobility Trapping Release Time (µs) 500
Mobility Trap Height (V) 15.0
Mobility Extract Height (V) 0.0
Trag Gate LUT table enabled FALSE
TriWave Trap Gate LookUp Table
Using Drift Time Trimming FALSE
Drift Time Bins 0
Using Mobility Delay after Trap Release TRUE
IMS Wave Delay (µs) 1000
Variable Wave Height Enabled FALSE
Wave Height Ramp Type Linear
Wave Height Start (V) 10.0
Wave Height End (V) 40.0
Wave Height Using Full IMS TRUE
Wave Height Ramp (%) 100.0
Wave Height Look Up Table
Variable Wave Velocity Enabled FALSE
Wave Velocity Ramp Type Linear
Wave Velocity Start (m/s) 1000.0

---



---

Wave Velocity End (m/s) 300.0
Wave Velocity Using Full IMS TRUE
Wave Velocity Ramp (%) 100.0
Wave Velocity Look Up Table
Backing 4.16e0
Source 7.38e-3
Sample Plate 1.00e-6
Trap 8.67e-3
Helium Cell 1.85e-4

IMS 7.98e-5
Transfer 7.25e-3
TOF 6.83e-7
IMSRFOffset 300
IMSMobilityRFOffset 250
TrapRFOffset 300
Use Automatic RF Settings TRUE
AutoStepWave1RFOffset 300
AutoStepWave2RFOffset 350
TransferRFOffset 350
MS Profile Type Auto P
MSProfileMass1 100
MSProfileDwellTime1 20
MSProfileRampTime1 20
MSProfileMass2 300
MSProfileDwellTime2 20
MSProfileRampTime2 40
MSProfileMass3 500
LockMassValidSigma 5
Acquisition mass range
Start mass 50.000
End mass 2000.000
Calibration mass range
Start mass 90.917
End mass 1449.848
Experiment Reference Compound Name: Leucine Enkephalin Single Point MS
Function Parameters - Function 1 - TOF MS FUNCTION
Scan Time (sec) 0.200
Interscan Time (sec) 0.015
Start Mass 50.0
End Mass 2000.0
Start Time (mins) 0.00
End Time (mins) 6.00
Data Format Continuum
Analyser Resolution Mode
ADC Sample Frequency (GHz) 3.0
ADC Pusher Frequency (µs) 69.0
ADC Pusher Width (µs) 1.75
Use Tune Page Cone Voltage YES
Use Tune Page Probe Temperature NO
API Probe Temp 500.0
Using Auto Trap Collision Energy (eV) 4.000000
Using Auto Transfer Collision Energy (eV) 2.000000
Sensitivity Normal
Dynamic Range Normal
Save Collapsed Retention Time Data No
Use Rule File Filtering No
FragmentationMode CID
Calibration Dynamic 2
Function Parameters - Function 2 - REFERENCE
Scan Time (sec) 1.000

---



---

Interscan Time (sec) 0.100
Start Mass 50.0

End Mass 2000.0
Start Time (mins) 0.00
End Time (mins) 6.00
Data Format Continuum
Analyser Resolution Mode
ADC Sample Frequency (GHz) 3.0
ADC Pusher Frequency (µs) 69.0
ADC Pusher Width (µs) 1.75
Use Tune Page Cone Voltage YES
Use Tune Page Probe Temperature NO
API Probe Temp 500.0
Using Auto Trap Collision Energy (eV) 4.000000
Using Auto Transfer Collision Energy (eV) 2.000000
Sensitivity Normal
Dynamic Range Normal
Save Collapsed Retention Time Data No
Use Rule File Filtering No
FragmentationMode CID
[LOCK SPRAY]
LockSprayType: Do not apply correction
LockSpray Reference Compound Name: Leucine Enkephalin Single Point MS
Scan Time (sec) 1.00
Interval 10
EDC Mass 0.0000
Mass Window +/- 0.5
Scans to Average 3.0
Reference Cone Voltage 30.0
Trap Collision Energy (eV) 4.0
LockSprayDRESetting 22.8100
[METHOD EVENTS:]
Timed Events Enabled: YES
API Probe Delay Temp: 20.0
Num of Timed Events: 4.0
Event Time Name Action System
1 -60.00 Flow State LC Sample
2 -60.00 Reservoir B LockSpray
3 -60.00 Refill Auto-Refill LockSpray
4 -60.00 Infusion Start LockSpray
Calibration Dynamic 2
ACE Experimental Record
Inlet Method File:
c:\projects\ibt\kk\2014\kk_20140905_martin_h_m.pro\acqudb\20140504_kk_c
---------- Run method parameters ----------
Waters GI Pump
1 ----------
Chromatographic Pump
Run Time: 7.00 min
Comment:
Solvent Selection B: B1
Low Pressure Limit: 0 psi
High Pressure Limit: 6000 psi



Solvent Name B: Methanol
Seal Wash: 6.0 min

System Pressure Data Channel: No
Flow Rate Data Channel: No
%A (CO2) Data Channel: No
%B Data Channel: No
Primary A (CO2) Pressure Data Channel: No
Accumulator A (CO2) Pressure Data Channel: No
Primary B Pressure Data Channel: No
Accumulator B Pressure Data Channel: No
Degasser Pressure Data Channel: No
[Gradient Table]
Time(min) Flow Rate %A %B Curve
1. Initial 2.500 98.0 2.0 Initial
2. 1.00 2.500 98.0 2.0 6
3. 4.00 2.500 70.0 30.0 6
4. 5.00 2.500 70.0 30.0 6
5. 6.00 2.500 98.0 2.0 6
6. 7.00 2.500 98.0 2.0 6
Gradient Start (Relative to Injection): 0 uL
Primary A (CO2) Temperature Data Channel: No
Accumulator A (CO2) Temperature Data Channel: No
ACQUITY Convergence Manager
Run Time: 7.00 min
ABPR Pressure Data Channel: No
CO2 Inlet Pressure Data Channel: No
[Gradient Table]
Time(min) Pressure(psi)
1. Initial 1600
Comment:
ABPR Pressure ON: true
Waters Acquity CM
Target Column Temperature: 45.0 C
Column Temperature Alarm Band: 5.0 C
Shutdown All Columns: No
Column Valve Position: Column 1
Equilibration Time: 0.1 min
External Valve 1: No Change
External Valve 2: No Change
External Valve 3: No Change
Comment:
Column Temperature Data Channel: No
Preheater Temperature Data Channel: No
Waters Acquity AutoSampler
Run Time: 7.00 min

---



---

Comment:
Load Ahead: Disabled
Injection Mode: Partial Loop With Needle Overfill
LoopOffline: Disable
Weak Wash Solvent Name:
Weak Wash Volume: 600 uL
Strong Wash Solvent Name:
Strong Wash Volume: 200 uL
Target Column Temperature: Off C
Column Temperature Alarm Band: Disabled

Target Sample Temperature: 15.0 C
Sample Temperature Alarm Band: Disabled
Full Loop Overfill Factor: Automatic
Syringe Draw Rate: Automatic
Needle Placement: Automatic
Pre-Aspirate Air Gap: Automatic
Post-Aspirate Air Gap: Automatic
Column Temperature Data Channel: No
Ambient Temperature Data Channel: No
Sample Temperature Data Channel: No
Sample Organizer Temperature Data Channel: No
Sample Pressure Data Channel: No
Switch 1: No Change
Switch 2: No Change
Switch 3: No Change
Switch 4: No Change
Chart Out: Sample Pressure
Sample Temp Alarm: Disabled
Column Temp Alarm: Disabled
Run Events: Yes
Needle Overfill Flush: Automatic
NoInjection: false
Sample Run Injection Parameter
Injection Volume (ul) - 2.00
---------- oOo ----------
End of experimental record.
---------- Waters GI Pump Postrun Report ----------
---------- oOo ----------
---------- Waters Acquity SM Postrun Report ----------
Software Version: 1.50.2736
Firmware Version: 1.52.332 (Feb 29 2012)
Checksum: 0x38dc8799
Serial Number: H12C2S096N
Sample Syringe Size: 100.0
Sample Loop Size: 10.0



Needle Size: 10.0
NeedleType: PEEK
Minimum Sample Temperature: 0.0
Maximum Sample Temperature: 0.0
Average Sample Temperature: 0.0
Minimum Column Temperature: 0.0
Maximum Column Temperature: 0.0
Average Column Temperature: 0.0
Measured Loop Volume: 10.030
Measured Loop Volume No Pressure: 10.030
---------- oOo ----------
---------- ACQUITY Convergence Manager Postrun Report ----------
---
Firmware Version: 1.50.43 (Mar 02 2012)
Software Version: 1.50.1185
Checksum: 0x718c4014
Serial Number: H12C2M145N
Minimum ABPR Pressure: 0.0 psi

Maximum ABPR Pressure: 0.0 psi
Average ABPR Pressure: 0.0 psi
Minimum CO2 Inlet Pressure: 0.0 psi
Maximum CO2 Inlet Pressure: 0.0 psi
Average CO2 Inlet Pressure: 0.0 psi
---------- oOo ----------
---------- Waters Acquity CM Postrun Report ----------
Software Version: 1.50.1678
Firmware Version: 1.52.115 (Mar 06 2012)
Checksum: 0x1a2b3344
Serial Number: F12CMP892G
Valve Position: 1
ColumnType: ACQUITY UPC² HSS C18 SB 1.8µm
Column Serial Number: 0102122711CC01
Total Injections on Column: 874
Minimum Column Temperature: 45.0
Maximum Column Temperature: 45.0
Average Column Temperature: 0.0
---------- oOo ----------
**Function 1**
Scans in function: 1486
Cycle time (secs): 0.215
Scan duration (secs): 0.200
Inter Scan Delay (secs): 0.015
Start and End Time(mins): 0.000 to 6.000
Ionization mode: AP+
Data type: Enhanced Mass

---



---

Function type: TOF MS
Mass range: 50 to 2000
**Function 2**
Scans in function: 34
Cycle time (secs): 1.100
Scan duration (secs): 1.000
Inter Scan Delay (secs): 0.100
Start and End Time(mins): 0.000 to 6.000
Ionization mode: ES+
Data type: Enhanced Mass
Function type: TOF MS
Mass range: 50 to 2000

# Appendix IV
# Characterization of carotenoid standards

Characterization of carotenoid standards using $UPC^2$-qTOF-MS was performed to provide the basis for characterization and identification of carotenoids from *Nannochloropsis oceanica*. The mass spectra of the standards bought from DHI (Denmark) with their corresponding retention times are given in Figure A4.1-A4.6. A total ion chromatogram (TIC) is given in figure A4.7.

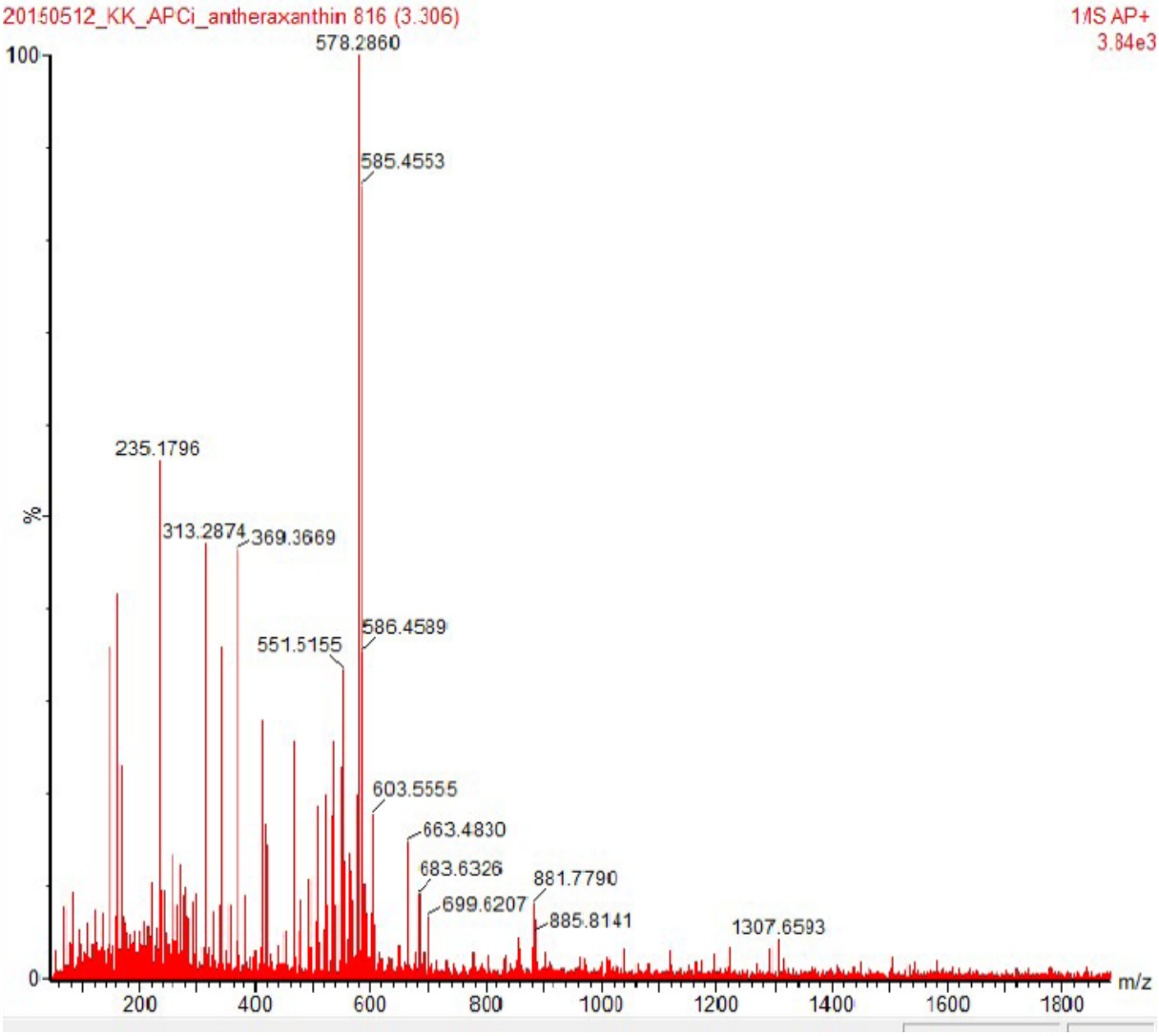


**Figure A4.1 – Mass spectrum of the antheraxanthin standard:** A mass of 586.46 and 585.46 eluted after 3.31 min was detected for the antheraxanthin standard.

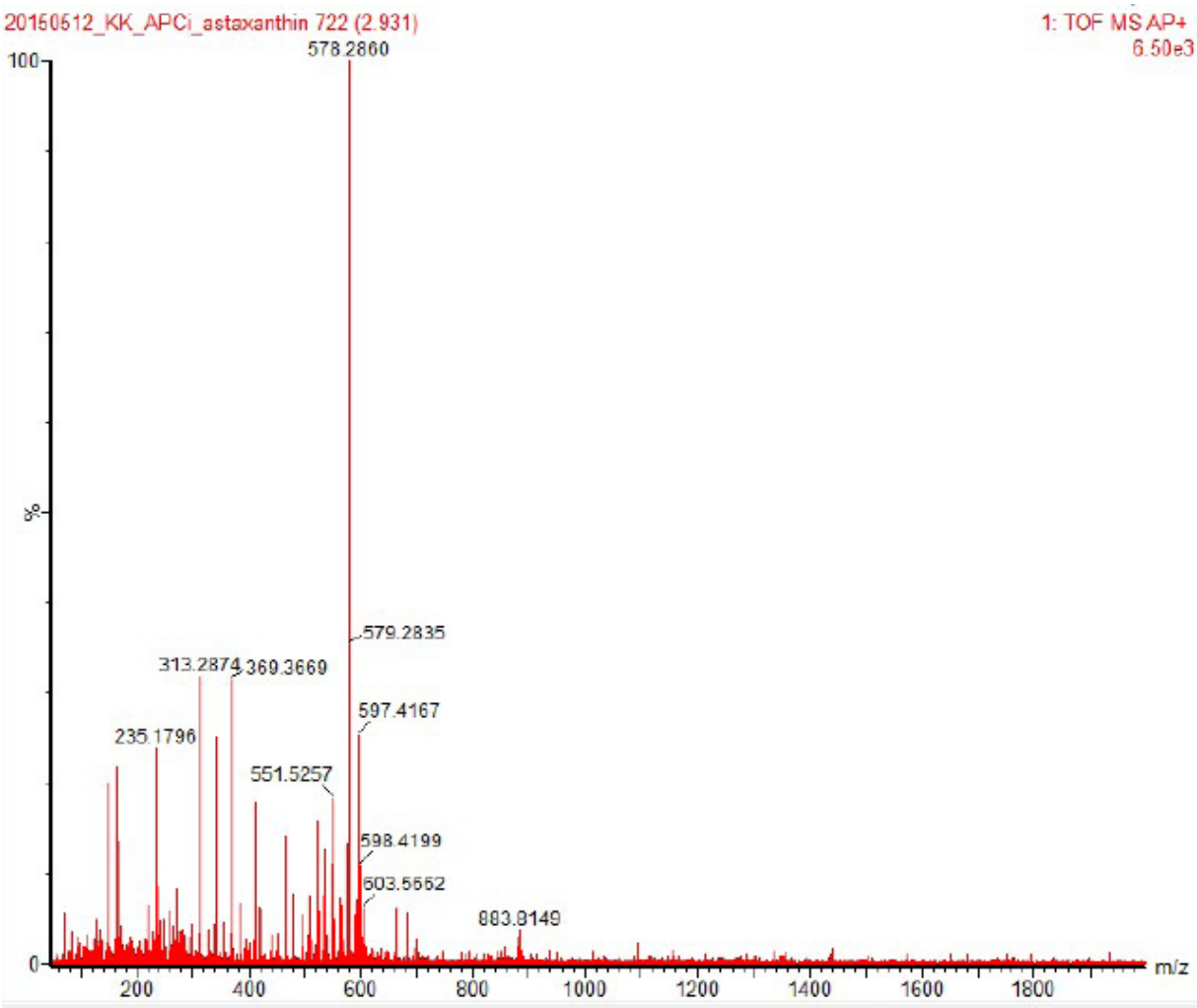


**Figure A4.2 – Mass spectrum of the astaxanthin standard:** A mass of 597.42 eluted after 2.93 min was detected for the astaxanthin standard.

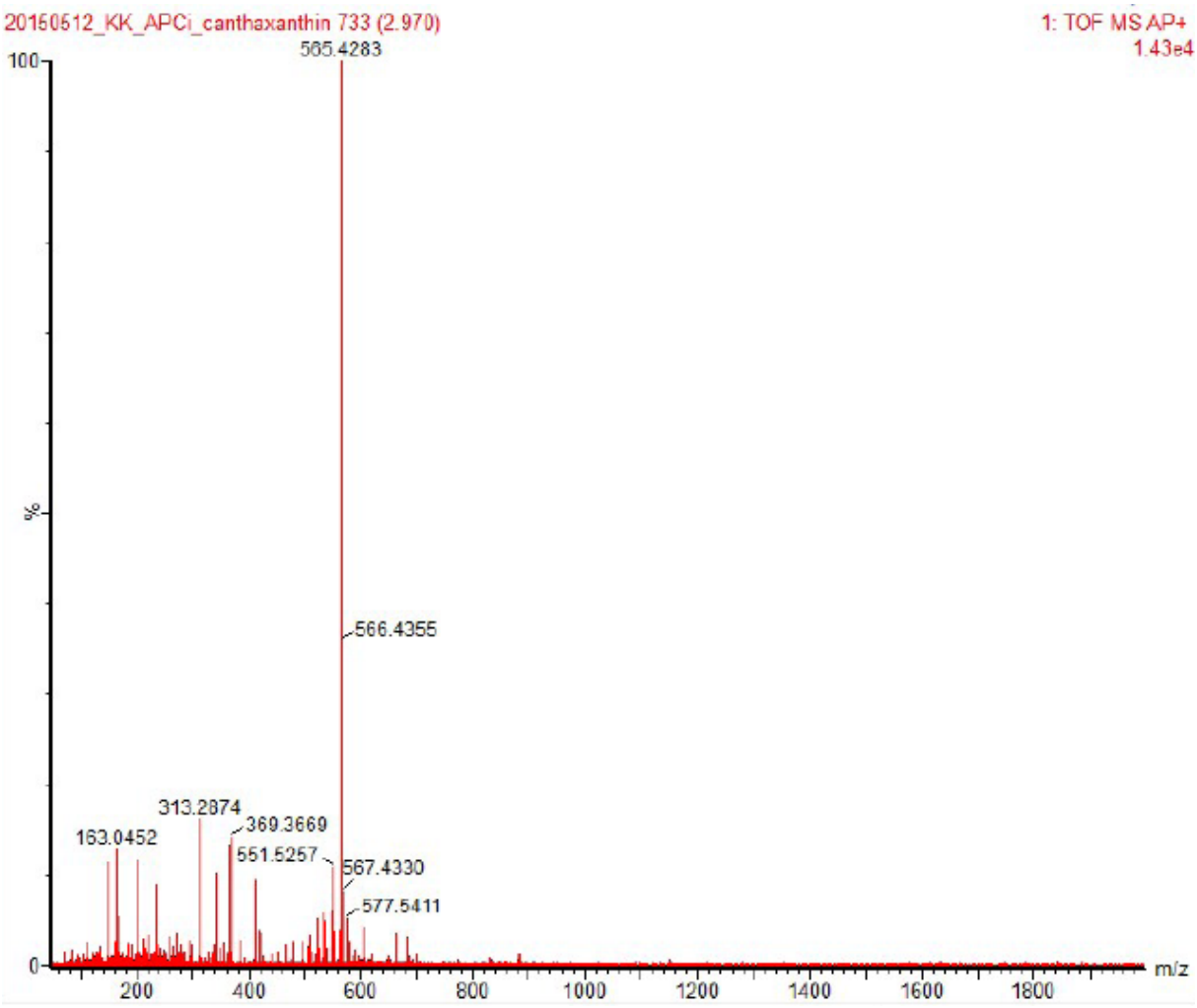


**Figure A4.3 – Mass spectrum of the canthaxanthin standard:** A mass of 565.43 eluted after 2.97 min was detected for the canthaxanthin standard.

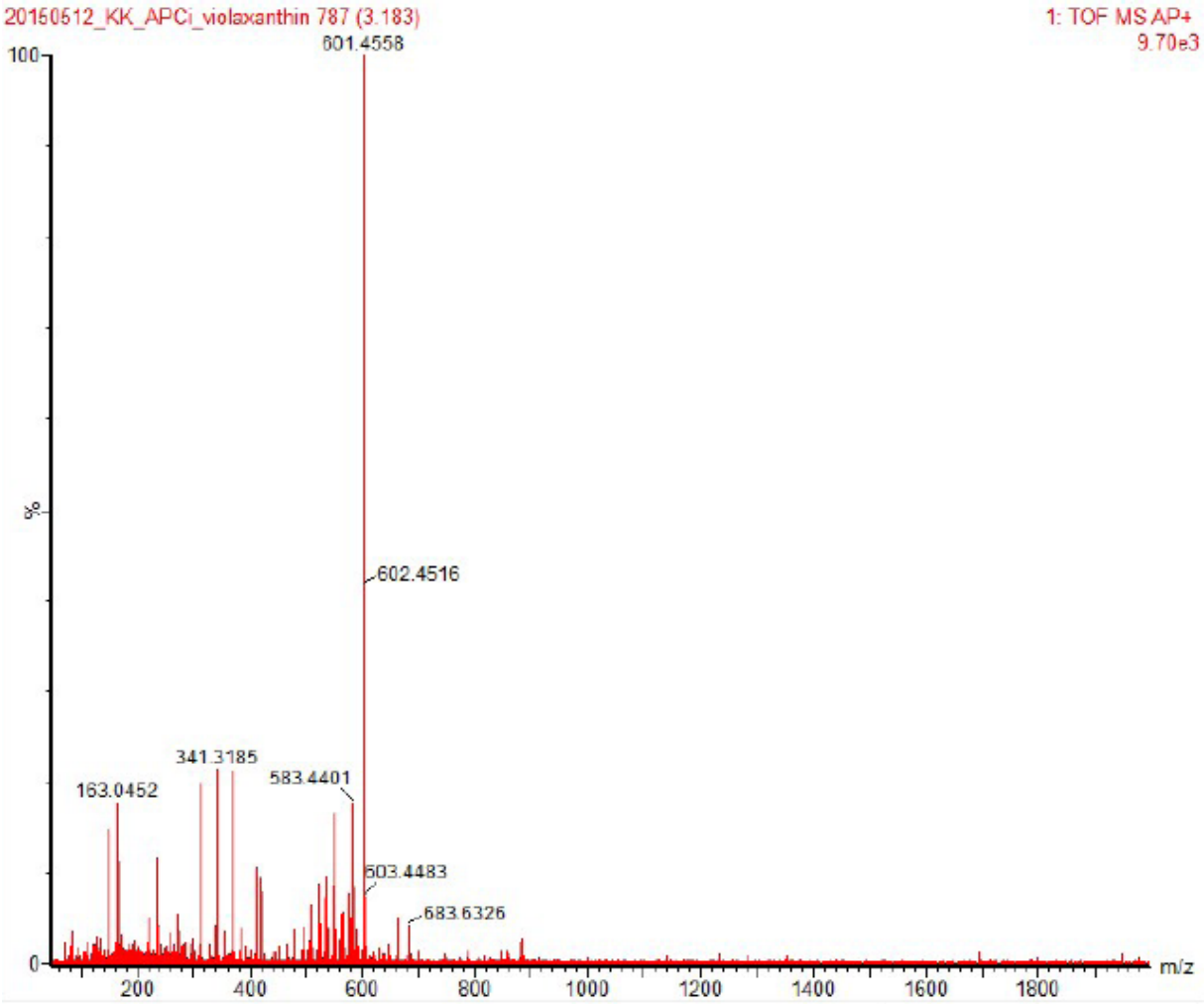


**Figure A4.4 – Mass spectrum of the violaxanthin standard:** A mass of 601.46 eluted after 3.18 min was detected for the violaxanthin standard.

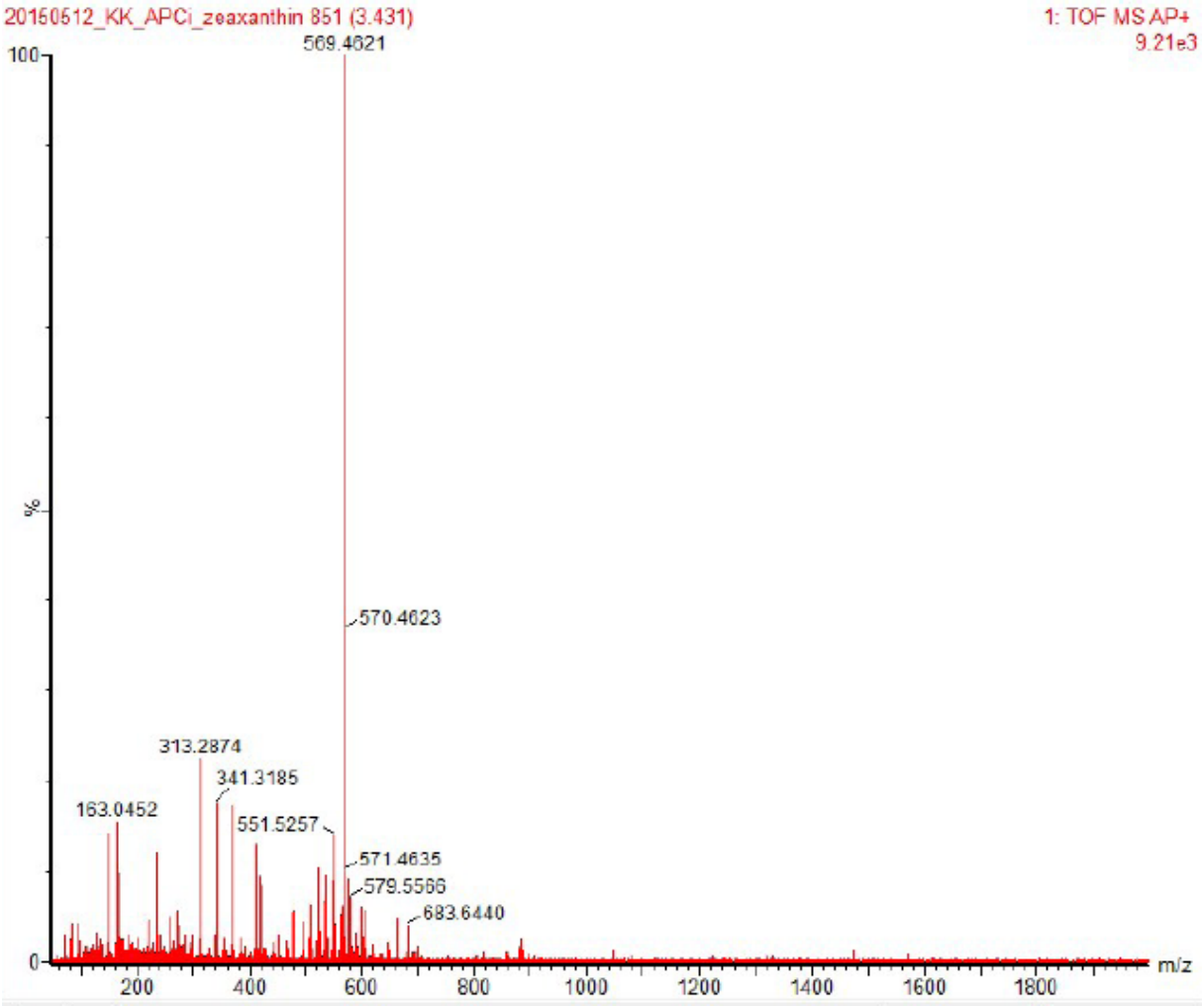


**Figure A4.5 – Mass spectrum of the zeaxanthin standard:** A mass of 569.46 eluted after 3.43 min was detected for the zeaxanthin standard.

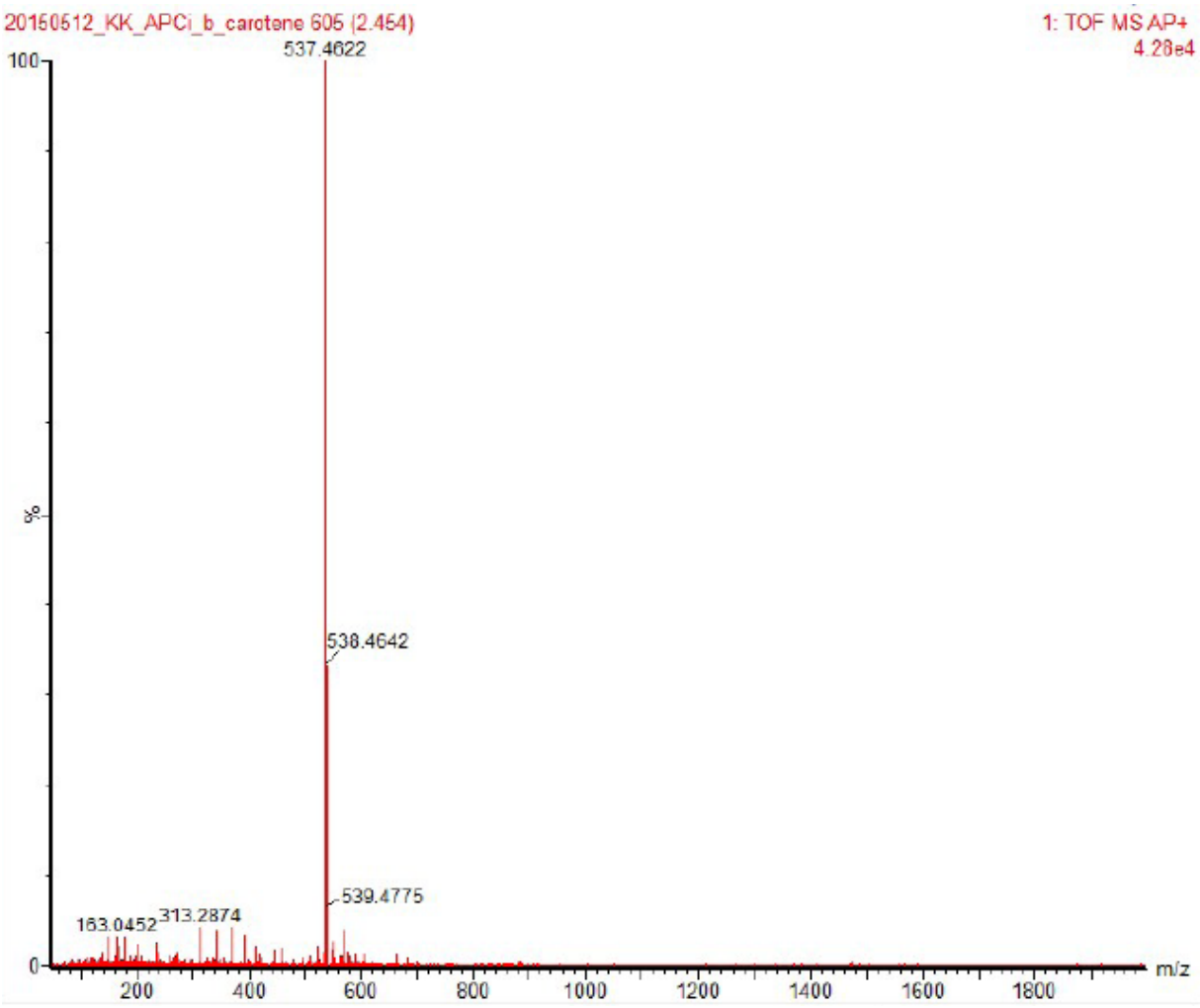


**Figure A4.6 – Mass spectrum of the β-carotene standard:** A mass of 537.46 eluted after 2.45 min was detected for the β-carotene standard.

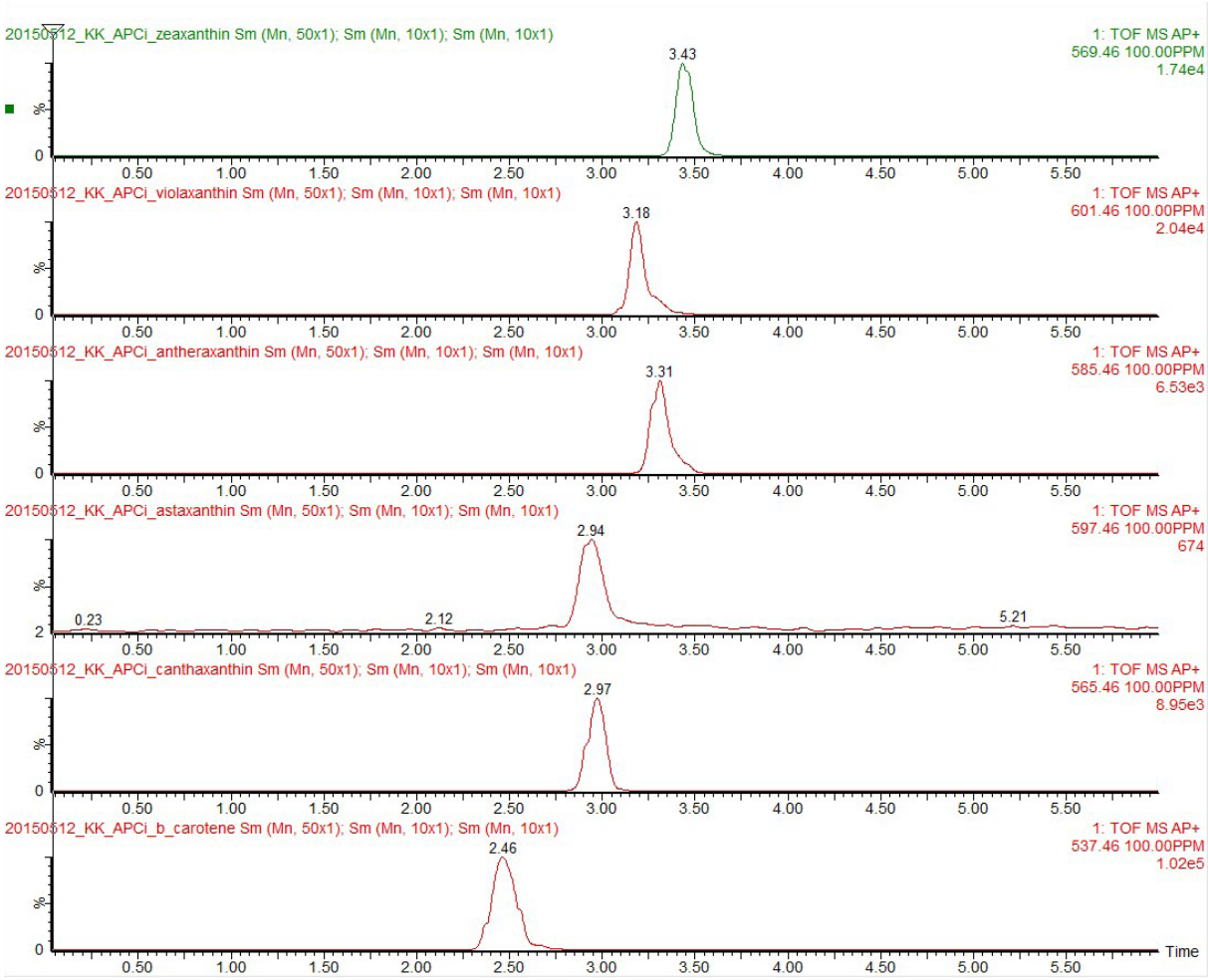


**Figure A4.7 – Total ion chromatograms for separated standards:** A TIC was created for each standard by summing up intensities of all peaks belonging to the same scan.

# Appendix V
# Additional recordings of 77 K spectroscopy

In this appendix, spectra recorded using 77 K spectroscopy are shown. Due to the relatively small differences observed between the biological replicates, only one typical recording is shown in the results section of chapter 4. The additional spectra are given here.

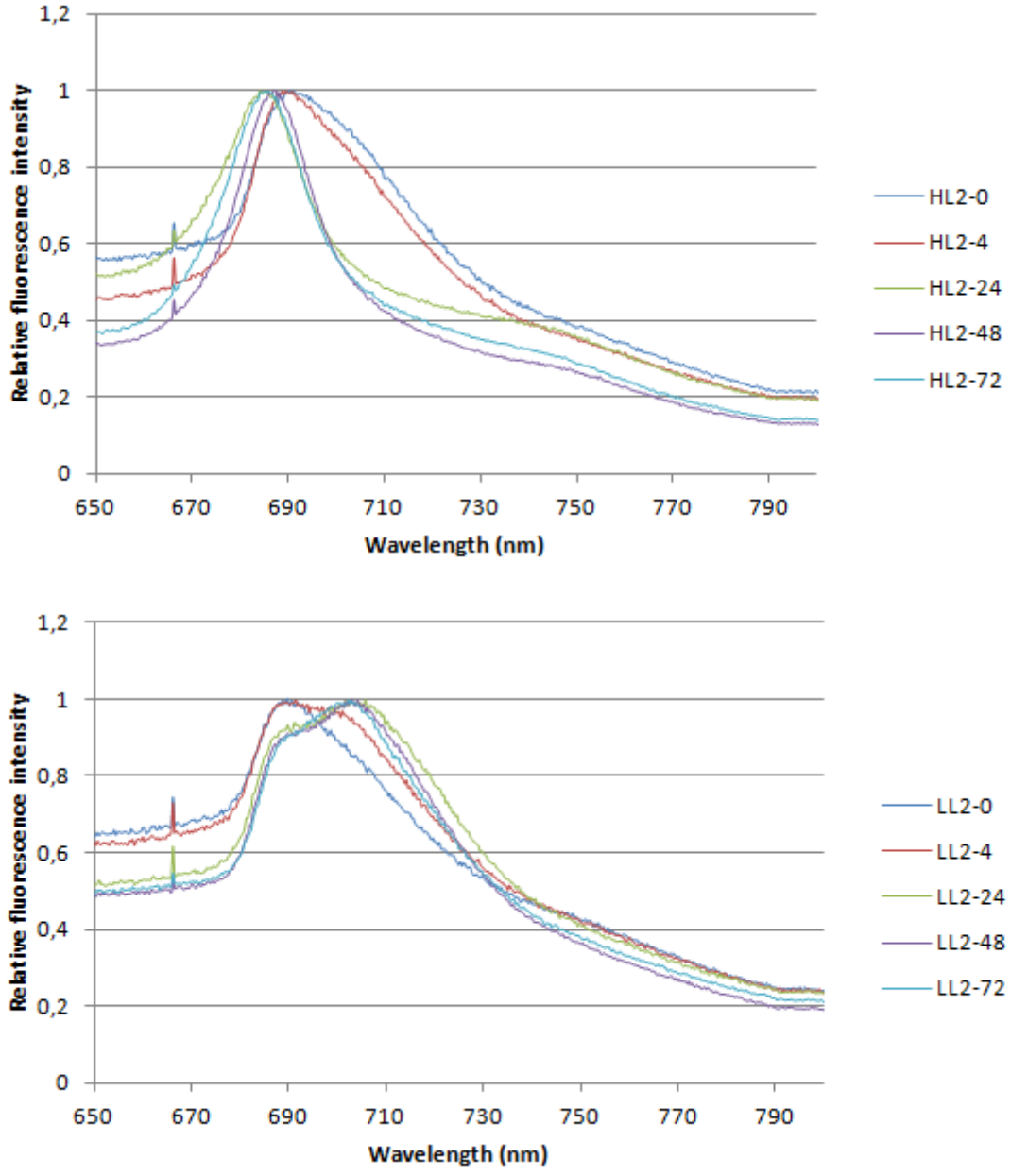


**Figure A5.1 -77 K fluorescence emission spectra of *Nannochloropsis oceanica:*** Comparison of fluorescence spectra over time (0-72h) under high light (HL) and lowlight (LL) conditions. The second parallel (biological replicate #2) .

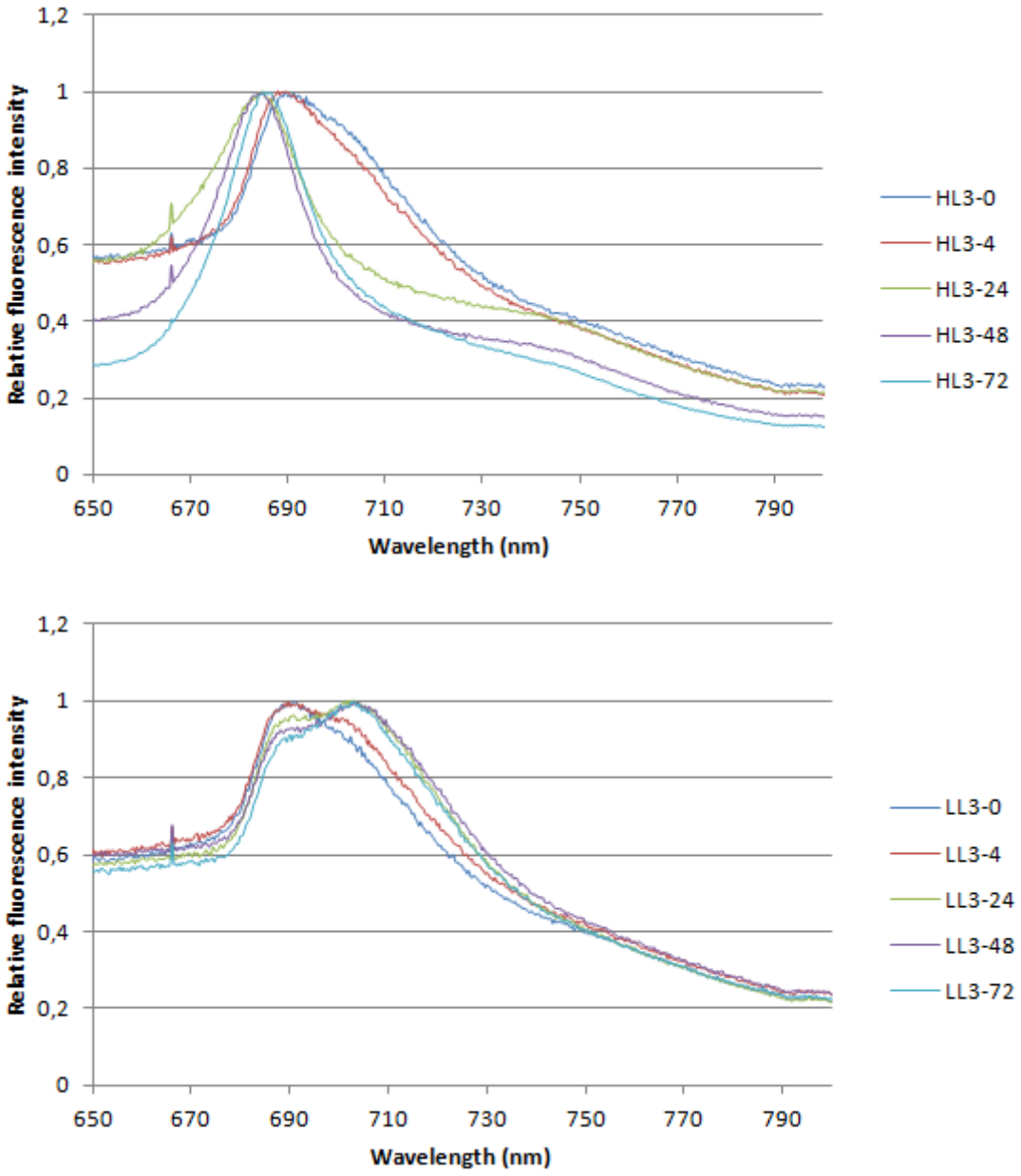


**Figure A5.2 -77 K fluorescence emission spectra of *Nannochloropsis oceanica:*** Comparison of fluorescence spectra over time (0-72h) under high light (HL) and lowlight (LL) conditions. The third parallel (biological replicate #3).

# Appendix VI
# PAM fluorometry induction curves

Appendix VI contains additional recordings of PAM fluorometry induction curves taken after 48 and 72 hours of exposure to high-light and low-light conditions.

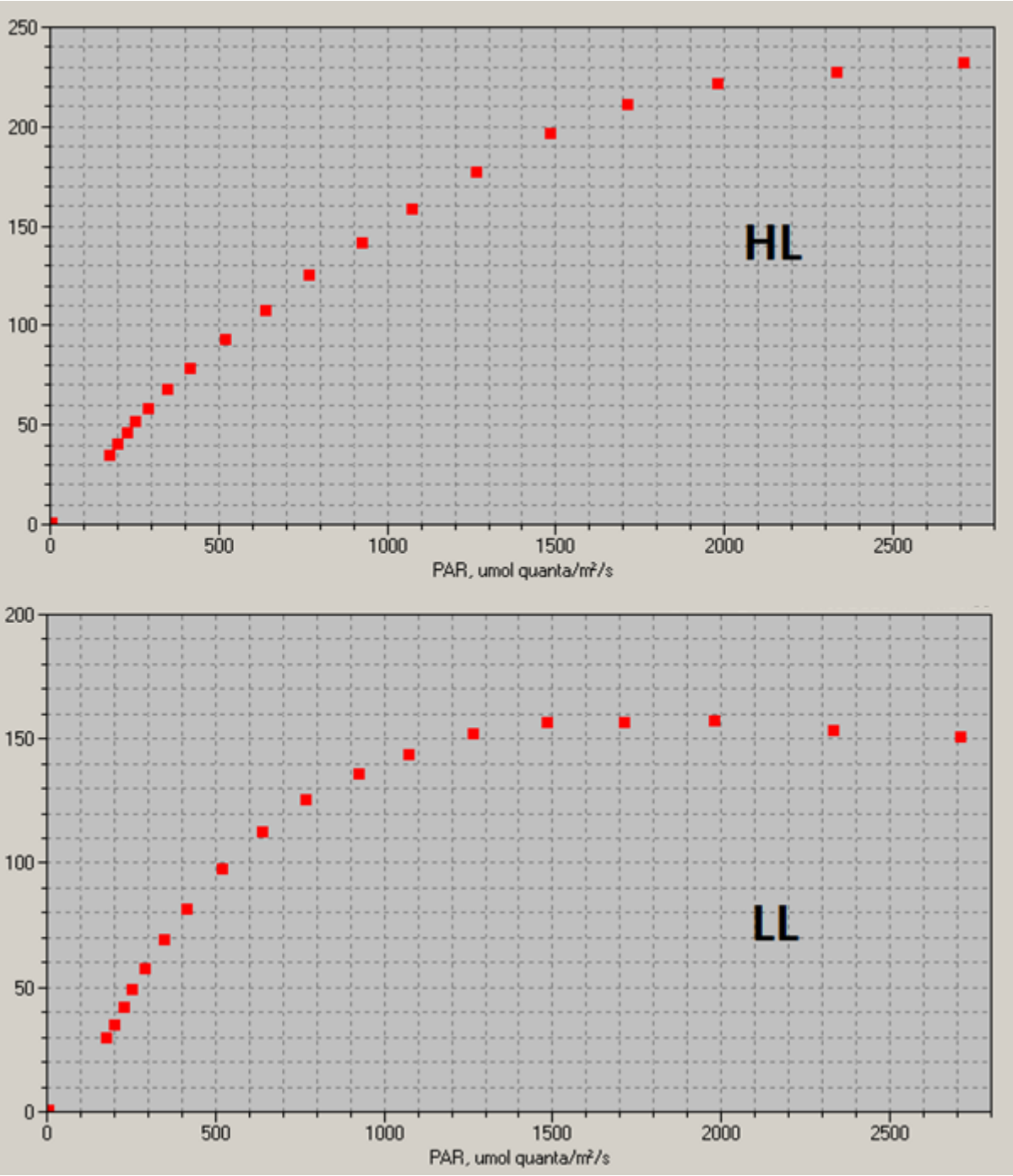


**Figure A6.1 – PAM fluorometry induction curves:** Relative rate of electron transport after 48 hours in low light (LL) and high light (HL) samples as a function of PAR.

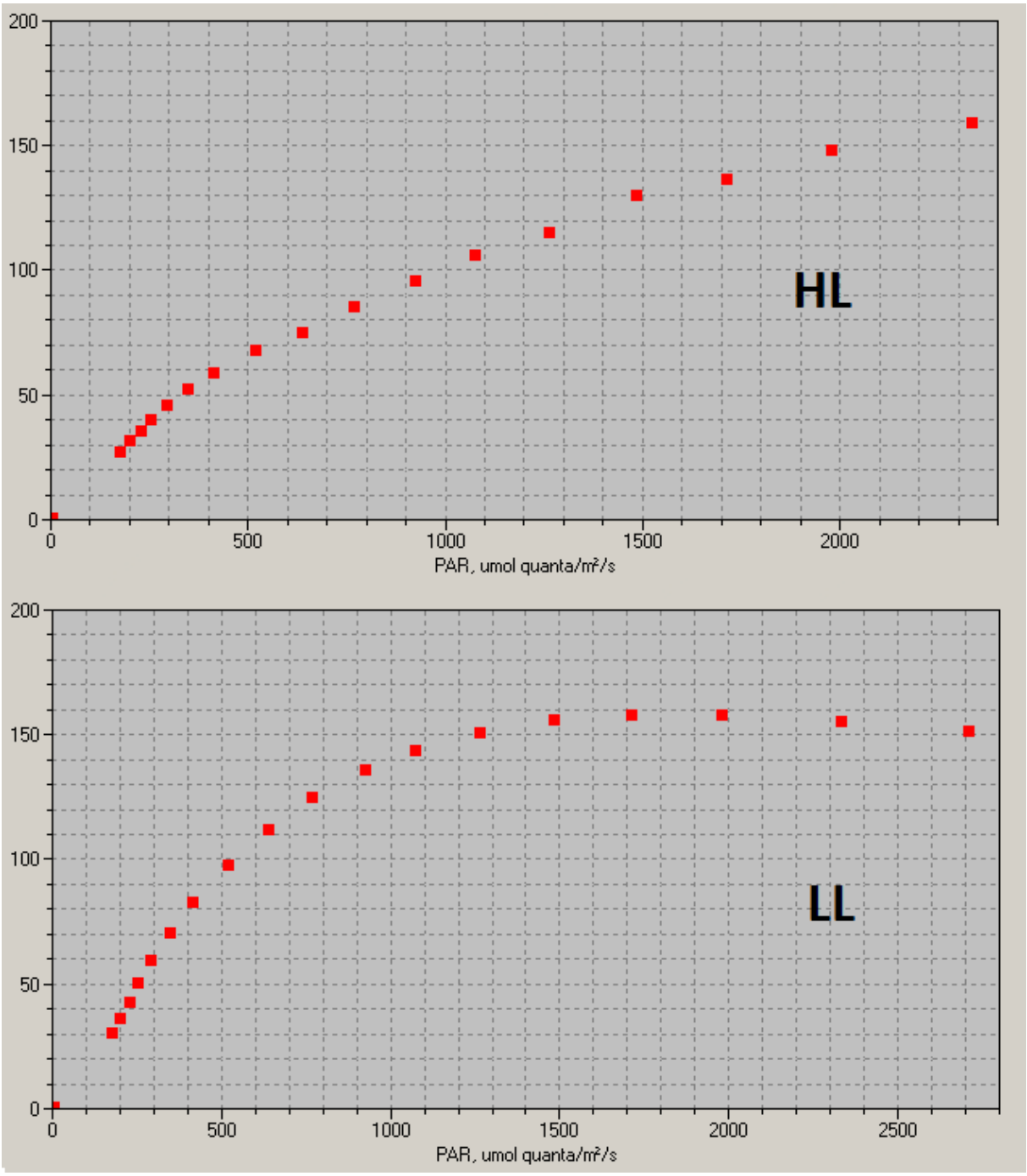


**Figure A6.2 – PAM fluorometry induction curves:** Relative rate of electron transport after 72 hours in low light (LL) and high light (HL) samples as a function of PAR.

# Appendix VII
# Characterization of photosynthetic lipids

Photosynthetic lipids extracted from *Nannochloropsis oceanica* were separated and characterized by UPC$^2$-qTOF-MS. Interpretation of the obtained mass spectrometry data was performed by utilizing the Progenesis QI software. The results of characterization of photosynthetic lipid composition presented in chapter 4 are an average of relative abundances of specific lipids between three biological replicates. The t = 0 samples were taken from the start culture, of which two sample replicates were prepared and analyzed. Appendix VII provides the detailed overview of the obtained mass spectrometric data with corresponding standard errors.

**Table A7.1 – Characterization of violaxanthin content:** Changes in relative abundance of violaxanthin in three biological replicas over time (0-72 hours) under high light (HL) and low light (LL) conditions, calculated average abundance and corresponding standard error (SE). Mass-to-charge ratio (m/z) and retention time for detected molecular ion are given at the top of the table.

| Violaxanthin | m/z | 601,4243 | | Retention time, min | 3,13738333 |
|---|---|---|---|---|---|
| **Time, hours** | **HL1** | **HL2** | **HL3** | **Average abundance** | **SE** |
| 0 | 9282,1768 | 10036,43 | | 9659,301449 | 377,124651 |
| 4 | 8707,0399 | 8375,014 | 9140,614 | 8740,889128 | 221,656691 |
| 24 | 5373,6728 | 5210,209 | 5499,988 | 5361,290063 | 83,8807726 |
| 48 | 2948,9382 | 5074,743 | 5403,434 | 4475,705147 | 769,257787 |
| 72 | 4127,1009 | 4184,194 | 4187,53 | 4166,275129 | 19,6107713 |
| **Time, hours** | **LL1** | **LL2** | **LL3** | **Average abundance** | **SE** |
| 0 | 9282,1768 | 10036,43 | | 9659,301449 | 377,1247 |
| 4 | 10691,49 | 12628,74 | 9084,384 | 10801,53813 | 1024,64614 |
| 24 | 12167,513 | 16759,25 | 14493,27 | 14473,34543 | 1325,55763 |
| 48 | 16673,152 | 16369,65 | 15979,58 | 16340,79587 | 200,735688 |
| 72 | 14938,923 | 14094,89 | 15453,32 | 14829,0459 | 395,973661 |

**Table A7.2 – Characterization of antheraxanthin content:** Changes in relative abundance of antheraxanthin in three biological replicas over time (0-72 hours) under high light (HL) and low light (LL) conditions, calculated average abundance and corresponding standard error (SE). Mass-to-charge ratio (m/z) and retention time for detected molecular ion are given at the top of the table.

| Antheraxanthin | m/z | 585,4285 | | Retention time, min | 3,36066667 |
|---|---|---|---|---|---|
| **Time, hours** | **HL1** | **HL2** | **HL3** | **Average abundance** | **SE** |
| 0 | 223,56652 | 250,8304 | | 237,1984347 | 13,6319177 |
| 4 | 307,54859 | 369,5343 | 292,04 | 323,0409832 | 23,673833 |
| 24 | 293,69706 | 311,9133 | 417,7984 | 341,1362591 | 38,6900829 |
| 48 | 464,87052 | 580,7901 | 741,6107 | 595,7571169 | 80,2377452 |
| 72 | 708,65566 | 793,5679 | 874,6984 | 792,307344 | 47,9365686 |
| **Time, hours** | **LL1** | **LL2** | **LL3** | **Average abundance** | **SE** |
| 0 | 223,56652 | 250,8304 | | 237,1984347 | 13,6319177 |
| 4 | 0 | 30,36983 | 12,4317 | 14,26717683 | 8,81491923 |
| 24 | 11,218974 | 47,98236 | 40,38466 | 33,1953298 | 11,2049313 |
| 48 | 26,868184 | 28,83912 | 16,74725 | 24,15151659 | 3,7455981 |
| 72 | 16,678539 | 0 | 0 | 5,559512837 | 5,55951284 |

**Table A7.3 – Characterization of zeaxanthin content:** Changes in relative abundance of zeaxanthin in three biological replicas over time (0-72 hours) under high light (HL) and low light (LL) conditions, calculated average abundance and corresponding standard error (SE). Mass-to-charge ratio (m/z) and retention time for detected molecular ion are given at the top of the table.

| Zeaxanthin | m/z | 569,4339 | | Retention time, min | 3,41421667 |
|---|---|---|---|---|---|
| **Time, hours** | **HL1** | **HL2** | **HL3** | **Average** | **SE** |
| 0 | 227,23 | 319,16 | | 273,1943207 | 45,9629998 |
| 4 | 148,19 | 254,94 | 277,01 | 226,712498 | 39,7767073 |
| 24 | 161,66 | 188,50 | 816,13 | 388,7632089 | 213,823319 |
| 48 | 1035,79 | 829,31 | 1427,73 | 1097,607154 | 175,491399 |
| 72 | 1003,11 | 1519,84 | 1923,26 | 1482,07064 | 266,295496 |
| **Time, hours** | **LL1** | **LL2** | **LL3** | **Average** | **SE** |
| 0 | 227,23132 | 319,1573 | | 273,1943207 | 45,963 |
| 4 | 0 | 147,1155 | 13,50603 | 73,55776882 | 46,949675 |
| 24 | 116,1165 | 408,6902 | 249,4748 | 262,4033631 | 84,568637 |
| 48 | 281,71026 | 326,463 | 289,6548 | 304,0866045 | 13,7855813 |
| 72 | 104,92901 | 86,39629 | 93,59069 | 95,66264821 | 5,39433301 |

**Table A7.4 – Characterization of oxidized PQ content:** Changes in relative abundance of oxidized PQ in three biological replicas over time (0-72 hours) under high light (HL) and low light (LL) conditions, calculated average abundance and corresponding standard error (SE). Mass-to-charge ratio (m/z) and retention time for detected molecular ion are given at the top of the table.

| Oxidized PQ | m/z | 749,621183 | | Retention time, min | 2,5083 |
|---|---|---|---|---|---|
| **Time, hours** | **HL1** | **HL2** | **HL3** | **Average** | **SE** |
| 0 | 5248,76852 | 5402,64013 | | 5325,70433 | 76,9358068 |
| 4 | 5922,41498 | 6012,27474 | 6016,2147 | 5983,63481 | 30,6310372 |
| 24 | 4920,42944 | 4749,65598 | 4884,2663 | 4851,45057 | 51,9568679 |
| 48 | 6400,40283 | 6093,44481 | 5542,80334 | 6012,21699 | 250,876923 |
| 72 | 6104,48236 | 6286,84871 | 5700,52979 | 6030,62029 | 173,23796 |
| **Time, hours** | **LL1** | **LL2** | **LL3** | **Average** | **SE** |
| 0 | 5248,76852 | 5402,64013 | | 5325,70433 | 76,9358068 |
| 4 | 5415,9371 | 6197,30905 | 4744,2273 | 5452,49115 | 419,866563 |
| 24 | 6464,02374 | 8365,60127 | 7235,44586 | 7355,02362 | 552,184572 |
| 48 | 8095,91068 | 7955,80212 | 7803,06908 | 7951,59396 | 84,5622696 |
| 72 | 6974,18596 | 7497,05159 | 7865,5802 | 7445,60592 | 258,605823 |

**Table A7.5 – Characterization of reduced PQ content:** Changes in relative abundance of reduced PQ in three biological replicas over time (0-72 hours) under high light (HL) and low light (LL) conditions, calculated average abundance and corresponding standard error (SE). Mass-to-charge ratio (m/z) and retention time for detected molecular ion are given at the top of the table.

| Reduced, PQ | m/z | 749,663099 | | Retention time, min | 1,7258 |
|---|---|---|---|---|---|
| **Time, hours** | **HL1** | **HL2** | **HL3** | **Average** | **SE** |
| 0 | 1045,84967 | 1068,48907 | | 1057,16937 | 11,3196971 |
| 4 | 2657,10644 | 2444,17724 | 2551,91978 | 2551,06782 | 61,4688403 |
| 24 | 7077,9967 | 6402,62132 | 6614,78214 | 6698,46672 | 199,403534 |
| 48 | 8845,69845 | 8054,99542 | 8428,51381 | 8443,06923 | 228,372295 |
| 72 | 6917,01409 | 7165,14508 | 7274,36499 | 7118,84139 | 105,72439 |
| **Time, hours** | **LL1** | **LL2** | **LL3** | **Average** | **SE** |
| 0 | 1045,84967 | 1068,48907 | | 1057,16937 | 11,3196971 |
| 4 | 439,714614 | 623,044695 | 501,168753 | 521,309354 | 53,8724189 |
| 24 | 59,3379796 | 138,05968 | 150,031938 | 115,809866 | 28,4466706 |
| 48 | 63,2835294 | 71,5775798 | 41,3811619 | 58,7474237 | 9,00718424 |
| 72 | 21,4584859 | 22,3568948 | 7,94824489 | 17,2545419 | 4,66037042 |

**Table A7.6 – Characterization of canthaxanthin content:** Changes in relative abundance of canthaxanthin in three biological replicas over time (0-72 hours) under high light (HL) and low light (LL) conditions, calculated average abundance and corresponding standard error (SE). Mass-to-charge ratio (m/z) and retention time for detected molecular ion are given at the top of the table.

| Canthaxanthin | m/z | 565,424419 | | Retention time, min | 3,14095 |
|---|---|---|---|---|---|
| **Time, hours** | **HL1** | **HL2** | **HL3** | **Average** | **SE** |
| 0 | 4,54273708 | 5,03690216 | | 4,78981962 | 0,24708254 |
| 4 | 5,90168219 | 7,73061786 | 7,10061852 | 6,91097286 | 0,53641574 |
| 24 | 2,2274713 | 2,61563871 | 1,96270898 | 2,26860633 | 0,18960343 |
| 48 | 0,75117106 | 3,10195953 | 2,26362128 | 2,03891729 | 0,68785185 |
| 72 | 1,45492305 | 2,67361401 | 1,89613169 | 2,00822292 | 0,35624207 |
| **Time, hours** | **LL1** | **LL2** | **LL3** | **Average** | **SE** |
| 0 | 4,54273708 | 5,03690216 | | 4,78981962 | 0,24708254 |
| 4 | 3,26921288 | 8,44808243 | 3,21797787 | 4,97842439 | 1,73489206 |
| 24 | 16,9353651 | 23,7895745 | 16,3355087 | 19,0201494 | 2,39099134 |
| 48 | 20,282477 | 17,1759721 | 12,760453 | 16,7396341 | 2,18235381 |
| 72 | 18,9376609 | 8,15133375 | 13,9142076 | 13,6677341 | 3,11618223 |

**Table A7.7 – Characterization of astaxanthin content:** Changes in relative abundance of astaxanthin in three biological replicas over time (0-72 hours) under high light (HL) and low light (LL) conditions, calculated average abundance and corresponding standard error (SE). Mass-to-charge ratio (m/z) and retention time for detected molecular ion are given at the top of the table.

| Astaxanthin | m/z | 597,395418 | | Retention time, min | 2,90505 |
|---|---|---|---|---|---|
| **Time, hours** | **HL1** | **HL2** | **HL3** | **Average abundance** | **SE** |
| 0 | 471,979236 | 477,232057 | | 474,605646 | 2,62641037 |
| 4 | 381,363167 | 373,614345 | 390,75942 | 381,912311 | 4,95696698 |
| 24 | 477,008511 | 456,307945 | 400,90206 | 444,739505 | 22,7187116 |
| 48 | 594,570055 | 610,450166 | 564,93506 | 589,985094 | 13,3375736 |
| 72 | 767,342751 | 771,56572 | 729,036946 | 755,981806 | 13,5274715 |
| **Time hours** | **LL1** | **LL2** | **LL3** | **Average abundance** | **SE** |
| 0 | 471,979236 | 477,232057 | | 474,605646 | 2,62641037 |
| 4 | 0 | 136,481115 | 69,1981119 | 68,5597423 | 39,3999972 |
| 24 | 174,747349 | 513,166638 | 438,268456 | 375,394148 | 102,626812 |
| 48 | 579,274881 | 436,129828 | 363,494666 | 459,633125 | 63,3892182 |
| 72 | 466,802615 | 333,395015 | 384,144805 | 394,780812 | 38,8769016 |

**Table A7.8 – Characterization of β-carotene content:** Changes in relative abundance of β-carotene in three biological replicas over time (0-72 hours) under high light (HL) and low light (LL) conditions, calculated average abundance and corresponding standard error (SE). Mass-to-charge ratio (m/z) and retention time for detected molecular ion are given at the top of the table.

| β-carotene | m/z | | 537,445338 | Retention time, min | 3,07833333 |
|---|---|---|---|---|---|
| **Time, hours** | **HL1** | **HL2** | **HL3** | **Average** | **SE** |
| 0 | 130,683333 | 122,645584 | | 126,664458 | 4,01887431 |
| 4 | 131,777846 | 134,473756 | 156,682682 | 140,978095 | 7,89076515 |
| 24 | 76,9953916 | 75,6443536 | 78,1804835 | 76,9400762 | 0,73263988 |
| 48 | 47,3063205 | 45,7214799 | 46,478465 | 46,5020884 | 0,45765652 |
| 72 | 49,1693668 | 64,3079355 | 51,3801491 | 54,9524838 | 4,72106087 |
| **Time, hours** | **LL1** | **LL2** | **LL3** | **Average** | **SE** |
| 0 | 130,683333 | 122,645584 | | 126,664458 | 4,01887431 |
| 4 | 561,283929 | 314,252846 | 390,87686 | 422,137879 | 73,0046286 |
| 24 | 245,898803 | 186,96459 | 198,916322 | 210,593238 | 17,9867836 |
| 48 | 195,420948 | 176,264986 | 194,541541 | 188,742492 | 6,24391579 |
| 72 | 198,632225 | 196,01004 | 199,912212 | 198,184826 | 1,14845696 |

**Table A7.9 – Characterization of β-carotene content:** Changes in relative abundance of β-carotene in three biological replicas over time (0-72 hours) under high light (HL) and low light (LL) conditions, calculated average abundance and corresponding standard error (SE). Mass-to-charge ratio (m/z) and retention time for detected molecular ion are given at the top of the table.

| Chlorophyll *a* | m/z | 891,526247 | | Retention time, min | 3,16238333 |
|---|---|---|---|---|---|
| **Time, hours** | **HL1** | **HL2** | **HL3** | **Average** | **SE** |
| 0 | 1265,13647 | 1309,19315 | | 1287,16481 | 22,0283415 |
| 4 | 1024,39916 | 926,88774 | 921,34492 | 957,543941 | 33,4658847 |
| 24 | 728,304519 | 700,171736 | 299,452816 | 575,976357 | 138,500078 |
| 48 | 192,607653 | 591,860429 | 291,175512 | 358,547865 | 120,076323 |
| 72 | 557,649732 | 353,207409 | 202,004072 | 370,953738 | 103,048788 |
| **Time, hours** | **LL1** | **LL2** | **LL3** | **Average** | **SE** |
| 0 | 1265,13647 | 1309,19315 | | 1287,16481 | 22,0283415 |
| 4 | 147,966033 | 834,228529 | 794,088806 | 592,094456 | 222,366321 |
| 24 | 836,49606 | 934,510465 | 1120,67895 | 963,895158 | 83,3418135 |
| 48 | 1089,57435 | 912,660947 | 932,781491 | 978,338931 | 55,9201774 |
| 72 | 1174,82882 | 1116,07431 | 1448,02165 | 1246,30826 | 102,272905 |